

Nanoparticles for Neurodegenerative Disorders

Enabling transport of a potential anti-Alzheimer's disease drug
across an advanced *in vitro* blood-brain barrier model

Dissertation

zur Erlangung des Grades des Doktors der Naturwissenschaften
der Naturwissenschaftlich-Technischen Fakultät III
Chemie, Pharmazie, Bio- und Werkstoffwissenschaften
der Universität des Saarlandes



von
Julia Stab
Saarbrücken
2016

Tag des Kolloquiums: 21.02.2017

Dekan: Prof. Guido Kickelbick

Berichterstatter: Prof. Günter Fuhr, Prof. Marc Schneider

Vorsitz: Prof. Gert Kohring

Akad. Mitarbeiter: Dr. Jens Neunzig

This study's experiments were performed at the Fraunhofer IBMT at St. Ingbert and Sulzbach, Germany at the department of bioprocessing & bioanalytics.

What is your name?

Auguste.

Last name?

Auguste.

What is your husband's name?

Auguste, I think...

An extract from Alois Alzheimer's interview with the severely demented Auguste Deter in 1901. She represents the first reported case of Alzheimer's disease.

Reprinted from Maurer *et al.*, Auguste D and Alzheimer's disease. *Lancet* 349, 1546-9 (1997).

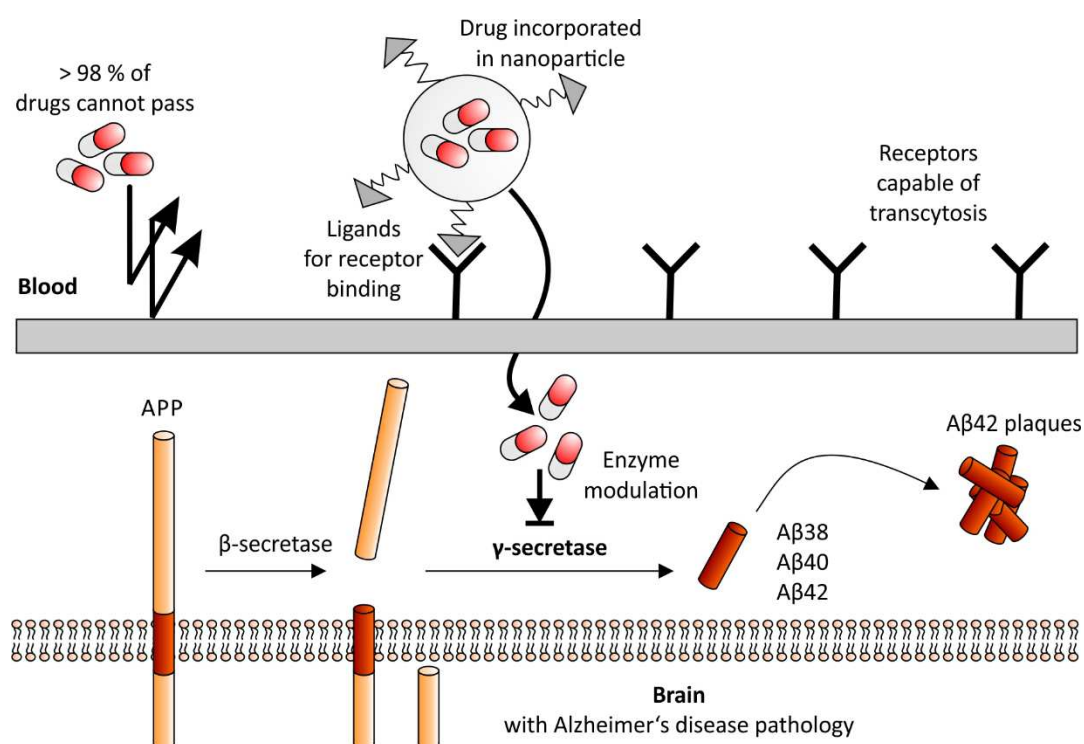
CONTENT

Abstract	I
Zusammenfassung	II
Abbreviations	III
1 Introduction	1
1.1 The blood-brain barrier: Obstacle in brain drug development	1
1.1.1 The shortage of brain medications.....	1
1.1.2 The structure of the blood-brain barrier	3
1.1.3 <i>In vitro</i> models try to predict <i>in vivo</i> success	5
1.1.4 Strategies for blood-brain barrier circumvention	7
1.2 Nanotechnology: Promising approach for brain delivery	8
1.2.1 What are nanoparticles?	8
1.2.2 Targeting nanoparticles to bio-structures.....	10
1.3 Dementia and Alzheimer’s disease: A rapidly growing problem	12
1.3.1 Case numbers, prognosis and treatment options	12
1.3.2 Discovery and neuropathology of Alzheimer’s disease.....	14
1.3.3 Etiology hypotheses of Alzheimer’s disease.....	16
1.3.4 Alzheimer’s disease variants	18
1.3.5 Alzheimer’s disease risk reduction factors.....	19
2 Aim of this thesis	21
3 Experimental procedures	22
3.1 Materials	22
3.2 Methods	26
3.2.1 Cell culture.....	26
3.2.2 Measurement of transendothelial electrical resistance of cell layers	29
3.2.3 Permeability of radiolabeled model substances	30
3.2.4 Characterization of the <i>in vitro</i> models by immunocytochemistry.....	32
3.2.5 Nanoparticle preparation and characterization.....	33
3.2.6 Fluorescence labeling of proteins	37
3.2.7 Nanoparticle plasma protein binding assay	37
3.2.8 Cellular binding studies	38
3.2.9 Cellular uptake studies	38
3.2.10 Determination of cytotoxic potential of nanoparticles.....	39
3.2.11 Nanoparticle-mediated drug transport experiments.....	40
3.2.12 Experimental definitions and visual display of data.....	42

4	Results & Discussion	43
4.1	Characterization of the <i>in vitro</i> blood-brain barrier model	43
4.1.1	Tight junction protein expression	44
4.1.2	Measurement of transendothelial electrical resistance	45
4.1.3	Permeability of radiolabeled model substances	46
4.1.4	Concluding remarks on characterization of the <i>in vitro</i> blood-brain barrier model	47
4.2	Nanoparticle preparation and characterization	48
4.2.1	Choice of basis material, synthesis and characterization of nanoparticles	49
4.2.2	Cellular viability of model cells after nanoparticle application	51
4.2.3	Influence on transendothelial electrical resistance development	52
4.2.4	Influence on marker permeability and barrier integrity of the <i>in vitro</i> BBB model	54
4.2.5	Concluding remarks on nanoparticle preparation and characterization	55
4.3	Nanoparticle-mediated drug transport across the <i>in vitro</i> barrier	56
4.3.1	Cellular binding of nanoparticles	57
4.3.2	Cellular uptake of nanoparticles	58
4.3.3	Drug transport studies	61
4.3.4	A β 42 reduction by flurbiprofen-loaded poly(lactic acid) nanoparticles	63
4.3.5	Cellular viability of the Alzheimer's disease model cells 7WD10	64
4.3.6	Summary drug transport	64
4.4	A suitable ligand for <i>in vivo</i> application: Apolipoprotein E3	68
4.4.1	Verification of receptor expression	68
4.4.2	ApoE binding to blood-brain barrier model cells	69
4.4.3	ApoE influence on barrier integrity and viability of primary BBB model cells	70
4.4.4	Binding and uptake of ligand-modified nanoparticles	72
4.4.5	Concluding remarks on ligand modification	74
5	Outlook & Scientific Context	75
5.1	Optimization of nanoparticles for flurbiprofen transport	75
5.2	Improving models: Can <i>in vitro</i> data predict <i>in vivo</i> outcome?	78
5.3	Further strategies and candidates profiting from nanotechnology	81
6	Conclusion	93
7	References	95
8	Appendix	112
8.1	List of publications	112
8.2	Curriculum Vitae	114
8.3	Acknowledgements	115

ABSTRACT

The blood-brain barrier (BBB) rigorously shields off the central nervous system from the periphery thereby protecting the fragile brain homeostasis. Yet, it also causes many potentially effective brain drugs to fail *in vivo* - not because of a lack of potency, but for they cannot enter the brain parenchyma. Nanoparticles enable brain drug delivery by acting as Trojan Horses, masking the original physicochemical properties of a drug and allowing targeted transport to biostructures, thereby enlarging the pool of brain drug candidates, such as potential anti-Alzheimer's disease (AD) drugs. Flurbiprofen (FBP) is a non-steroidal anti-inflammatory drug (NSAID) that lowers amyloid beta ($A\beta$) and AD prevalence in high dose long-term treatment. Still, an FBP enantiomer failed in clinical trials with AD patients, likely for its poor brain penetrating capacity. This study revisits FBP as an anti-AD drug by packing the drug into poly(lactic acid) nanoparticles (PLA-FBP NP). PLA-FBP NP crossed an advanced *in vitro* BBB model (consisting of primary porcine brain capillary endothelial cells (pBCEC) on Transwell® inserts to allow a blood and a brain compartment separation). Also, PLA-FBP NP reduced $A\beta_{42}$ burden (generated by AD model cells) in the brain compartment – notably without destroying barrier integrity. These promising *in vitro* findings highlight the potential of nanotechnology-based approaches as a chance in BBB crossing for the prevention and treatment of neurodegenerative disorders.



Graphical abstract of this thesis. The drug flurbiprofen might positively impact amyloid- β ($A\beta$) burden, but failed in clinical trials for it crosses the blood-brain barrier insufficiently *in vivo*. When the drug is incorporated in nanoparticles, it crosses a primary porcine *in vitro* blood-brain barrier model and reduces amyloid- β levels in the brain-representing compartment. Flurbiprofen mediates amyloid- β reduction by modifying the enzyme activity of γ -secretase.

ZUSAMMENFASSUNG

Die Blut-Hirn-Schranke (BHS) trennt Peripherie und Zentralnervensystem voneinander um die fragile Hirn-Homöostase zu schützen. Allerdings scheitern daher viele potentiell effektive Neurotherapeutika *in vivo* – sie können die BHS oft nicht überschreiten. Nanopartikel können den Transport ins Gehirn vermitteln indem sie als Trojanische Pferde die physikochemischen Eigenschaften der Substanzen maskieren und einen zielgerichteten Transport erlauben. Dies vergrößert die Anzahl potentieller Neuropharmaka, z.B. gegen die Alzheimer Krankheit (AD). Flurbiprofen (FBP) gehört zu den nicht-steroidalen Antirheumatika, die Amyloid beta (A β) und die AD-Prävalenz bei hoch dosierter Langzeitgabe verringern können. Dennoch verliefen klinische Studien mit AD Patienten enttäuschend, wahrscheinlich, weil FBP die BHS nur schlecht passiert. Diese Arbeit greift FBP wieder auf, indem die Substanz in Polymilchsäure-Nanopartikel (PLA-FBP NP) verpackt wird. PLA-FBP NP konnten ein *in vitro* BHS Modell (basierend auf primären porcinen Hirnkapillarendothel-Zellen (pBCEC) auf Transwell® Einsätzen zur Teilung in Blut- und Hirn-Kompartiment) überwinden. Darüber hinaus konnten die Nanopartikel A β 42 im Hirn-Kompartiment (produziert von AD Modell-Zellen) reduzieren – ohne dabei die Barriere-Integrität zu zerstören. Diese vielversprechenden *in vitro* Daten unterstreichen das Potenzial Nanotechnologie-basierter Ansätze zur Überwindung der BHS für die Therapien und Prävention neurodegenerativer Erkrankungen.

ABBREVIATIONS

°C	Degrees Celsius
μ	Micro
ACHE	Acetylcholine esterase
AD	Alzheimer's disease
AEBSF	4-(2-Aminoethyl)benzenesulfonyl fluoride hydrochloride
AIDS	Acquired immune deficiency syndrome
ALS	Amyotrophic lateral sclerosis
ApoE3	Apolipoprotein E3
APP	Amyloid precursor protein
ATP	Adenosine triphosphate
BACE1	β-secretase 1 (also known as β-site amyloid precursor protein cleaving enzyme 1, β-site APP cleaving enzyme 1, membrane-associated aspartic protease 2, memapsin-2, aspartyl protease 2, and ASP2)
BBB	Blood-brain barrier
BSA	Bovine serum albumin
Cld-3	Claudin 3
Cld-5	Claudin 5
CLSM	Confocal laser scanning microscopy
CNS	Central nervous system
COX-1,-2	Cyclooxygenase-1,-2
CSF	Cerebrospinal fluid
CYP	Cytochrome P450
DAPI	4',6-diamidino-2-phenylindole
DHA	Docosahexaenoic acid
DMEM	Dulbecco's modified Eagle medium
DMSO	Dimethyl sulfoxide
dpm	Decays per minute
EDC	1-Ethyl-3-(3-dimethylaminopropyl)-carbodiimide
EDTA	Ethylenediaminetetraacetic acid
ELISA	Enzyme-linked immunosorbent assay
Em	Emission
EMA	European medicines agency
ESAM	Endothelial selective adhesion molecule
Ex	Excitation
FBP	Flurbiprofen
FBS	Fetal bovine serum
FCS	Fetal calf serum
FDA	Food and drug administration
g	Gravity
g	Gram
GI	Gastrointestinal
GPC	Gel permeation chromatography
GTP	Guanosine triphosphate
h	Hour
HAART	Highly active antiretroviral therapy
HD	Huntington's disease
HEPES	4-(2-hydroxyethyl)-1-piperazineethanesulfonic acid

HIV	Human immunodeficiency virus
HPLC	High-performance liquid chromatography
HRP	Horseradish peroxidase
HSA	Human serum albumin
JAM	Junctional adhesion molecules
LDLR	Low density lipoprotein receptor
LRP1	Low density lipoprotein receptor-related protein 1
LRP2	Low density lipoprotein receptor-related protein 2 (also known as Megalin)
MAO	Monoamine oxidase
MEM	Minimum essential medium
MES	2-(<i>N</i> -morpholino)ethanesulfonic acid
MHC	Major histocompatibility complex
MPTP	1-methyl-4-phenyl-1,2,3,6-tetrahydropyridine
MRI	Magnetic resonance imaging
MS	Multiple sclerosis
NaCl	Potassium chloride
NCS	New born calf serum
NEAA	Non-essential amino acids
NRG1	Type III neuregulin 1
NSAID	Non-steroidal anti-inflammatory drug
O/W	Oil/water
Occl	Occludin
PBCA	Poly(butyl cyanoacrylate)
PBS	Phosphate buffered saline
PD	Parkinson's disease
PDI	Polydispersity index
PEG	Poly(ethylene glycol)
Pen/Strep	Penicillin streptomycin solution
PFA	Paraformaldehyde
PLA	Poly(lactic) acid
PLGA	Poly(lactic-co-glycolic acid)
PSEN 1, PSEN 2	Presenilin 1, Presenilin 2
PVA	Polyvinyl alcohol
Resazurin	7-Hydroxy-3H-phenoxazin-3-one 10-oxide
ROS	Reactive oxygen species
RT	Room temperature
RXR	Retinoid X receptor
SDS	Sodium dodecyl sulfate
SEM	Standard error of the mean
TER	Transendothelial electrical resistance
TJ	Tight junction
UK	United Kingdom
US	United States of America
VD	Vascular dementia
W/O/W	Water/oil/water
ZO-1	Zonula occludens

1 INTRODUCTION

A strong barrier surrounds the human brain, rigorously and reliably shielding off most substances and pathogens to protect the fragile central nervous system (CNS) homeostasis. However, this barrier also often prevents successful drug treatment in case of brain-associated diseases.

1.1 The blood-brain barrier: Obstacle in brain drug development

Disorders of the brain are a significant problem today, including depression, schizophrenia, dementia, Alzheimer's and Parkinson's disease, epilepsy, cerebrovascular disease and brain tumors [1], but research and development for CNS disease drugs is highly complex. Substances may often show promising *in vitro* results in preclinical testing, but they often fail to benefit *in vivo*. Although the number of drugs for CNS treatment has steadily grown, too few drugs acting on the CNS have entered the market [2] – even though treatment tactics with small molecule drugs often may exist (Figure 1A). The limiting factor is the delivery to the brain. For example, in the early stage of the acquired immune deficiency syndrome (AIDS), the human immunodeficiency virus (HIV) infects the brain [3]. HIV can be significantly reduced by highly active antiretroviral therapy (HAART) in the periphery, but the cocktail of small molecule drugs partially cannot penetrate the brain parenchyma, hampering HIV treatment if the virus settles down in the CNS of the patient [3, 4].

1.1.1 The shortage of brain medications

Transport of drugs to the brain is an exception rather than a rule: nearly 100 % of large molecule drugs and more than 98 % of small molecule drugs cannot gain access to the brain, leading to a very limited number of potential neuropharmaceuticals. Generally, only substances with a molecular mass less than 400-500 Da that form less than 8-10 hydrogen bonds in solvent water can diffuse to the brain in relevant amounts if no specific transport molecule is available. Also, the drug must not avidly bind to plasma proteins or be a substrate to the brain's efflux transporters [5]. Only very few CNS disorders (depression or schizophrenia) respond to drugs of this category (Figure 1A).

The brain seems to be fenced off from the rest of the body (as illustrated in Figure 1B). In the whole body autoradiogram of a mouse, sacrificed after intravenous injection of radiolabeled histamine, the CNS appears completely white; the overall rest of the body appears black and grey representing the amount of infused histamine (white areas in the abdomen represent air-filled intestinal loops). Whereas histamine (which only is approximately 100 Da in mass) perfused all capillaries in the periphery, it does not appear in the entire brain and spinal cord.

More than a century ago, Paul Ehrlich laid the foundation for the experiments leading to the discovery of the blood-brain barrier (BBB) by using trypan dyes [6, 7] that he originally developed in search of drugs against protozoa of the species *Trypanosoma*, which cause sleeping sickness (African trypanosomiasis). Peripheral injections of trypan dyes lead to staining of the whole body of laboratory animals – with exception of the brain (Figure 1C).

Edwin Goldman, systemically refined the experiments [7–9] and injected trypan blue in different animals (mice, rats, frogs, guinea pigs, rabbits, dogs and monkeys), and he also observed the same phenomenon. The dye distributed rapidly to the complete body with exception of the CNS. To rule out that this effect was due to a poor brain affinity, Goldman performed the correct verifying experiments and injected the dyes not only to the periphery, but to the cerebrospinal fluids of the animals' brains (Figure 1D). Vice versa, the CNS was stained, but not the body of the animal. He therefore proved that the distribution was independent from the dyes' affinity, but that the dyes were caught in either the blood or the brain compartment of the body – dependent on the injection site. The actual structures responsible for separating the blood and the brain could only be proved to exist by Reese and Karnovsky with the introduction of scanning electron microscopy in the 1960s [10].

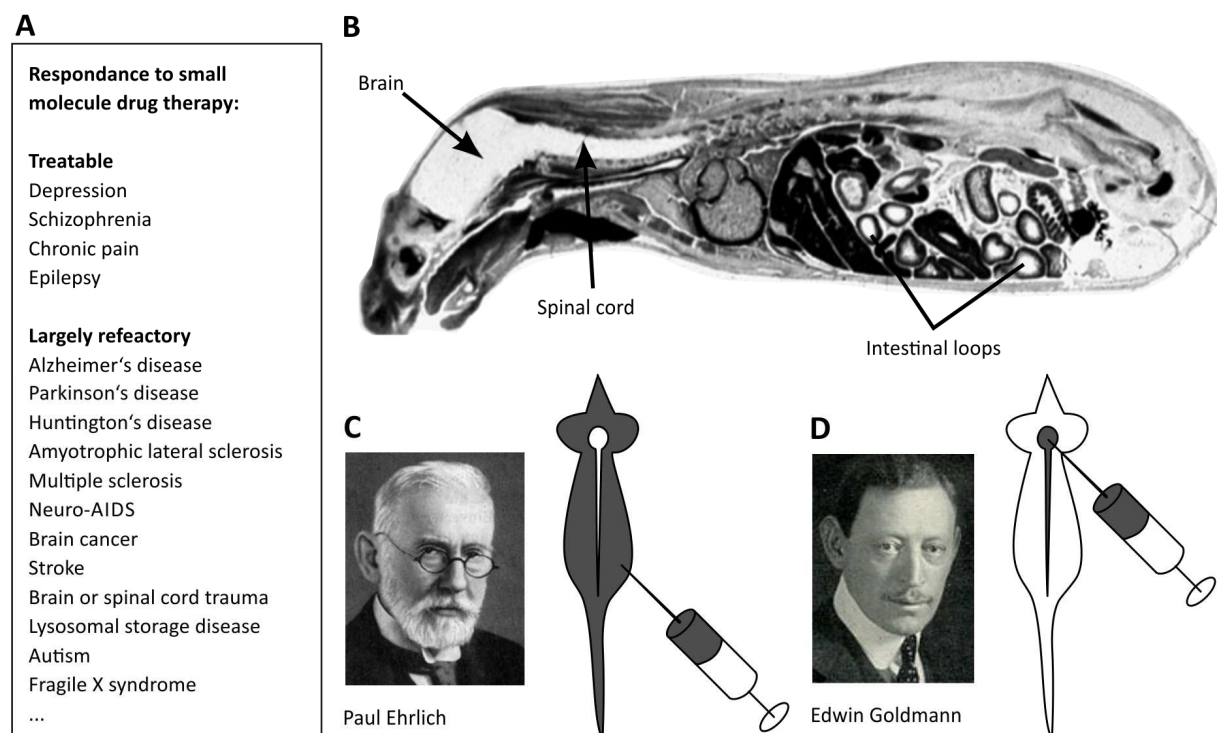


Figure 1: The blood-brain barrier restricts body distribution of substances. (A) Drug therapy for brain disorders is difficult, even with small molecule drugs (adapted and modified from Partridge [2]). Exceptions: L-dopa for Parkinson's disease and cytokines for multiple sclerosis can enter the brain. (B) Autoradiogram of a mouse 30 minutes after intravenous injection of radiolabeled histamine. No signal was detected in the central nervous system, but everywhere else in the periphery (adapted and modified from Partridge [2]). (C) Scheme of first experiment that hinted at the existence of such a barrier. Ehrlich developed trypan dyes that stained the periphery if injected into animals [6, 7]. (D) Goldman systematically refined the experiments [7–9]. Not only staining the periphery by intravenous dye application was feasible, but also the inversion of the experiment. Injecting dyes into the CNS only stained the brain and cerebral fluids. These data proved the existence of a barrier between blood and brain parenchyma.

1.1.2 The structure of the blood-brain barrier

Today we know that all higher organisms possess a blood-brain barrier (BBB) to maintain the unique and fragile homeostasis of a complex nervous system. A tight network of over 600 km of microvessels provides the human CNS with nutrients and exports toxic metabolites – nearly the linear distance between Hamburg and Munich (Figure 2A). Endothelial cells, growing on a basal lamina composed of collagen and laminine, line these cerebral microvessels and hence represent the barrier's cornerstones. Astrocytes (which cover more than 90 % of the capillary's surface), pericytes and neurons provide biochemical support via release of growth factors [11]. Together they are often called the "neurovascular unit" (Figure 2B).

The very specialized brain endothelial cells – distinct from most other endothelia in the body – connect with each other and form a **physical barrier** (Figure 2C). The foundations are transmembrane tight junction (TJ) proteins that seal the paracellular pathway and play a key role in maintaining barrier function. Without accurate tight junction protein expression, the cellular barrier lacks appropriate resistance and is permeable to various substances. The first identified tight junction protein was zonula occludens [12]. Later, occludin and the very important claudin group were shown to block the aqueous pathway and force most molecules to take the transcellular route [13, 14]. Claudin derives from the Latin word "claudere", meaning "to shut, to block".

Transcellular transport is highly regulated, thus resulting in a **transport barrier** (Figure 2C). Transporters on both sides of the endothelial layer import valuable nutrients and export noxious metabolites. Examples are glucose and amino acids that have their own transport system to maintain brain homeostasis: the brain only constitutes 2 % of body weight, but requires up to 20 % of the basal metabolism. Other valuable molecules are transported by receptor-mediated transcytosis: insulin, transferrin or apolipoproteins bind to their specific receptor protein at the BBB and are imported by clathrin-mediated endocytosis. This pathway leads to the formation of endosomes that are later acetated by proton pumps (and then are called lysosomes) before degradation. Another import process is adsorptive transcytosis: plasma proteins fuse with the plasma membrane of the endothelial cells due to their specific surface charge and are also transported across the barrier and released at the brain site.

Different enzymes in the brain parenchyma contribute to the **metabolic barrier** (Figure 2C) function: peptidases and nucleotidases outside of the cell can degrade peptides and adenosine triphosphate (ATP); monoamine oxidase (MAO) and members of the cytochrome P450 (CYP) family inside the cell inactivate many neuroactive and toxic compounds [15].

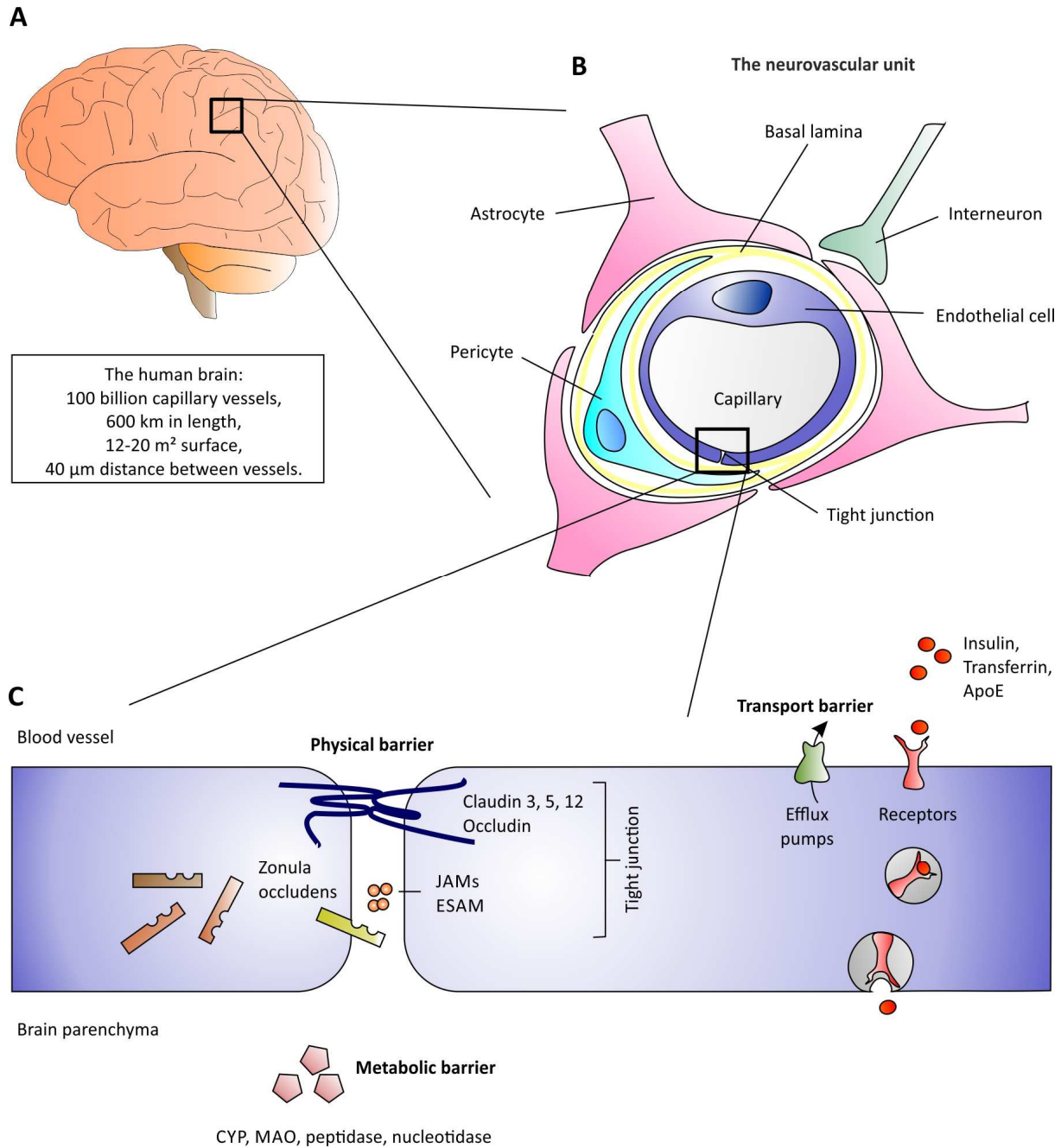


Figure 2: Simplified structure of the blood-brain barrier. (A) Schematic human brain that is lined with billions of blood capillary vessels, resulting in a remarkable large network. Brain data in the box from [2, 16–18]. (B) The neurovascular unit is composed of brain endothelial cells, basal lamina, pericytes, astrocytes and neurons. (C) Tight junctions seal the gaps between endothelial cells and represent the physical barrier. Efflux transporters (P-glycoprotein) possess many substrates that are exported if they cross the blood-brain barrier. Extra- and intracellular enzymes degrade a plethora of substances if they enter the brain parenchyma. JAM = Junctional adhesion molecules, ESAM = endothelial selective adhesion molecule, MAO = monoamine oxidase, CYP = cytochrome P450 (CYP1A and CYP2B). Modified after Abbott *et al.* [11].

1.1.3 *In vitro* models try to predict *in vivo* success

The BBB represents one of the most challenging hindrances in the body and therefore needs to be taken into account when trying to develop new CNS drugs. Today most of these studies are performed in laboratory animals, and consequently are expensive, labor intensive and under debate concerning ethical legitimation. Furthermore, it is often hard to choose or develop an appropriate animal model (transgenic or inbred strains, species variants). Generally, a robust, relatively simple, but still widely useable model is needed. Consequently, numerous *in vitro* models of the BBB emerged in order to complete and accelerate *in vivo* and human studies and to simplify the overwhelming complexity of this structure [19–21].

In vitro approaches have various advantages compared to animal studies:

- Less expense,
- High throughput for drug permeability experiments,
- Simplified working environment,
- Less variability,
- Higher reproducibility,
- Higher versatility (manipulating possibilities).

However, *in vitro* cellular models that aim at predicting permeability of drugs across the BBB need to fulfil certain criteria (summarized from Gumbleton and Audus [21]): First of all, the model must represent the permeability data for low (e.g., inulin or sucrose) and high (e.g., diazepam or propranolol) brain-penetrating substances, which can be set as an internal reference for the potential new CNS drug in debate. Secondly, the model must reflect the limited paracellular pathway, which forces substances to take the transcellular route across the BBB. Monitoring transendothelial electrical resistance (TER) indicates BBB integrity, but still provides only limited information regarding paracellular restriction. Thus, permeability studies with marker solutes are recommended. Thirdly, the model should possess a cell architecture that resembles the *in vivo* conditions, including morphology, cell-cell contacts, and expression of BBB relevant receptors, transporters and proteins. For nanoparticle-mediated drug transport studies, the expression of receptors that are capable of transcytosis is of utmost importance. Also, efflux pumps, most importantly P-gp, may have an enormous impact on BBB transit capacitance and therefore should be expressed accurately in an *in vitro* BBB model. Finally, a model ideally should allow easy handling and culturing, as well as high yield of cells for screening or high-throughput experiments. An immortalized cell line that stably expressed all abovementioned features would therefore be the optimal BBB model. However, until today, all brain endothelium cell lines failed to depict a realistically restricted paracellular pathway, drawing attention to primary cells as BBB model.

Immortalized brain endothelial cell lines are a very basic tool to mimic the BBB *in vitro*, advantages mainly comprise time and cost efficacy as well as low variability in experiments. Commonly used cell lines for BBB research are the murine bEnd3 [21, 22] and HBMEC [23], derived from human material. HBMEC was described as the most suitable human BBB model cell line, compared to 3 other cell lines, although HBMEC only expresses crucial proteins like claudin-5 or zonula occludens on a very low level [23]. Another disadvantage of cell lines is their low TER: bEnd3 cells exhibit TER values lower than $60 \Omega \cdot \text{cm}^2$ in general [21]; HBMEC display TER values lower than $50 \Omega \cdot \text{cm}^2$ in cell cultures [23].

Primary capillary endothelial cell cultures are a compromise between *in vivo* experiments and cell line based *in vitro* models, since BBB characteristics are generally better than in simple models (like bEnd3), but the experiments are not defined as animal studies. However, since yields of brain capillary endothelial cells from rodents are relatively low (e.g. 1-2 million cells per rat brain), large experimental setups need a vast amount of animals to be sacrificed, raising ethical concerns. Bovine (first described by Bowmann *et al.* [24]) and porcine species gained more and more attention as an alternative source for brain capillary endothelial cells, since cell yields are higher: for bovine material ~50 million viable cells per brain are reported [21]; the preparation protocol for porcine material used in this study usually results in 20-30 million cells per brain. Bovine models were widely neglected in Europe after bovine spongiform encephalopathy (BSE) appeared in the nineties, and the generation of porcine models was focused on, pioneered by the group of Galla [25]. TER of porcine BBB model used in this study can exceed $500 \Omega \cdot \text{cm}^2$ depending on the surface grown on [26, 27].

In vitro models were continually refined, and today range from static horizontal cell culture systems to advanced three dimensional (3D), flow-based cocultures [28–31]. For example, NDIV-BBB [28, 29], μ BBB [30] and SyM-BBB [31] take into account the blood flow through a 3D vessel construct to induce shear stress and limit sedimentation of samples to depict realistic local concentration of drugs, leading to better predictability of drug transport *in vivo*.

But all in all, regardless of all efforts made to optimize *in vitro* BBB models, mimicking the BBB on a cellular level is a challenging task and is associated with serious drawbacks as it is for any *in vitro* cellular model: cells cultivated *ex situ* lose their natural environment and lack external stimuli and physiological factors. They may modify expression of organ-specific, relevant features such as transporters, proteins and ligands which can lead to altered characteristics *in vitro*. Thus, *in vitro* findings always need to be verified within *in vivo* experiments.

1.1.4 Strategies for blood-brain barrier circumvention

Strategies to deliver drugs to the brain *in vivo* are rare and often appear rather harsh: One common invasive approach is, for example, to inject hyperosmolar mannitol solution within the carotid artery. The osmotic shock shrinks the cells and disrupts the intercellular connections, so that co-applied drugs can pass the endothelial cell layer. Also, ultrasonic sound waves are used to forcibly break down the blood-brain barrier [32]. These techniques are not specific and allow uncontrolled passage of drugs; adverse side effects may comprise changes in neuropathology, brain vasculopathy and seizures [33–37]. Even more radical is intraventricular injection of drugs or implantation of depots (Figure 3). *Ipsa facto*, these are brain surgery procedures with all associated risks like intracranial infections [38] or brain edema [39]. Furthermore, in the brain parenchyma the drug concentration decreases logarithmically with the diffusion distance, leading to a very low bioavailability even close to the injection site [2, 40, 41].

Non-invasive methods improve the treatment procedure, but they are rarely successful. The modification of drugs to improve blood-brain barrier crossing can lead to loss of function, whereas the intranasal application via the *nervus olfactorius* (a window in the blood-brain barrier) drastically decreases bioavailability [42]. Inhibition of efflux transporters (like P-glycoprotein) [43] allows some drugs to penetrate into the brain parenchyma, but entails severe, mostly intolerable adverse effects. A promising approach to combine the beneficial characteristics of non-invasive techniques is to use nanoparticles as drug carriers. Various studies showed that intravenous injection of drug-loaded nanoparticles can lead to drug release in the brain (for review see [39], also see 1.2.2): The nanoparticles can be transcytosed at the BBB by receptor-mediated pathways. The incorporated or adsorbed drug itself is not modified and can perform its original task after the particle matrix releases it into the brain.

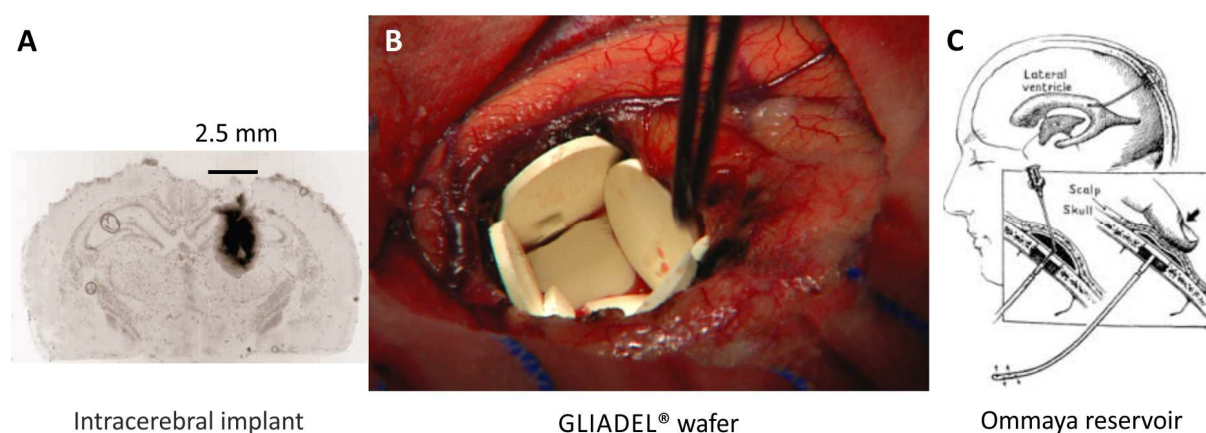


Figure 3: Invasive strategies for blood-brain barrier circumvention. (A) Intracerebral implant (2 mm disc with ^{125}I -labeled nerve growth factor (NGF)) releases the drug only at the local depot site (autoradiogram of rat brain). Adapted from Pardridge [44]. (B) Implantation of GLIADEL[®] wafers (polymer loaded with chemotherapeutics for the treatment of recurrent gliomas) during human brain surgery. Adapted from Lesniak and Brem [45]. (C) Ommaya reservoir allows intraventricular injection of drugs. Adapted and modified from Mehta *et al.* [46].

1.2 Nanotechnology: Promising approach for brain delivery

Pharmacology today faces the challenge of efficient drug transport and distribution to desired organs. The advantages are seductive compared to classical, non-targeted administration of drugs: Specific transport allows a higher therapeutic value at the desired site of action and reduces adverse side effects in the periphery, therefore being advantageous compared to classical, non-targeted administration of drugs. For the treatment of brain disorders, nanomaterials represent an interesting pharmacological tool to overcome the otherwise insurmountable structure of the blood-brain barrier. In brief, nanoparticles can act as molecular *Trojan horses* [47].

1.2.1 What are nanoparticles?

Nanotechnology is a versatile, advantageous and fast emerging biomedical field and a plethora of nano-sized formulations is being developed right now. For pharmaceutical purposes, nanoparticles are defined as solid, biodegradable colloids, with diameters ranging from 1 to 1,000 nm, and bearing drugs or other biologically active substances [48, 49]. Usually, nanoparticles intended for therapeutic approaches consist of at least two components: a basis polymer to form the particles and one pharmaceutically active substance that can be incorporated, adsorbed or chemically bound [49]. The preparation method depends on the basis material and can either be achieved by polymerization or dispersion processes. Natural macromolecules as basis material include human serum albumin (HSA), sodium alginate, chitosan or gelatin (for review of nanoparticle preparation see [50]). Common examples for synthetic, biocompatible polymers for nanoparticle preparation are poly(lactic acid) (PLA) and poly(glycolic acid) (PGA), or a copolymers from PLA and PGA, resulting in poly(lactic-co-glycolic acid) (PLGA) (Figure 4A), which are approved by the United States food and drug administration (FDA) [51–53] and frequently serve as basis material for nanoparticle preparation [54]. The human body metabolizes these polyesters into glycolic acid and lactic acid. These acids then are decomposed within the citric acid cycle to form water (H₂O) and carbon dioxide (CO₂), which explains their excellent biocompatibility [55]. Current examples of approved drugs that utilize PLA and PLGA as material for implants or microparticles are Trenantone [56] , Profact [57] or Zoladex [57].

For successful application in clinic, therapeutic nanoparticles are expected to be at least [39, 47, 49]:

- non-toxic
- non-immunogenic
- non-inflammatory
- preferentially biodegradable
- functionally targeted to desired bio-structures
- capable of prolonged circulation in the bloodstream

Regarding biomedical applications, the usage of nanoparticles may differ strongly despite preparative similarities. The desired function can either be a therapeutic effect of transported substances, the diagnosis of a disease state or molecular imaging in clinic or research. Drugs can be incorporated or conjugated to the surface of nanoparticles; detection molecules (contrast agents, radionuclides or fluorophores) can be added; and targeting structures (antibodies or ligands) can be coupled to the surface (Figure 4B) (for review see [58]). The biological stability of the biodegradable nanoparticles influences pharmacokinetics [54]: the drug release from nanoparticles can be altered by variation of size, basis material composition or coatings to allow a broad release profile ranging from immediate to retarded.

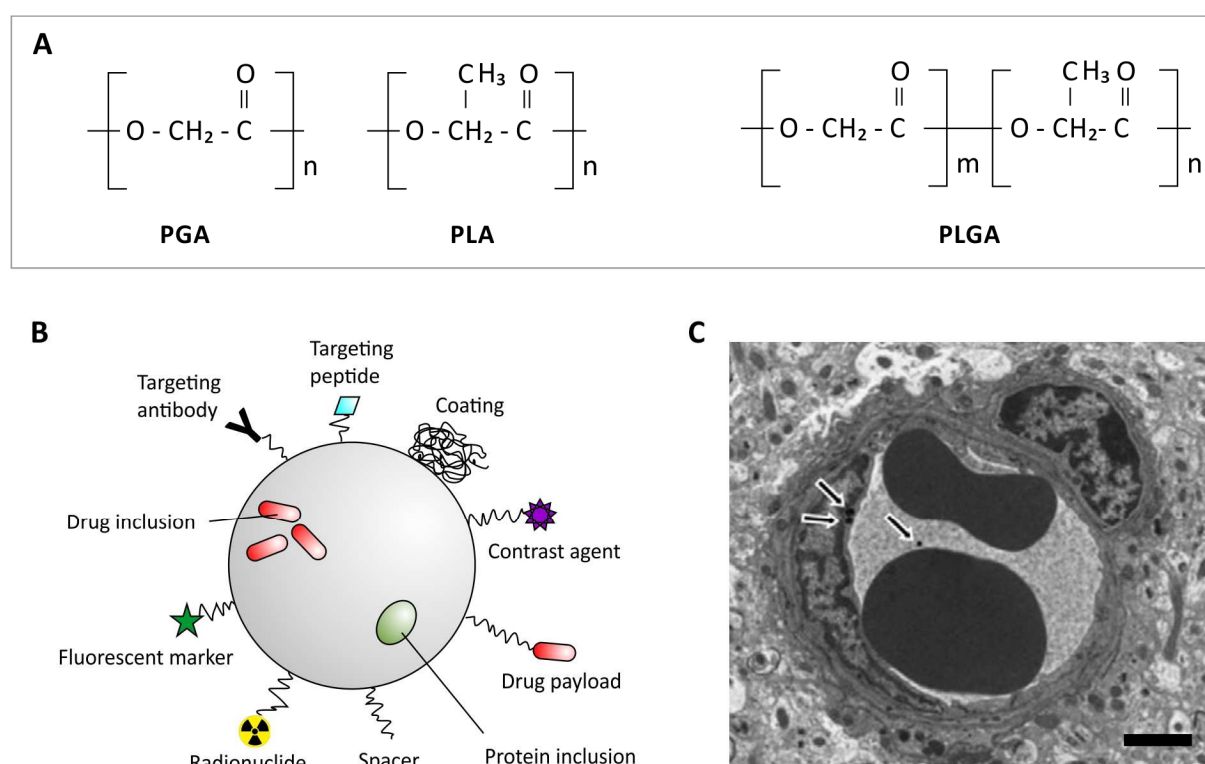


Figure 4: Nanoparticle basis materials and modifications for biomedical application. (A) Chemical structure of poly(glycolic acid) (PGA), poly(lactic acid) (PLA) and poly(lactic-co-glycolic acid) (PLGA). **(B)** A multi-functionalized nanoparticle can carry: Ligands for imaging (contrast agents for magnet resonance spectroscopy, radionuclides for positron emission tomography (PET) or single-photon emission computed tomography (SPECT)), shell coating for enhanced circulation time in the bloodstream (e.g. with poly ethylene glycol (PEG)), fluorescent markers for *in vitro* application, ligand-modification for targeted transport (e.g. peptides, antibodies). Drugs and proteins for therapeutic purposes can be bound to the surface of the nanoparticles or incorporated. Image adapted and modified from Re *et al.* [58]. **(C)** Nanoparticles can be targeted to bio-structures: mouse brain slice in electron microscopy, arrows indicate endocytosed nanoparticles in brain endothelial cells and nanoparticles in the blood stream after intravenous injection, scale bar 2 μm , reprinted from Zensi *et al.* [59].

1.2.2 Targeting nanoparticles to bio-structures

Body distribution

Nanoparticles are often injected intravenously to avoid the biological barriers of the gastrointestinal tract. However, after entering the bloodstream, they usually accumulate in organs of the reticulo-endothelial system (liver, spleen, lungs and bone marrow), and are thereby hindered in fulfilling their original purpose. Fortunately, targeting strategies to bio-structures exist. The next sections summarize the success of nanoparticles for brain targeting.

Brain targeting options

Nanoparticles are an elegant way to overcome the challenging blood-brain barrier with minimal invasive damage. By masking the original physico-chemical properties of a drug, nanoparticles allow transporting substances that could not enter the brain by themselves. The fundamental idea is that ligand-modified nanoparticles mimic biomolecules that have a specific receptor at the blood-brain barrier.

Guiding drug-loaded nanoparticles to the brain was first achieved by surfactants. Kreuter *et al.* [60, 61] and Schroeder *et al.* [62, 63] tested more than a dozen different surfactant coatings for nanoparticles that influenced BBB transit capability. Interestingly, incubating nanoparticles with polysorbate 80 (Tween®80) or poloxamer 188 (Pluronic® F-68) causes anchoring of lipoproteins from blood plasma [64, 65] or serum of the culture medium [39, 49, 66–68]. These lipoproteins, for example apolipoproteins E and/or A-I, adsorb to the nanoparticles' surface and can interact with receptors at the BBB, resulting in cellular uptake of the drug-loaded nanoparticles *in vitro* and *in vivo* [26, 47, 69–75].

A tangible example is loperamide, an opioid drug that cannot enter the brain and therefore has no analgesic effect. When loperamide-loaded nanoparticles are injected into mice, these animals become less sensitive in nociceptive experiments, proving drug transport to the brain. Kreuter *et al.* showed an analgesic effect of apolipoprotein-modified nanoparticles in nociceptive experiments in 2002 [66]. Later, Chen *et al.* [76] investigated the differences in brain transport capacity comparing loperamide-loaded PLGA-PEG-PLGA nanoparticles coated with either Tween®80 or Pluronic® F-68. Direct coupling of apolipoprotein onto the nanoparticles' surfaces to enable BBB crossing (Figure 4C), can even increase the effect compared to Tween®80-coated nanoparticles [77, 78].

The mechanism of nanoparticle uptake was proposed to be endo- and transcytosis mediated by receptors of the low density lipoprotein (LDL) receptor family [49, 60] (that is also expressed on BBB-forming endothelia [79, 80]). For example, Tween®80-coated PBCA nanoparticles were shown to be taken up by neuronal cells in *in vitro* primary cells, and the uptake could be blocked by LDLR antibodies [72].

Wagner *et al.* [81] further investigated the endocytosis processes and confirmed that ApoE-modified nanoparticles are actively transported via LDL receptor family members in *in vitro* experiments by using the receptor-associated protein (RAP). RAP blocks binding sites of most LDL receptor family members and after co-incubating RAP with ApoE-modified nanoparticles, binding capacity to BBB model cells was drastically reduced [81]. The prominent role of the LDL receptor related protein (LRP1) was highlighted by adding soluble purified LRP1 fragments when ApoE-modified nanoparticles were incubated on BBB model cells [81]. Binding to the cells was inhibited when fragments expressing the binding domain II or IV of LRP1 were added, verifying LRP1 involvement [81], because the domains (which are capable of binding numerous LPR1 ligands [82]) sequester the nanoparticles before they can bind to the cellular LRP1 receptors expressed on the BBB cells.

Present-day examples for compound-loaded nanoparticles for brain delivery are listed in Table 1, many of them focusing on brain tumors or pain management. Another hot topic is the treatment of neurodegenerative disorders.

Nanoparticles for Alzheimer's disease

Nanotechnology offers the chance to rethink drug treatment strategies that are ineffective due to their inability to transit the BBB. It suddenly seems possible to choose from a larger variety of substances in the anti-neurodegeneration drug development- but how could we use this new pharmacological tool? Which substances would stand a chance against dementia and Alzheimer's disease? Are there any treatment options right now that nanoparticles could improve? To answer these questions, we need to take a closer look at the nature of these diseases.

Table 1: Selected examples of drugs and substances bound to nanoparticles for brain delivery in *in vivo* studies. Adapted and modified from Li and Sabliov [83] and Wohlfart *et al.* [39].

Compound	Purpose	Basis material [#]	Surface modification [§]	Reference
Camptothecin	Anticancer drug	SLN	Pluronic [®] F 68	[84]
Dalargin	Analgesic drug	PBCA	Tween [®] 80	[61, 84]
Dexamethasone	Steroidal drug	PLGA	Alginate hydrogel	[85]
Doxorubicin	Anticancer drug	PBCA	Tween [®] 80	[86]
Etoposide	Anticancer drug	Tripalmitin	Without coating	[87]
FITC	Fluorescent marker	PLA	Tween [®] 80	[88]
Gemcitabine	Anticancer drug	PBCA	Tween [®] 80	[89]
Kyotorphin	Analgesic drug	PBCA	Tween [®] 80	[62]
Loperamide	Opiate receptor agonist	PBCA, HSA, PLGA	Tween [®] 80, ApoE3, ApoA1, ApoB100, (R)-g7 peptide	[78, 90, 91]
Methotrexate	Anticancer drug	PBCA	Tween [®] 80	[92]
Rivastigmine	Anti-Alzheimer's drug	PBCA	Tween [®] 80	[93]
Sulpiride	Atypical antipsychotic drug	PLA	Maleimide PEG	[94]
Tacrine	Anti-Alzheimer's drug	PBCA	Tween [®] 80	[95]
Tubocurarine	Muscle relaxants	PBCA	Tween [®] 80	[96]

[#]Abbreviations: SNL=solid lipid nanoparticles, PBCA=poly(butyl cyanoacrylate), PLGA=poly(lactic-co-glycolic acid), PLA=poly(lactic acid), HSA=human serum albumin. [§]Trade names: Tween[®]80=polysorbate 80, Pluronic[®] F 68=poloxamer 188.

1.3 Dementia and Alzheimer's disease: A rapidly growing problem

A long life expectancy accompanies an increased risk to develop dementia of the Alzheimer's disease type. On the one hand, the obstacle of the blood-brain barrier complicates treatment of neurodegenerative disorders. On the other hand, often the etiology and neuropathological processes are far from being understood - preventing the development of causal approaches.

1.3.1 Case numbers, prognosis and treatment options

Dementia is not a specific disease itself, but rather a collective term to depict symptoms like memory, communication and cognitive deficiencies [97] that are often responsible for disabilities in the elderly. The name derives from the Latin word *dementia* meaning *irrationality*.

Today, more than 46 million people in the world suffer from dementia (population numbers in 2015 for comparison: Colombia 48.2 million, Spain: 46.4 million [98]). The *World Alzheimer Report 2015* predicts that these numbers will almost double every 20 years [99] due to demographic changes (Figure 5A) and even corrected the estimates to be more than 10 % compared to the *World Alzheimer Report 2009*. Regarding global incidence, in 2015 over 9.9 million new cases will occur, meaning one new case every 3.2 seconds [99]. Up to 80 % of dementia cases are supposed to be caused by Alzheimer's disease (Figure 5B). The situation is expected to rapidly aggravate, because life expectancy immensely increased during the last century (Figure 5C) and age is the main risk factor for Alzheimer's disease [100, 101].

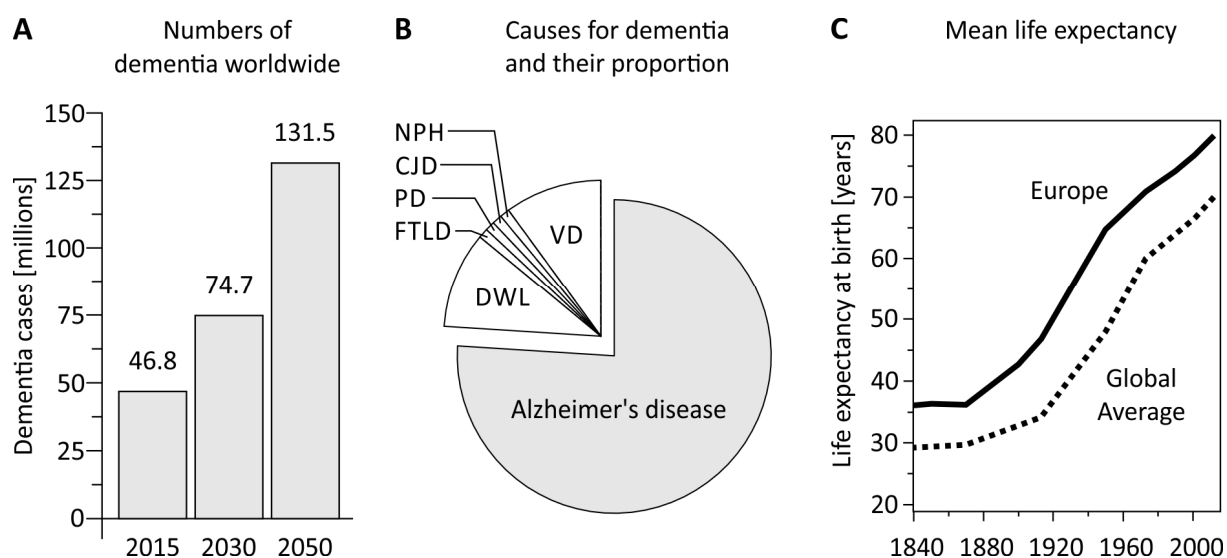


Figure 5: Dementia and Alzheimer's disease facts. (A) Estimated number of people suffering from dementia worldwide at different time points (data from *World Alzheimer Report 2015* [99]). (B) Causes and types of dementia displayed in percent of all dementia cases (data from *Alzheimer's Association* [97]). DWL=dementia with Lewy bodies, FTLD= frontotemporal lobar degeneration, PD= Parkinson's disease, CJD= Creutzfeldt-Jakob disease, NPH=normal pressure hydrocephalus, VD= vascular dementia. (C) Mean life expectancy for Europe and the world, data from Riley [102].

Mortality and Morbidity

Some Alzheimer's disease cases are not recognized for years, but once diagnosed, patients only live for an additional four to eight years on average [103, 104]. They do not die of the Alzheimer's symptoms themselves, but of the on-going loss of body functions as well as secondary infections like pneumonia. Death certificates often listed these acute conditions as the primary cause of death rather than the underlying Alzheimer's disease – even though later disease stages directly contribute to death by drastically promoting terminal conditions. Tinetti *et al.* reported that dementia was the second most important contribution to death after heart failure in the elderly [105]. Therefore, Alzheimer's disease is likely to cause more deaths than officially recorded, but already nowadays, it is the sixth-leading cause of death in the United States. Compared to other major diseases, deaths attributed to Alzheimer's disease drastically increased in recent years [97], reflecting various facts: a rise in the actual number of deaths attributed to Alzheimer's disease, better survival chances for other life threatening diseases and an improved reporting pattern for causes of death [97].

Are there any treatment options?

Unfortunately, nothing prevents or cures the cognitive degradation and constantly proceeding helplessness of Alzheimer's disease patients. Today, no causal therapy exists. Patients may only receive moderate symptomatic relief from three different acetylcholine esterase (AChE) inhibitors (donepezil, galantamine and rivastigmine) and one *N*-Methyl-D-aspartate (NMDA) receptor inhibitor (memantine) [106] that are on the market. Whether patients really benefit from these substances is highly controversial [107–109]. Attendant symptoms for cognitive impairment (like depression, schizophrenia and aggression) are commonly treated either pharmacologically or psychotherapeutically [106, 110, 111].

Recently, the development of causal, disease-modifying strategies has been in the focus of attention and many substances have advanced to clinical trials. Unfortunately, they failed eventually and did not stop or slow down cognitive decline in patients (for example [112]). In contrast to symptomatic improvement, these drugs are not expected to be efficient in a few months, complicating and increasing costs of clinical trials. Many believe that these drugs will not be beneficial to patients after the disease has already been recognized. Upon diagnosis of Alzheimer's disease, neuronal damage and synaptic dysfunction have already occurred and are unlikely to be reversible.

1.3.2 Discovery and neuropathology of Alzheimer's disease

What happens in the brain of an Alzheimer's disease patient? More than 100 years ago, Dr. Alois Alzheimer (Figure 6A) gave a remarkable lecture at a Psychiatrists Meeting in Tübingen, Germany [113]. He presented a case report of his former patient Auguste Deter (Figure 6B): she was severely demented and died at the early age of 55 at the Frankfurt Psychiatric Hospital. When Dr. Alzheimer autopsied her brain, he noticed aggregated plaques and neurofibrillary tangles. Surprisingly, the chairpersons and audience gave little attention to Alzheimer's topic. The next year, he published an article about Deter's case, called "Über eine eigenartige Erkrankung der Hirnrinde" [113–115]. His former mentor, Emil Kraepelin, noticed the significance of Alzheimer's findings, published a report in the 8th edition of his famous textbook *Psychiatrie* [116] and proposed the name *Alzheimer's disease* for the illness.

Today, pathologists reconfirm the two primary cardinal lesions that Alois Alzheimer found in Auguste Deter's brain. Firstly, extracellular plaques (Figure 6C, D) consisting of amyloid- β peptide ($A\beta$) that evolve after proteolytic cleavage of the amyloid precursor protein (APP) (described in detail in 1.3.3) and secondly, intracellular neurofibrillary tangles (NFTs) that consist of hyperphosphorylated τ protein leading to loss of synaptic function and eventually neuronal death [117]. Release of τ also triggers further neurodegeneration since it is neurotoxic itself [118]. During the course of the disease, neurons and synapses progressively perish (especially in the cortex and sub-cortex) [119]. Furthermore, the innate immune system responds with the activation of inflammatory processes in the diseased brain (for review see [120]) that can be advantageous in early stages, but promotes further neuronal cell death in late stages. Loss of brain mass compared to a non-diseased brain (Figure 6E, F) often is reported in the advanced disease stages of Alzheimer's disease [121]. It is very challenging to determine if one pathological structure described above "drives the disease, is a natural bystander or just represents an unsuccessful repair attempt" [122], especially in end stages of Alzheimer's disease when numerous biochemical pathways change and result in altered gene expression and protein levels compared to the healthy brain.

These massive alterations in severe Alzheimer's dementia obviously influence mental and physical health of affected patients. Deter's symptoms were typical for a late disease stage: She lost track of time and space, and could not remember where she put things. She could not remember details from her own history and gave answers that had no connection to the question. She increasingly lost language, visuospatial ("where-am-I") and behavioural skills [123] as well as became unsocial in her family life. Like the majority of patients in the advanced stages of the disease [124], she became completely helpless and lost muscle mass and mobility. Around 1905, Deter's condition worsened and she became confined to bed, was confused, incontinent and unable to feed herself [125].

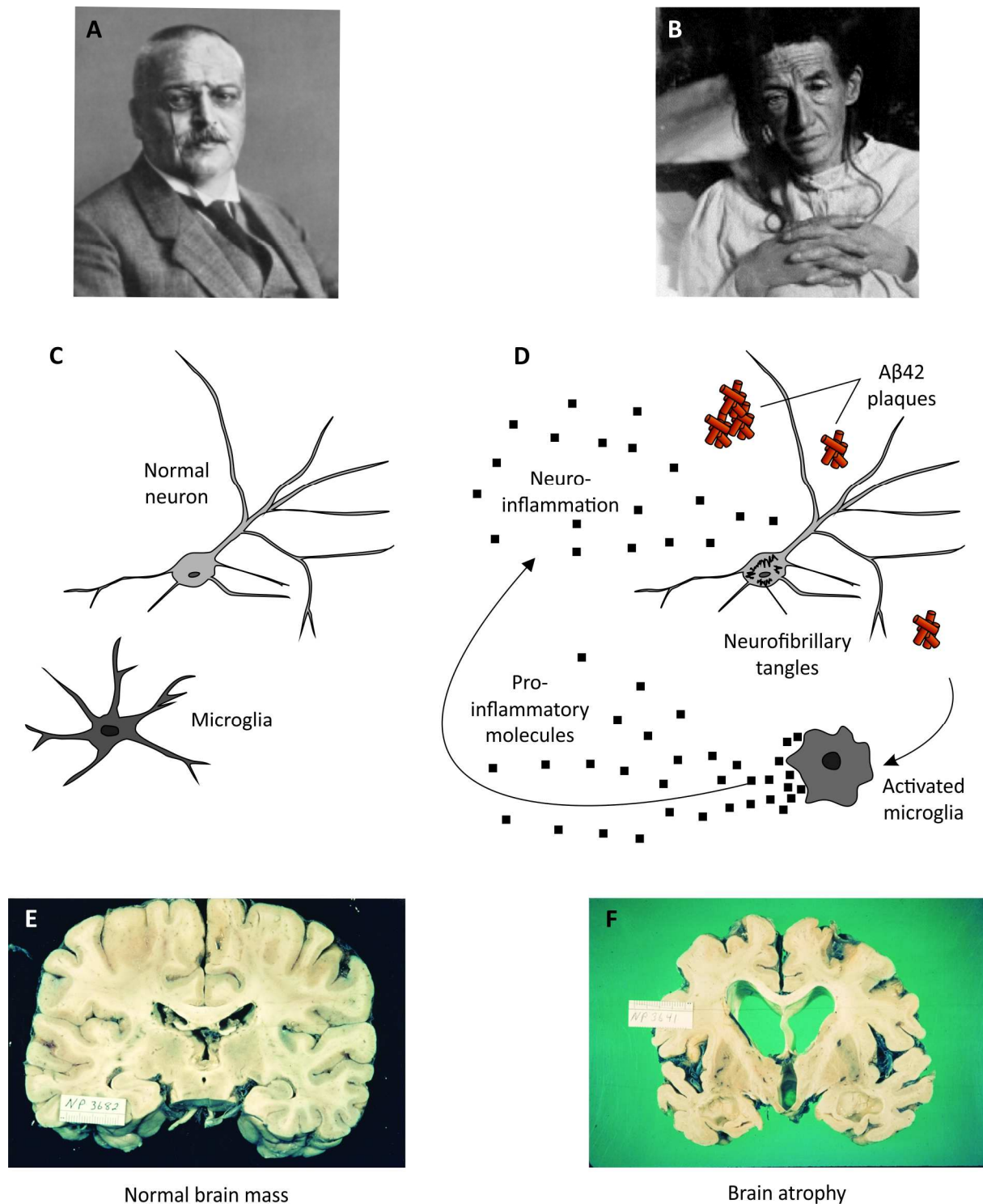


Figure 6: The discovery of Alzheimer's disease. (A) Alois Alzheimer, German neuropathologist and namesake of Alzheimer's disease, reprinted from Hippus and Neundörfer [113]. (B) The first person diagnosed with Alzheimer's disease, Auguste Deter, reprinted from Maurer *et al.* [126]. She died early (55 years old) after a secondary infection in 1906. Alzheimer post mortem investigated her brain and noticed severe abnormalities. (C-D) Schematic differences between a brain of a (C) healthy person and a (D) patient suffering from severe Alzheimer's disease. Notice the two cardinal findings that are characteristic for Alzheimer's disease: neurofibrillary tangles and senile plaques composed of A β peptide. Also, activated microglia release pro-inflammatory molecules, such as chemokines, interleukines and reactive oxygen species in the diseased brain. (E) Normal brain compared to a (F) brain from an Alzheimer's disease patient with diffuse atrophy in the cortex and enlargement of the ventricle. Brain atrophy indicates a dementia of the Alzheimer's type, but is not a clear diagnostic tool, images copied from Bird [127].

1.3.3 Etiology hypotheses of Alzheimer's disease

Why exactly people develop Alzheimer's disease is not elucidated up to today (except for an inherited variant with causal gene mutations [128–132]). Most likely, the disease is a consequence of multiple factors rather than one deciding cause. Age is the main risk factor as well as genetic predisposition exists, but many questions remain. Scientists continue to try to understand and explain Alzheimer's disease etiology. The first hypothesis was based on the loss of cholinergic activity in 1982 [133]. Today, the most common hypothesis, suggested by John Hardy and colleagues in 1991 [134], blames aggregated amyloid- β peptide plaques as a causal event in Alzheimer's disease. George Bartzokis questioned the amyloid hypothesis as the actual cause of Alzheimer's disease and proposed his myelin breakdown hypothesis [135, 136] in 2004 as a response (see below).

The cholinergic hypothesis

In Alzheimer's disease, levels of choline acetyltransferase (ChAT) and acetylcholine (ACh) (synthesized by ChAT) are low [133], which promotes the downfall of cholinergic neurons. This is expected to contribute to the disease, but is likely not a primary event in Alzheimer's disease development. It rather appears that deposition of amyloid plaques negatively affects cholinergic neurons and consequently lowers ACh synthesis, then (as a secondary event) resulting in further damages of cholinergic neurons and lower ACh receptor expression [133, 137–139]. Acetylcholine esterase (AChE) inhibitors target this effect in Alzheimer's disease therapy. By inhibiting the degrading enzyme, ACh concentration and duration are elevated, thereby easing the patients' symptoms in early and moderate disease stages.

The amyloid hypothesis

According to the widely postulated amyloid- β hypothesis [134, 140, 141], the accumulation of the neurotoxic A β plaques causes Alzheimer's disease, caused by either elevated A β 42 production in the diseased brain or by decreased physiologic A β 42 clearing processes. A β plaques derive from the amyloid precursor protein (APP) that is naturally expressed in the brain (Figure 7).

Special proteases – so-called α -, β - and γ -secretases - sequentially cleave the transmembrane APP and different APP fragments evolve. In the non-amyloidogenic pathway, α -secretase cleaving results in a soluble APP α fragment, which will not form plaques (Figure 7A). In the amyloidogenic pathway, consecutive cleaving of β - and γ -secretases occurs (Figure 7B). Firstly, β -secretase (also called BACE1) cuts off a soluble APP β fragment and leaves a 99 amino acid long fragment in the plasma membrane. Secondly, the γ -secretase cleaving leads to the neurotoxic peptide composed of 42 amino acids (A β 42), which is highly hydrophobic and tends to form complexes – resulting in the characteristic extracellular plaque formation (Figure 7B). Regulating secretase activity can therefore influence A β 42 burden: γ -secretase blockers reduce A β 42 level by complete enzyme inhibition, whereas γ -secretase

modulators elegantly promote a switch from A β 42 to A β 38 without affecting other important pathway, such as Notch (Figure 7C), a highly conserved, evolutionary ancient cell signaling pathway present in most multicellular organisms (for review see [142]).

The myelin breakdown hypothesis

Another model was postulated by Bartzokis in 2004 [135, 136]. He criticized that the amyloid hypothesis does not explain recent failures in clinical trials, when A β burden reduction failed to reduce cognitive decline. Bartzokis proposed that myelin (produced by oligodendrocytes) is involved in essential circuit functions and is especially vulnerable to damage, thereby promoting Alzheimer's disease. Hardy countered that the amyloid hypothesis was accurate, but that the damage after A β deposition already occurred, was irreversible [128].

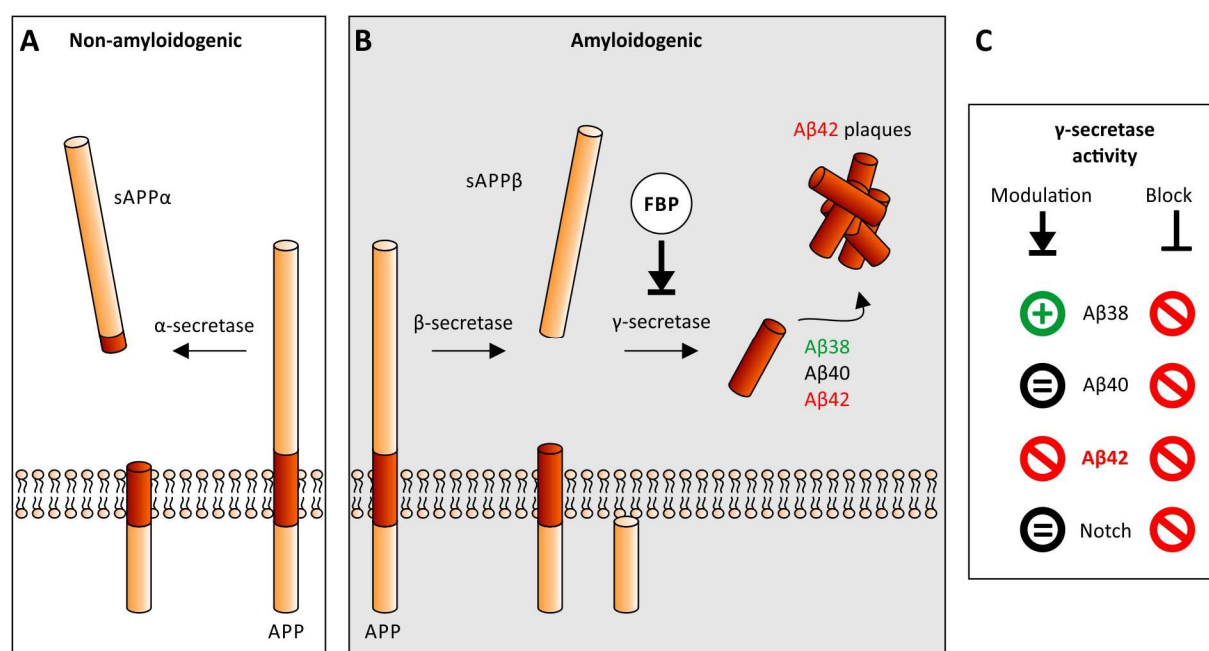


Figure 7: The molecular generation of A β plaques. (A) A β plaques derive when the amyloid precursor protein (APP), which is expressed in the healthy brain, undergoes a specific proteolytic pathway. Most of the APP is cleaved by α -secretase, leading to a non-toxic, soluble fragment (sAPP α) and a smaller fragment in the membrane (non-amyloidogenic). (B) The other cleaving pathway results in neurotoxic A β species: APP is first cleaved by β -secretase, which leaves a 99 amino acid long fragment in the membrane. In the next step, the γ -secretase complex cuts off the upper 38-43 amino acids, leading to the amyloidogenic A β 42. This A β species is highly hydrophobic and hence forms complexes (A β plaques). Flurbiprofen (FBP) and other non-steroidal anti-inflammatory drugs can modulate γ -secretase activity and therefore might be beneficial for Alzheimer's disease therapy. Adapted and modified from LaFerla *et al.* [143]. (C) γ -secretase activity can be pharmacologically regulated: while γ -secretase blockers result in decreases of A β 38, A β 40 and A β 42 production and a down regulated Notch pathway, γ -secretase modulators switch the preference from A β 42 to A β 38 without affecting A β 40 levels or Notch signaling (for further information see [144]).

1.3.4 Alzheimer's disease variants

Two variants of Alzheimer's disease exist: A rare, early onset familial variant caused by gene mutations and a much more common sporadic variant with no obvious cause:

Familial Alzheimer's disease

In the familial variant, causal mutations in APP processing genes facilitate the formation of neurotoxic A β species (Figure 7). Either the *APP* gene itself or γ -secretase-encoding genes (*PSEN-1* or *-2*) are mutated – both resulting in elevated A β 42 production. In the Swedish *APP* mutation variant (N/L670/671K/M), more A β 42 is produced because the β -secretase prefers the mutated APP variant, thereby favoring the amyloidogenic pathway [128–132]. Causal gene mutation cases only comprise up to 10 % of patients. A recent article reported that Auguste Deter was one of them. After exhumation of her body for genome analysis, a mutation associated with familial Alzheimer's disease was found [145].

Sporadic Alzheimer's disease

Far more patients (90-95 %) suffer from the sporadic variant with no obvious cause. The main risk factor is aging, but various other factors may have an impact (e.g., infections or cardiovascular diseases). In terms of genetics, genome-wide association studies revealed risk correlations [128], like variations in endosomal vesicle recycling genes [146, 147]. Also, altered cholesterol homeostasis can lead to AD, especially apolipoprotein E (ApoE) variations play a major role in incidence: People carrying one or two copies of the E4 allele of apolipoprotein E (ApoE4) have an increased risk compared to other isoforms (such as the most common variant ApoE3) [148]. In the central nervous system, ApoE serves as the major carrier for cholesterol, playing a key role in synaptogenesis and repair mechanisms, which may directly cause faster AD progression. Interestingly, the different ApoE isoforms differ in their cholesterol transport capacity – and ApoE4 is the least efficient. Other interesting relationships between cholesterol and Alzheimer's disease exists: intracellular cholesterol has been found to interfere with A β production [149] and A β can modulate cholesterol metabolism in the brain [150]. ApoE4 expressing cells also seem to be less effective in A β clearance and degradation and a negative effect in immunomodulation is suspected [151–154]. Furthermore, altered innate immune system responses [155] can increase the risk for AD [156, 157]: For example, fibrillary amyloid can bind to the complement factor C1 that activates the classical complement cascade [158, 159] promoting an inflammatory response. In addition, astroglia and microglia bear Toll-like receptors that recognize fibrillary amyloid. The role of these activated microglia can at the same time be beneficial (involved brain repair) and harmful (pro-inflammatory) [160–162]. Furthermore, variants in innate immunity genes can be a risk factor for Alzheimer's disease [155].

1.3.5 Alzheimer's disease risk reduction factors

A minority of people seems to have a considerably lower risk of Alzheimer's disease than the rest of the population: For example, a recent study reported of a natural *APP* gene mutation in a cohort of Icelanders that is associated with a lower risk for Alzheimer's disease and dementia [163]. Also nutrition factors, such as intake of long-chain Ω -3 polyunsaturated fatty acids, are debated to protect from Alzheimer's disease, but so far failed to be effective in clinical trials [164–167]. Even psychosocial factors (higher education, sports) are discussed to potentially lower the disease risk (for review see [168]). Remarkably, retrospective epidemiologic studies revealed that patients suffering from rheumatoid arthritis actually are less likely to develop Alzheimer's disease [169]. Apparently, their pain medication evokes a protective effect.

Painkillers against Alzheimer's disease?

Patients affected with rheumatism receive high doses of non-steroidal anti-inflammatory drugs (NSAIDs) for a long period. Numerous epidemiologic studies suggested that a sustained intake of NSAIDs during the therapy of rheumatoid arthritis reduced the risk of developing Alzheimer's disease [169]. Consequently, NSAIDs were proposed for the treatment and prevention of Alzheimer's disease nearly 25 years ago [170]. Scientists believed that NSAIDs either were beneficial due to their anti-inflammatory properties or because they might directly target the amyloid processing [171–173]. In fact, NSAIDs are able to lower neurotoxic $A\beta$ species [174, 175] by modulating γ -secretase activity (Figure 7C). For example, sulindac sulphide, ibuprofen and indomethacin were shown to lower neurotoxic $A\beta_{42}$ production *in vitro* and *in vivo* rodent models [174, 175].

The flurbiprofen failure

Another promising NSAID candidate for Alzheimer's treatment was flurbiprofen (FBP). The enantiomer of the racemic mother molecule R-flurbiprofen (Tarenflurbil, FlurizanTM) can lower $A\beta_{42}$ species *in vitro* [176–178] (Figure 7C), but elegantly lost its influence on the cyclooxygenases (COX) 1 and 2. This feature was sought for in order to reduce the classical severe side effects mediated by COX activity alteration during high dose NSAID therapy.

For several years, *Myriad Genetics* (an American molecular diagnostic company) conducted research and clinical trials to investigate R-flurbiprofen's potency for Alzheimer disease therapy, but discontinued the development in 2008 [179–181]. R-flurbiprofen still showed some benefits in a phase II clinical trial for patients with mild Alzheimer's disease, but failed in a phase III clinical trial, because it did not significantly improve patients' thinking ability or influenced daily activities [182–184].

Flurbiprofen (like many other NSAIDs) only poorly distributes to the brain parenchyma and hence may have failed to reduce A β 42 in a satisfactory quantity *in vivo*. Although the substance is fairly lipophilic and consequently is expected to readily cross the BBB, distribution in the CNS is limited, because flurbiprofen tightly binds to plasma proteins [185]. Therefore, availability of flurbiprofen in the brain – if applied in low to moderate doses - is very restricted, potentially prohibiting a neuroprotective effect regarding Alzheimer's disease pathology. In fact, only >5 % of applied acidic NSAIDs (ibuprofen, flurbiprofen, ketoprofen, naproxen) reach the brain or the cerebrospinal fluid (CSF) [177, 185–188]. *In vitro* experiments suggest that flurbiprofen efficiently decreases amyloid burden in cellular Alzheimer's disease models at concentrations of 50 μ M and higher [68, 172]. In contrast, less than 1.5 μ M of ibuprofen or flurbiprofen is achieved at normal plasma concentration in *in vivo* experiments [185–188]. Higher doses (as given in rheumatoid arthritis) would be required to achieve a desired NSAID effect in the brain in patients, but the severe gastrointestinal side effects and toxicity rules out high dose treatment.

Therefore, it is desired to improve the NSAIDs' bioavailability in the brain in order to increase a potential therapeutic effect while reducing peripheral doses and associated side effects. Packing flurbiprofen into nanoparticles is expected to increase brain distribution by reducing plasma protein binding and masking the physicochemical characteristics of the drug. Nanoparticle-mediated brain transport has been shown to be effective in various cases, and can be further optimized by specific ligand coupling to even increase active nanoparticle uptake mechanisms.

2 AIM OF THIS THESIS

Brain drug development is a highly complex task, regarding that the vast majority of substances cannot cross the blood-brain barrier (BBB) *in vivo*. Unfortunately, many of the *in vitro* models of the BBB – originally intended to facilitate brain drug development – actually rather confuse the situation, because they often do not reflect the insurmountable obstacle of the BBB. By being more permeable than the *in vivo* BBB, unsuited *in vitro* BBB models lead to a plethora of false positive brain drug candidates. Therefore, a great need exists for reliable *in vitro* screening methods in order to predict BBB crossing capacity. Thus, substances that show little promise for *in vivo* success could be better identified and the enormous expenses of further investigation could be restricted.

This thesis aims at identifying and investigating an *in vitro* model that displays excellent barrier qualities. Nevertheless, the *in vitro* model is supposed to be only moderately complex in order to allow high-throughput approaches for pharmaceutical industries in the long term. Here, primary brain material from the domestic pig *Sus scrofa* was selected, because it is expected to be advantageous for BBB model formation compared to a cell-line based approach for various reasons, including high genetic comparability to humans and large availability from slaughter processes intended for food production. The suitability of the model was intended to be assessed by state-of-the-art techniques, such as investigating the expression of essential tight junction proteins and BBB-relevant receptors, defining transendothelial electrical resistance and determining the permeability capacitance of radiolabeled marker substances across the barrier.

After verifying a proper barrier function of the *in vitro* model, this thesis intends to address the question: *Are nanoparticles a potential tool to allow transport of drugs that could not enter the brain by themselves?* Specifically, this work should focus on the non-steroidal anti-inflammatory drug (NSAID) flurbiprofen. Flurbiprofen was proposed as an anti-Alzheimer's disease drug, because it showed promising results in A β 42 reduction *in vitro* and *in vivo* experiments and nevertheless failed in clinical trials, probably due to its poor distribution to the CNS. This study aims at revisiting the drug by incorporating it into nanoparticles for BBB transit. Various nanoparticular characteristics, such as influence on the barrier formation, the viability or integrity of BBB model cells should be investigated in this thesis. The actual drug transport capacity of the nanoparticles and, eventually, the ability to reduce A β 42 should be assessed, and possibly increased by optimizing the nanoparticular formulations by surface modifications or adjusting the choice of basis material to influence drug release profiles.

In addition, this work aims at discussing to what extent other diseases could profit from NSAID-loaded nanoparticles and which other pathways could causally be targeted in Alzheimer's disease pathology, benefitting from nanotechnology.

3 EXPERIMENTAL PROCEDURES

3.1 Materials

Utensils and consumables

Item	Supplier
CELLSTAR® aspirating pipettes	Greiner Bio-One, Frickenhausen, Germany
CELLSTAR® cell culture flasks	Greiner Bio-One, Frickenhausen, Germany
CELLSTAR® multiwell culture plates	Greiner Bio-One, Frickenhausen, Germany
CELLSTAR® serological pipettes, div. sizes	Greiner Bio-One, Frickenhausen, Germany
Culture slides, glass, div. sizes	BD Bioscience, Heidelberg, Germany
FACS tubes (Polystyrene, Round-Bottom Tube)	Becton Dickinson, Heidelberg, Germany
Microscopy chamber	ibidi, Martinsried, Germany
Plastic scintillation vials	PerkinElmer, Boston, USA
Storage bottles, polystyrene, div. sizes	Corning, Wiesbaden, Germany
Transwell® inserts (3 µm and 0.4 µm pore size)	Corning, Wiesbaden, Germany
VACUETTE® EDTA Tubes	Greiner Bio-One, Frickenhausen, Germany
Vacuum filtration system	TPP, Trasadingen, Switzerland
Verex™ HPLC vials	Phenomenex, Aschaffenburg, Germany

Antibodies

Primary antibodies			
Name	Antigen	Host	Supplier
Anti-ApoA4	Apolipoprotein A4 (ApoA4)	Mouse	Cell Signaling, Boston, USA
Anti-ApoE3	Apolipoprotein E3 (ApoE3)	Mouse	Cell Signaling, Boston, USA
Anti-ApoER	Apolipoprotein E Receptor (ApoER)	Mouse	Acris, Herford, Germany
Anti-Cld-3	Claudin 3 (Cld-3)	Rabbit	abcam, Cambridge, UK
Anti-Cld-5	Claudin 5 (Cld-5)	Rabbit	abcam, Cambridge, UK
Anti-LDLR	LDL Receptor (LDLR)	Rabbit	abcam, Cambridge, UK
Anti-LRP1	Low Density Lipoprotein Receptor-related Protein 1 (LRP1)	Mouse	Kind gift from C. Pietrzik, Mainz
Anti-LRP2	Low Density Lipoprotein Receptor-related Protein 2 (LRP2)	Mouse	abcam, Cambridge, UK
Anti-Occl	Occludin (Occl)	Rabbit	abcam, Cambridge, UK
Anti-ZO-1	Zonula occludens (ZO-1)	Rabbit	ZYTOMED, Berlin, Germany

Secondary antibodies			
Name	Conjugation	Isotype	Supplier
Goat Anti-Mouse	Alexa Fluor® 488	IgG	Invitrogen, Molecular Probes, Eugene, USA
Goat Anti-Rabbit	Alexa Fluor® 488	IgG	Invitrogen, Molecular Probes, Eugene, USA
Rabbit-Anti-Mouse	Horseradish peroxidase	IgG	Santa Cruz, Dallas, USA

Spectra data of dyes and conjugates

	Excitation [nm]	Emission [nm]
Alexa Fluor® 488	495	519
CellTracker™ Blue CMAC	353	466
CellTracker™ Red CMTPX	577	602
DAPI	358	461
Lumogen® F Orange 240	524	539
PromoFluor-488 Premium	490	516
PromoFluor-633	635	658

Chemicals, biologicals and kits

Item	Supplier
¹⁴ C-diazepam	Hartmann Analytic, Braunschweig, Germany
¹⁴ C-inulin	PerkinElmer, Boston, USA
Acetonitrile	Sigma-Aldrich, Steinheim, Germany
AESBF	Sigma-Aldrich, Steinheim, Germany
alamarBlue® cell viability assay reagent	Invitrogen, Karlsruhe, Germany
ApoE3 human recombinant, expressed in E. coli	Sigma-Aldrich, Steinheim, Germany
Aqua ad iniectabilia	Berlin-Chemie, Berlin, Germany
Aβ42 human ELISA Kit	Life Technologies, Darmstadt, Germany
BD Cytofix/Cytoperm™ Kit	BD Biosciences, San Diego, USA
Bovine Serum Albumin	PAA Laboratories, Pasching, Germany
Carboxy-(PEG)4-amine	Thermo, Langensfeld, Germany
CellTracker™ Blue CMAC and Red CMTPX	Invitrogen, Karlsruhe, Germany
Collagen from human placenta, type IV	Sigma-Aldrich, Steinheim, Germany
Collagenase	Biochrom, Berlin, Germany
Dichloromethane	Sigma-Aldrich, Steinheim, Germany
Dispase® II (neutral protease, grade II)	Roche Diagnostics, Mannheim, Germany
Coomassie Brilliant Blue R-250	Bio-Rad Laboratories, Munich, Germany
Divinylsulfone	Sigma-Aldrich, Steinheim, Germany
DMEM/F-12	Invitrogen, Karlsruhe, Germany
DNase	Roche Diagnostics, Mannheim, Germany
EasyColl Separating Solution	Biochrom, Berlin, Germany
EDC	AppliChem, Darmstadt, Germany
Ethyl acetate	Sigma-Aldrich, Steinheim, Germany
FACS-Flow, -Clean, -Rinse	Becton Dickinson, Heidelberg, Germany
Fetal Bovine Serum	Sigma-Aldrich, Steinheim, Germany
Fetal Bovine Serum Gold	PAA Laboratories, Pasching, Austria
Flurbiprofen	Sigma-Aldrich, Steinheim, Germany
Geneticin®	Invitrogen, Karlsruhe, Germany
Gentamicin	Invitrogen, Karlsruhe, Germany
HEPES	Invitrogen, Karlsruhe, Germany
Hydrocortisone solution	Sigma-Aldrich, Steinheim, Germany
L-glutamine	Invitrogen, Karlsruhe, Germany
Lumogen® F Orange 240	BASF, Ludwigshafen, Germany
M199	Invitrogen, Karlsruhe, Germany
MANNIT 20 %, mannitol solution	Serag-Wiessner, Naila, Germany
MEM NEAA	Invitrogen, Karlsruhe, Germany
MEM Vitamins	Invitrogen, Karlsruhe, Germany
Newborn Calf Serum	Biochrom, Berlin, Germany
N-hydroxysulfoxuccinimide	Sigma-Aldrich, Steinheim, Germany
Nu-Serum™ IV	BD Biosciences, Heidelberg, Germany
Ovalbumin from hen egg white	Sigma-Aldrich, Steinheim, Germany
Paraformaldehyde	Sigma-Aldrich, Steinheim, Germany
Penicillin-Streptomycin	Invitrogen, Karlsruhe, Germany
Phosphate buffered saline	Invitrogen, Karlsruhe, Germany
Phosphate buffered saline, pH 7.2	Invitrogen, Karlsruhe, Germany
Poly(lactic acid) (PLA)	Sigma-Aldrich, Steinheim, Germany
Polyvinyl alcohol (PVA)	Sigma-Aldrich, Steinheim, Germany
Potassium chloride solution (0.075 M)	Sigma-Aldrich, Steinheim, Germany
PromoFluor-488 Premium Labeling Kit	PromoCell, Heidelberg, Germany
PromoFluor-633 Labeling Kit	PromoCell, Heidelberg, Germany
Protein Assay	Bio-Rad Laboratories, Munich, Germany
RESOMER® RG502H and RG752H	Evonik Industries, Essen, Germany
Sodium chloride	Sigma-Aldrich, Steinheim, Germany
Solvable™	PerkinElmer, Boston, USA
Trifluoroacetic acid	Sigma-Aldrich, Steinheim, Germany
Trypsin EDTA	Invitrogen, Karlsruhe, Germany
Tween®80	Sigma-Aldrich, Steinheim, Germany
Ultima Gold, Scintillation fluid	PerkinElmer, Boston, USA
VECTASHIELD® Hard Set™ mounting medium (+/- DAPI)	Vector Laboratories, Burlingame, USA

Software

Software	Provider
CellQuest Pro	Becton Dickinson, Heidelberg, Germany
cellZscope® 2.1.2	nanoAnalytics, Münster, Germany
ChemStation® 1.7	Agilent Technologies, Waldbronn, Germany
CorelDRAW® Graphics X6	Corel Corporation, Ottawa, Canada
Leica Application Suite X (LAS X)	Leica Microsystem, Heidelberg, Germany
Microsoft Office 2010 & 2013	Microsoft Corporation, Redmond, USA
OriginPro 9.1G	OriginLab Corporation, Northampton, USA
QuantaSmart software	PerkinElmer, Boston, USA
Zeiss ZEN 2009	Zeiss, Jena, Germany

Hardware

Item	Supplier
Agilent 1200 and 1260 Infinity HPLC device	Agilent Technologies, Waldbronn, Germany
Analytical balance CP64	Sartorius, Göppingen, Germany
Biofuge stratos	Heraeus, Hanau, Germany
CASY® Cell Counter + Analyzer System	OLS OMNI Life Science, Bremen, Germany
CC-12 camera	Soft imaging systems, Münster, Germany
cellZscope® device	nanoAnalytics, Münster, Germany
Centrifuge 3K18	Sigma Laboratory Centrifuges, Osterode am Harz, Germany
Centrifuge 5810R	Eppendorf, Hamburg, Germany
Centrifuge Biofuge Pico	Thermo Scientific, Langenselbold, Germany
Centrifuge Biofuge R	Thermo Scientific, Langenselbold, Germany
Dispersion tools S25N-10G and S25NK-19G	Ultra Turrax®, IKA, Staufen, Germany
Excitation light source, mercury lamp X-Cite®, series 120	Lumen Dynamics Group Inc., Mississauga, Canada
Flow cytometer FACS Calibur	Becton Dickinson, Heidelberg, Germany
Gemini® NX 250-C18 column	Phenomenex, Aschaffenburg, Germany
Heraeus® BBD6220 Incubators	Thermo Scientific, Langenselbold, Germany
Leica TCS SP8 confocal microscope	Leica Microsystem, Heidelberg, Germany
Microscopes CKX31 and IX70	Olympus, Hamburg, Germany
Mini centrifuge	Biozym Scientific, Hessisch Oldendorf, Germany
Poroshell 120 EC-C18 column	Agilent Technologies, Waldbronn, Germany
Poroshell 120 UHPLC Guard EC-C18 Pre-column	Agilent Technologies, Waldbronn, Germany
TECAN infinite® 200 microplate reader	Tecan Group, Maennedorf, Switzerland
Tri-Carb 2910TR, liquid scintillation counter	PerkinElmer, Boston, USA
TSKgel Super SW3000 column	Tosoh Bioscience, Stuttgart, Germany
Ultra Turrax® device T25 digital	Ultra Turrax®, IKA, Staufen, Germany
Zeiss LSM 510 confocal microscope	Zeiss, Jena, Germany
Zetasizer PN3702	Malvern Instruments, Malvern, UK

Origin of cell lines and primary cells

Cells	Type	Biological source	Provider
7WD10	Human APP gene transfected cell line	<i>Cricetulus griseus</i>	Kind gift from Claus Pietrzik, Institute for Pathobiochemistry, Mainz University, Germany
bEnd3	Polyoma middle T antigen transformed brain endothelioma cells	<i>Mus musculus</i>	LGC Promochem, Wesel, Germany
HBMEC	SV-40 transfected human brain microvascular endothelial cells	<i>Homo sapiens</i>	Kind gift from Kwang Sik Kim, Division of Pediatric Infectious Diseases, Johns Hopkins University School of Medicine, Baltimore, USA
pBCEC	Primary porcine brain capillary endothelial cells	<i>Sus scrofa domestica</i>	Freshly prepared from primary material from local slaughterhouse (Zweibrücken, Germany)

Media composition & coatings for cell culture

Medium stocks were prepared in a maximum volume of 500 ml, only small volumes were pre-heated to 37 °C prior to use in cell culture. All basis media were obtained from Gibco®, Life Technologies. Fetal calf serum was obtained from PAA or Sigma-Aldrich.

Growth surfaces for endothelial cells (pBCEC, bEnd3, HBMEC) were pre-coated with 0.1 mg/ml collagen type IV from human placenta in 0.25 % acetic acid / PBS (1:4). A total of 180 µl/cm² of this solution was incubated for 2 hours at 37 °C, washed with PBS and cells were seeded when the growth surfaces were still moist.

Cell type	Basis (Cat. No. Gibco®) medium	Sera	Antibiotics	Additives
7WD10	MEM α (22571)	10 % FCS	1 % Pen/Strep 400 µg/ml Geneticin®	
bEnd3	DMEM (41965)	10 % FCS		
HBMEC	RPMI 1640 (21875)	10 % FCS 10 % Nu-Serum	1 % Pen/Strep	2 mM L-glutamine 1 mM sodium pyruvate 1x MEM NEAA 1x MEM Vitamins
pBCEC 1 st	M199 (31150)	10 % NCS	1 % Pen/Strep 1 % Gentamycin	0.7 mM L-glutamine
pBCEC 2 nd	DMEM/F-12 (11039)	0 or 5 % FCS	1 % Pen/Strep 1 % Gentamycin	1.5 mM L-glutamine 550 nM hydrocortisone

3.2 Methods

3.2.1 Cell culture

All cell culture work was performed under sterile conditions to avoid contamination with bacteria, fungi or other microorganisms. Consumable materials and reagents were either sterilized by the supplier or autoclaved, ethanol-sterilized or sterile-filtered prior to use. All applied chemicals were of highest purity. Mycoplasma contamination of cell lines was tested for in frequent intervals.

Cultivation of cell lines

Endothelial cell lines of murine and human origin (bEnd3, HBMEC) were cultured at 37 °C, 5 % CO₂ and 95 % relative air humidity in an incubator. For splitting, cells were washed with PBS and incubated with trypsin-EDTA (0.5 %) until more than 90 % of the cells detached. Addition of culture medium inhibited the trypsin effect and rinsed off the remaining cells. After centrifugation, the cell sediment was resuspended in medium and cultured accordingly to further application. bEnd3 and HBMEC were allowed to reach confluence before splitting and seeding.

Isolation and cultivation of primary porcine brain capillary endothelial cells

Primary porcine brain capillary endothelial cells (pBCEC) were dissected following a protocol of Wagner *et al.* [26]. Directly after slaughtering fresh porcine skulls from *Sus scrofa domestica* (Figure 8A) were kindly provided by the local slaughterhouse in Zweibrücken, Germany. Slaughtering occurred in accordance with the guideline 93/119/EC of the European Community on the protection of animals at the time of slaughter or killing from 22.12.1993. At the Fraunhofer IBMT, skulls were sprayed with disinfecting agent and the skullcap was removed (Figure 8B) to prepare cerebral tissue. The outermost layers of the meninges (*Dura mater* and *Arachnoidea mater*) were removed. The brain was carefully detached from the brainstem (*Truncus encephali*) and transferred to a transport buffer. All following steps were performed under sterile conditions in an airflow hood. The remaining meningeal membrane (*Pia mater*) and major blood vessels were stripped off (Figure 8C) and the grey matter was collected and minced into pieces (Figure 8D). For homogenization and release of capillary fragments, the gray matter was digested with the same volume of dispase II solution at 37 °C for 70 minutes under stirring. Afterwards, the capillary fragments were divided from the connective tissue with the aid of a discontinuous density gradient (30 min, 4 °C, and 822 g, without brake) (Figure 8E). The fatty supernatant was removed after centrifugation and capillary fragments were transferred to fresh medium. After centrifugation (20 min, 4 °C, 235 g) to wash out remaining percoll, the cells were digested in collagenase II solution (20 min, 37 °C, 150 rpm on a shaking incubator) with frequent resuspensions. This step allows separation of brain capillary cells from non-endothelial tissue, because

collagenase II segregates intercellular connections and the basal lamina. Subsequently, DNase was added at 37 °C for 3 minutes to prevent clumping of capillary fragments due to unleashed DNA. Next, the cell suspension was filtered with the aid of a cell strainer (70 µm pore size) in order to discard larger undigested microvascular capillary fragments and to singularize cells. After centrifugation (10 min, 4 °C, 376 *g*) the cell pellet was resuspended in 1 ml DMEM and transferred onto a continuous density gradient (20 min, 10 °C, 312 *g*, no brake), that was freshly prepared (45 min, 21 °C, 14,500 *g*, no brake). This second density gradient allowed separation of brain capillary endothelial cells from other cells and permitted a homogenous, pure cell culture. The upper fraction containing the pBCEC was collected and transferred to PBS for centrifugation (10 min, 4 °C, 258 *g*). To remove remaining erythrocytes, the pellet was resuspended twice in 1 ml erythrocyte lysis buffer and subsequently centrifuged (5 min, 4 °C, 165 *g*) (Figure 8F). Finally, the cells were washed two times in DMEM and resuspended in a medium containing 10 % newborn calf serum (pBCEC 1st) for counting and seeding.

After Isolation, pBCEC were plated at a density of 3.5×10^6 cells/cm² on collagen IV-coated surfaces. To remove unattached cells and debris, a medium exchange was performed 1 hour after the initial seeding. Approximately 24 hours after seeding, the medium was changed to hydrocortisone-containing medium (pBCEC 2nd) in order to support transendothelial electrical resistance (TER) development of the confluent monolayer, unless otherwise stated. pBCEC were not passaged and used for further experiments within 1 week after isolation, usually after 4 to 5 days in culture.

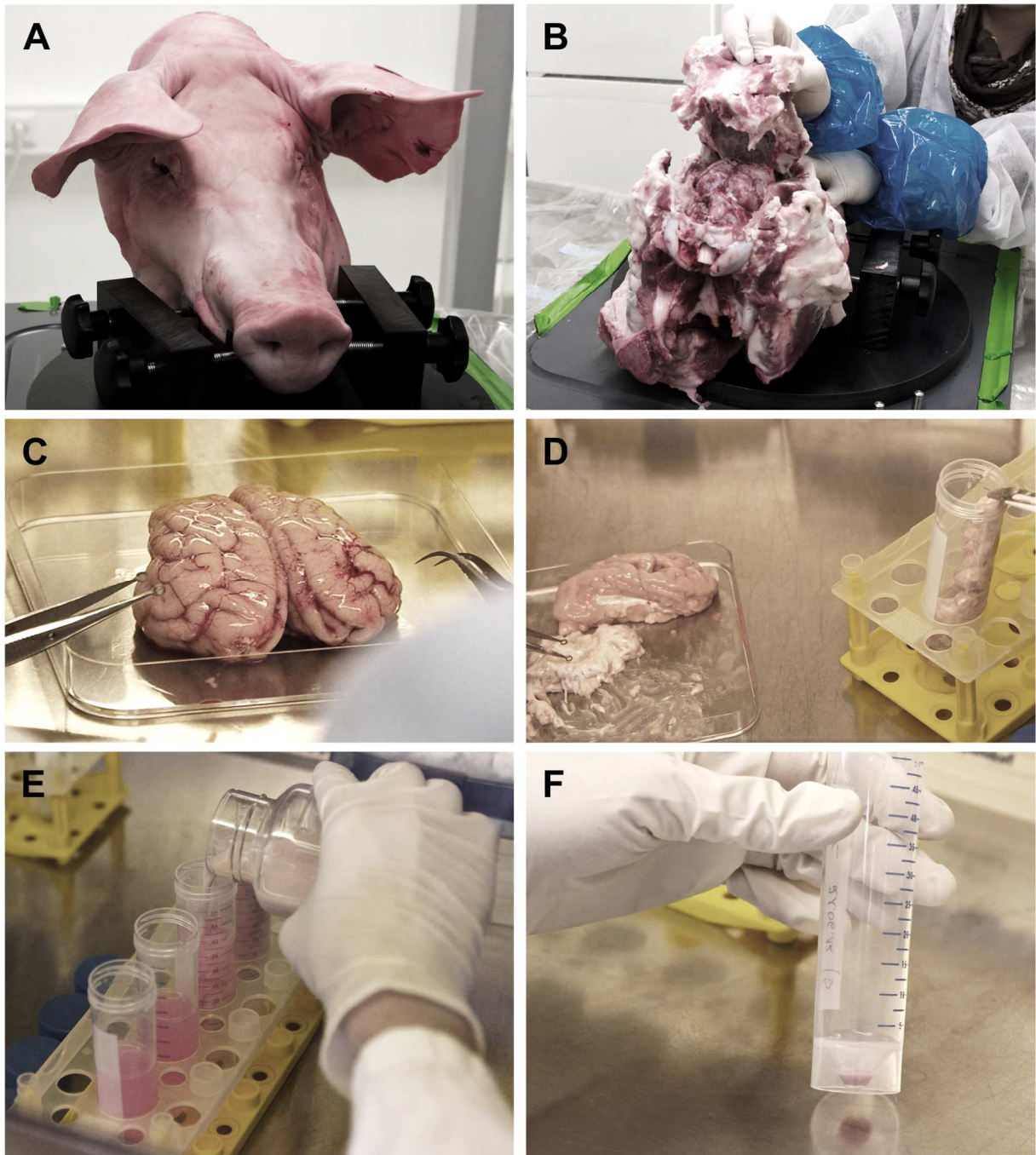


Figure 8: Selected steps of pBCEC preparation. (A) Skulls obtained from the local slaughter house. **(B)** Removal of skullcap after opening with a hatchet. **(C)** Isolated brain before removal of meningeal membranes. **(D)** Homogenization of the grey matter and preparation for dispase II digestion. **(E)** Digested brain tissue transferred to discontinuous gradient for removal of fatty supernatant. **(F)** Final pBCEC pellet after various enzymatic digestion and centrifugation steps.

3.2.2 Measurement of transendothelial electrical resistance of cell layers

In the body, epithelial and endothelial cells form barriers to regulate diffuse permeation of solutes. A direct correlation between permeability and transendothelial electrical resistance (TER) exists as tight cell layers show high TER values [189]. Therefore, TER measurement is suitable for quantifying leakage of barrier forming tissue.

In this work, pBCEC were plated on human collagen IV-coated ($131 \mu\text{g}/\text{cm}^2$) Transwell® inserts and subsequently placed in the cellZscope® device, which allows non-invasive real-time monitoring of TER development. Transwell® controls consisted of a collagen IV-coated insert without cells. Except for sample applications and medium exchanges, the module stayed in an incubator ($37 \text{ }^\circ\text{C}$, 5 % CO_2 , 95 % relative air humidity) and was connected to an external controller and computer, allowing automated, long-term measurements. A cellZscope® device can monitor TER and capacitance (C_{cl}) of cell layers that grow on porous membranes between two electrodes and form an interface between two compartments. When small alternating current voltage (V_{ac}) is applied, the electrical impedance of the cell system can be measured. Ideally, the cell layer limits ion current in this setup.

Principle of measurement

Barrier properties can be evaluated by extracting data from equivalent circuits and corresponding mathematical models that allow separating the total impedance (Z) spectrum from the impedance spectrum of the cells. Although cell layers are complex systems, their electronic features can be modelled by basic elements.

The relevant components for a cell layer's total impedance are the ohmic resistance TER and the capacitance C_{cl} (Figure 9). The TER describes the parallel connection of the paracellular paths while the capacitance C_{cl} of the cell layer comprises both apical and basolateral membranes. R_{med} is approximated and models the culture medium's ohmic resistance in the apical (R_{med1}) and basolateral (R_{med2}) compartment (Figure 9). The interface between the electrodes' metal and the cell culture medium is called constant phase element (CPE) and displays a complex impedance behaviour. It is empiric and based on the two parameters A_{cpe} , n_{cpe} . The cellZscope® software uses CPE as a mathematical model to describe the frequency-dependence of the electrode-medium interface's impedance. Total impedance of the system is calculated by the applied equivalent circuit and the corresponding mathematical models that are based on the five parameters TER, C_{cl} , R_{med} , A_{cpe} and n_{cpe} . Obtained data from the cellZscope® device is fitted by resulting algorithms to extract the parameters TER and C_{cl} .

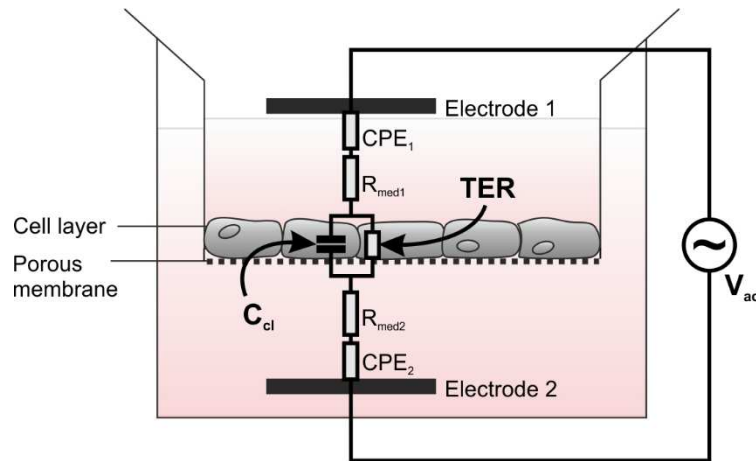


Figure 9: Schematic measurement of transendothelial electrical resistance (TER) and capacitance (C_{cl}) of a cell layer. Frequency dependent impedance is recorded and an electric equivalent circuit is used to analyze the data. Adapted and modified from nanoAnalytics [189].

3.2.3 Permeability of radiolabeled model substances

The quality of *in vitro* BBB model systems cannot only be monitored by measurement of the TER, but also by determination of the permeability of different marker substances, which is more sophisticated and sensitive.

The permeability of a BBB model is expressed by the percentage of measured decays per minute (dpm) values of a radiolabeled substance from apical (blood-representing) and basolateral (brain-representing) Transwell® compartments. Although Becquerel (Bq) is the *Système international d'unités* (SI)-derived unit of radioactivity, the unit Curie (Ci) is still widely used in scientific publications and industry and was therefore also calculated in this study.

For the evaluation of the obtained data, the following conversion factors are essential:

$$1 \text{ Bq} = 60 \text{ dpm}$$

$$1 \text{ dpm} = 0.016 \text{ Bq}$$

$$1 \text{ dpm} = 1.67 \times 10^{-8} \text{ MBq}$$

$$1 \text{ Bq} = 2.7027 \times 10^{-11} \text{ Ci}$$

$$1 \text{ MBq} = 27.027 \text{ } \mu\text{Ci}$$

For permeability assays pBCECs were isolated and prepared as described (see 3.2.1) and seeded on Transwell® inserts (Figure 10A) placed in a cellZscope® device. Permeability experiments occurred during maximum TER plateau, usually at day 4 to 5 post seeding. As a paracellular marker ^{14}C -inulin was chosen (Figure 10B). Inulin is not able to cross the BBB *in vivo* and therefore its low permeability represents a good indicator for intact barrier integrity. To verify physiological conditions, a transcellular marker was also applied (Figure 10B). For this purpose, ^{14}C -diazepam was selected. Diazepam is also known as Valium® and can diffuse through endothelial cell *in vivo*. For barrier characterization experiments, 0.35 $\mu\text{Ci}/\text{Transwell}^\circ$ of ^{14}C -inulin or ^{14}C -diazepam (DZP) were added to the apical compartment. After 2 hours incubation, medium from the apical and basolateral Transwell® compartment was transferred to a plastic vial containing 6 ml scintillation fluid and placed into a liquid scintillation counter (LSC). The decay per minute (dpm) and counts per minute (cpm) data were calculated by the QuantaSmart software with program settings for a single dpm assay and a measured energy level from 0 to 156 keV.

In order to further verify physiological conditions, the BBB model was opened by adding hyperosmotic 1.1 M mannitol solution. In this case, permeability experiments were performed with the radiolabeled markers solved in 1.1 M mannitol solution (Figure 10C) with an approximate osmolality of 1,100 mOs/ml.

After the marker incubation, Transwell® membranes were solubilized in 1 ml Solvable™ for 4 h at 60 °C, transferred to scintillation fluid and also measured in LSC analysis equally like samples from basolateral or apical compartment.

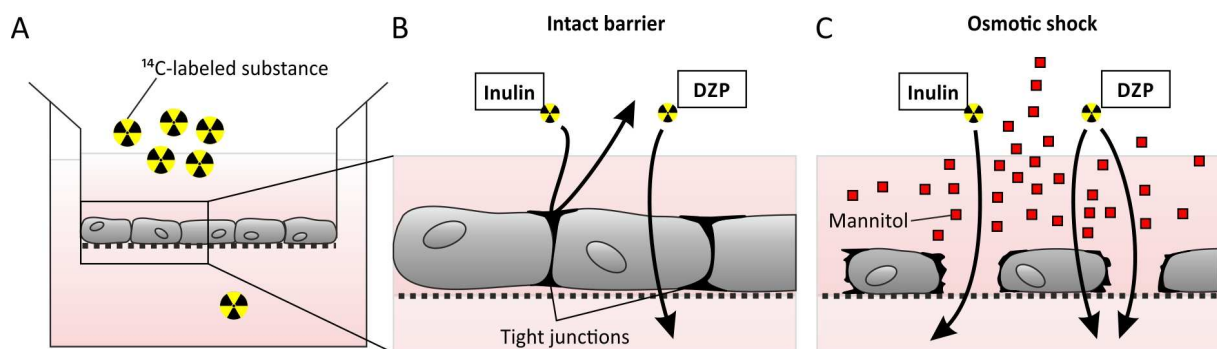


Figure 10: Schematic experimental design for permeability assays. (A) pBCEC on Transwell® inserts were incubated with radiolabeled marker substances when TER values were appropriate (4-5 days after preparation). After 2 hours, medium was analyzed for radioactive decays per minute (dpm) in a liquid scintillation counter. (B) ^{14}C -inulin served as a paracellular marker, tight junctions should largely prohibit diffusion across an intact barrier. ^{14}C -diazepam (DZP) passes the BBB transcellularly *in vivo* and should be detected in the basolateral compartment of the *in vitro* model. (C) When mannitol is added, pBCEC osmotically shrink, and ^{14}C -inulin should be able to pass by the disrupted tight junctions.

3.2.4 Characterization of the *in vitro* models by immunocytochemistry

For the characterization of the *in vitro* BBB models, primary cells or endothelial cell lines were stained with different antibodies for relevant markers and subsequently analyzed either by confocal laser scanning microscopy (CLSM) (qualitative) or flow cytometry (quantitative). Primary and secondary antibodies used for characterization are listed in section 3.1.

Qualitative immunocytochemistry

Primary pBCECs were stained with various antibodies against tight junction proteins (Cld-3, Cld-5, ZO-1, Occl). Cells were fixed with 1 % paraformaldehyde or acetone for 5-10 minutes and blocked by 5 % fetal calf serum (FCS) or bovine serum albumin (BSA) for 20 minutes. The primary antibody was diluted in PBS and incubated at room temperature for 1 hour or at 4 °C overnight. Cells were washed twice with PBS before applying the secondary antibody for 1 hour. After washing with water or PBS, cell culture slides were allowed to dry for up to 1 hour. Cover glasses and VECTASHIELD® Hard Set™ mounting medium (with DAPI) were added and again left to dry in a refrigerator for at least two hours. Samples were then analyzed with the aid of a confocal laser scanning microscope (CLSM).

Quantitative immunocytochemistry

For determination of the receptor status of the *in vitro* BBB model, flow cytometry analysis was performed after immunostaining for receptors of the low density lipoprotein receptor family (LDLR, LRP1, LRP2, ApoER). The pBCEC, bEnd3 or HBMEC were detached from growth surface by trypsin-EDTA incubation (0.5 %, 37 °C, 5-10 min). After washing, 3×10^5 – 1×10^6 cells were transferred to FACS tubes and incubated with BD Cytofix/Cytoperm solution for 20 min at 4 °C and subsequently with blocking solution (5 % FCS in PBS) for 30 min at 4 °C in order to prevent unspecific antibody binding. Then, blocking solution was removed and cells were incubated with 50 µl primary antibody (0.5-1 µg in PBS) for at least 1 hour at 4 °C. Afterwards, cells were washed again and incubated with the secondary antibody (0.5-1 µg in 50 µl PBS) for 30 min at 4 °C in the dark, washed again and resuspended in FACS-Fix solution before further analysis. Washing was performed with BD Perm/Wash solution and PBS. Samples were analyzed by flow cytometry with a FACS Calibur device. An electronic gate was set for a mother population of adequate control cells (treated identically, but without primary antibody incubation). 10,000 cells were recorded for each investigated sample and analyzed with the *CellQuest Pro* software. For analysis, a threshold was set for fluorescence intensity of the control population. Sample signals exceeding the threshold were counted as “positive” for the respective staining, (expressed either as “% positive”).

3.2.5 Nanoparticle preparation and characterization

All nanoparticles used in this study were prepared at the Institute for Pharmaceutical Technology and Biopharmacy (IPTB) at Münster University by Dr Iavor Zlatev and Bastian Raudszus.

Drug-loaded human serum albumin (HSA) nanoparticles

To prepare drug-loaded human serum albumin (HSA)-based nanoparticles two protocols were used. For the **solvent displacement** technique 0.5 ml aqueous HSA solution (40 mg/ml; pH 8) and 0.4 ml FBP (10 mg/ml) in water (pH 8) were added to 0.1 ml of water and were incubated for 2 h in a Thermomixer® (20 °C, 650 rpm). Afterwards, 4 ml ethanol 90% (m/m) were added dropwise in a velocity of 1 ml/min under constant stirring. After centrifugation (10 min, 16,000 g) and washing, the synthesized nanoparticles were collected and the amount of incorporated FBP was detected by HPLC analysis. Solvent displacement with PEG₄₀₀₀ was performed the like solvent displacement technique above, but instead of ethanol, 4 ml PEG₄₀₀₀ (300 mg/ml) in water (pH 5.5, 5.8 or 6.1) were added. The **inverse solvent displacement** technique was similar to the solvent displacement technique, but instead of adding ethanol to a HSA solution, the process was inverted, resulting in addition of the aqueous HSA-FBP solution (described above) to 4 ml ethanol 90% (m/m). Next, 11.6 µl glutaraldehyde (80 mg/ml) in water were added and stirred overnight.

Drug-loaded poly(lactic-co-glycolic acid) (PLGA) nanoparticles

For preparation of poly(lactic-co-glycolic acid) (PLGA) nanoparticles two different techniques and two different PLGA polymers (differing in proportions of lactide and glycolide) were used. For **oil/water (o/w) emulsion diffusion technique**, either 100 mg RESOMER® RG502H (lactide : glycolide 50:50) or 100 mg RESOMER® RG752H (lactide : glycolide 75:25) and 10 mg FBP were dissolved in 1 ml ethyl acetate (organic phase). Then, 2 ml polyvinyl alcohol (PVA) in water (10 mg/ml) was added (aqueous phase). For O/W emulsion, the sample was homogenized in an UltraTurrax® device (30 min, 21,000 rpm, dispersion tool S25N-10G). The emulsion was then transferred to 8 ml PVA in water (10 mg/ml) and magnetically stirred in an exhaust hood for at least 3 hours for ethyl acetate evaporation. The thereby produced nanoparticles were centrifuged and redispersed five times in PBS (pH 8) or water for washing. For detection of incorporated FBP, 20 µl nanoparticle suspension were added to 980 µl acetone and mixed for 5 min at 20 °C with a Thermomixer® device (20 °C, 700 rpm). After centrifugation (20 min, 20,000 g), FBP content was analyzed by HPLC.

For **water/oil/water (w/o/w) emulsion evaporation technique**, 0.5 ml FBP (20 mg/ml in water, pH 12.3) and 2.5 ml RESOMER® RG502H in dichloromethane (40 mg/ml) was homogenized by UltraTurrax® (1 min, 18,000 rpm, dispersion tool S25N-10G), resulting in a pre-emulsion. For w/o/w double emulsion, the pre-emulsion was added to 14 ml PVA in hydrochloric acid (10 mg/ml, pH 2.2)

and again homogenized by UltraTurrax® (5 min, 18,000 rpm, dispersion tool S25NK-19G). The pH was adjusted to 5.8 by NaOH. For dichloromethane removal, the sample was stirred on a magnetic stirrer (220 rpm) overnight under an exhaust hood. The produced nanoparticles were centrifuged and redispersed five times in PBS (pH 8) or water for washing. The detection of incorporated FBP was performed by HPLC analysis as described above for o/w emulsion diffusion technique prepared PLGA nanoparticles.

Drug-loaded poly(lactic acid) nanoparticles

Nanoparticles based on poly(lactic acid) (PLA) were produced by an **emulsion diffusion technique** (Figure 11A) as previously described [68]. In brief, the organic phase (100 mg PLA and 10 mg FBP dissolved in 2 ml dichloromethane) and aqueous phase (12 ml polyvinyl alcohol (2%, w/v)) were homogenized with an Ultra Turrax® device (24,000 rpm, 30 min) in an ice bath. If visualization of the nanoparticles for flow cytometry and microscopy analysis was aimed for, the organic phase also contained 150 µg Lumogen® F Orange 240. Dichloromethane removal occurred by stirring overnight at room temperature under an appropriate exhaust hood. Nanoparticles were then collected by centrifugation and redispersed and washed in purified water.

For lyophilization, trehalose (3 % w/v) was added as a cryoprotective agent. Lyophilization steps were performed as indicated in Figure 11A. Lyophilized nanoparticles were freshly reconstituted in cell culture medium (40 mg/ml) and vortexed prior to experiments.

For determination of flurbiprofen loading, high-performance liquid chromatography (HPLC) analysis was performed: 1 ml acetonitrile was added to 1 mg nanoparticles and incubated for 5 min at room temperature (RT). After centrifugation (20,000 g; 10 min), the 20 µl aliquots of the supernatant were measured with a HPLC device at a flow rate of 1 ml/min. The mobile phase consisted of acetonitrile and 0.1 % (v/v) trifluoroacetic acid (57.5 : 42.5, v/v), detection occurred at 245 nm wavelength.

After preparation, particle diameter, polydispersity index (PDI), and zeta potential of drug-loaded nanoparticles (redispersed in purified water) were analyzed with the aid of a Malvern Zetasizer Nano ZS. In this study, only nanoparticles with a PDI < 0.1 were used for further experiments, because the population distribution of the nanoparticles is then assumed to be monodisperse (Figure 11B, C).

For surfactant coating, Tween®80 was added in a final concentration of 1 % to the freshly redispersed nanoparticles 30 min before incubation on cells and shaken at RT at 600 rpm.

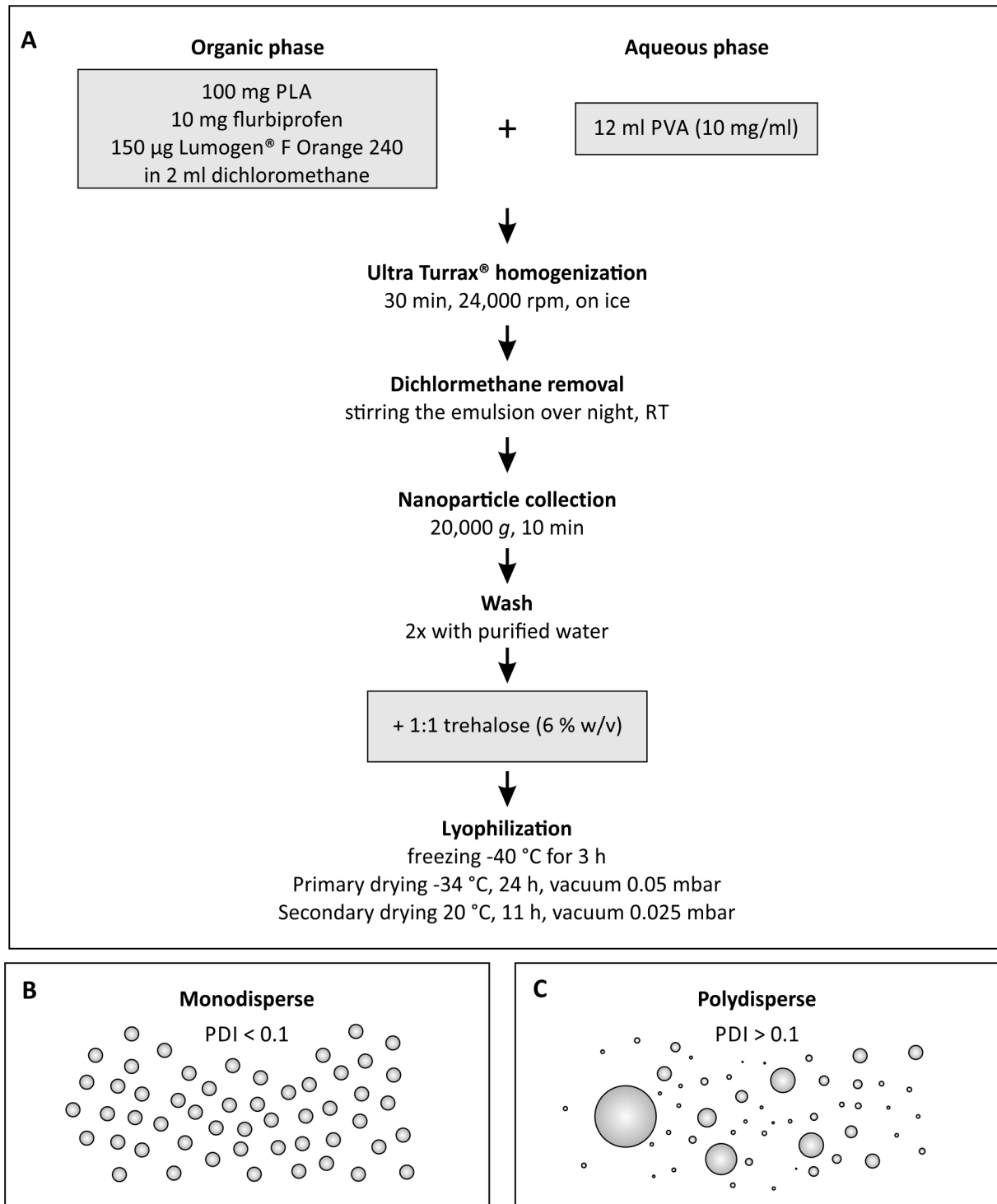


Figure 11: Preparation and characterization of fluorescence-labeled, flurbiprofen-loaded poly(lactic acid) nanoparticles (PLA-FBP-Lum NP) by oil/water (O/W) emulsion diffusion technique. (A) Preparation overview. The organic phase (consisting of poly(lactic acid) (PLA), flurbiprofen and a Lumogen® dye, all solved in dichloromethane) was added to the aqueous phase (polyvinyl alcohol (PVA)) and was subsequently homogenized with an Ultra Turrax® device in an ice bath to avoid vaporization of the organic phase. Dichloromethane was removed by stirring overnight (220 rpm) under an exhaust hood. Nanoparticles were collected by centrifugation and redispersion in purified water. Before freeze drying in a lyophilization device as indicated, trehalose solution was added as a cryoprotective agent. After drying, the vials were sealed and stored at 4 °C until use. **(B), (C)** Scheme of two different nanoparticle populations that might display the same mean diameter. Notice that the particles in **(B)** share a common size distribution whereas the size and shape of the population in **(C)** strongly varies. These characteristics are important for cellular uptake and cytotoxicity. The polydispersity index (PDI) challenges this problem. If a particle population shows a PDI smaller than 0.1, a population of equal size and shape (=monodisperse) as shown in **(B)** can be assumed.

Ligand-modified poly(lactic acid)nanoparticles

For apolipoprotein E3 (ApoE3) or ovalbumin modification, 15 mg PLA NP were mixed with a 5-fold molar excess of divinylsulfone for 5 minutes in 0.1 M NaOH (introducing amine-reactive vinylsulfone groups to the particle surface). The nanoparticles were collected at 10,000 *g* and washed 3 times with purified water. Afterwards nanoparticles were redispersed and incubated in 125 μ l carboxy-(PEG)4-amine solution (4 mg/ml) overnight at room temperature and 700 rpm, resulting in PEGylated nanoparticles that were purified by centrifugation (10,000 *g*, 10 min) and redispersed in water. Afterwards, 80 μ l of 1-ethyl-3-(3-dimethylaminopropyl)-carbodiimide (EDC) solution (30 mg/ml) and a N-hydroxysulfosuccinimide (Sulfo-NHS) solution (10 mg/ml) were added and incubated for 15 min at room temperature and 600 rpm, buffered by 2-(*N*-morpholino)ethanesulfonic acid (MES) at pH 4.6. The reaction leads to linking of an amine-reactive Sulfo-NHS ester to the PEGylated nanoparticles, allowing to covalently bind an amine-containing molecule (like a protein) to the nanoparticles' surface. Excess reagent was removed by centrifugation (10,000 *g*, 5 min). Nanoparticles were redispersed in water, centrifuged a second time and then incubated with 5 mg/ml ApoE3 or ovalbumin in PBS (pH 7.5) for 3 hours. To determine the amount of unbound ApoE3 or ovalbumin, nanoparticles were centrifuged (15,000 *g*, 15 min) and the supernatant was analyzed in 20 μ l aliquots by gel permeation chromatography (GPC) at a flow rate of 0.35 ml/min. The mobile phase was PBS (pH 6.8) containing 0.1 % sodium dodecyl sulfate (SDS). Detection was performed at 280 nm wavelength.

As for drug-loaded nanoparticles, particle diameter, polydispersity index (PDI) and zeta potential of ligand-modified nanoparticles (redispersed in purified water) were analyzed with a Zetasizer device. Lyophilization of the ligand-modified nanoparticles was performed as described above for drug-loaded nanoparticles (Figure 11A).

3.2.6 Fluorescence labeling of proteins

Lyophilized human, recombinant apolipoprotein E3 and the control protein ovalbumin were labeled with a fluorescent marker to allow detection in flow cytometry. A commercially available kit, PromoFluor-633 Labeling Kit was used according to the manufacturer's instructions. Samples were lyophilized after preparation and freshly resolved prior to experimental use. The fluorescent label allowed detection at Ex 637/Em 657 nm. Protein labeling was performed at the IPTB at Münster University by Dr Iavor Zlatev.

3.2.7 Nanoparticle plasma protein binding assay

The investigation and analysis of the protein corona of PLA-FBP NP after incubation with human plasma was performed by Dr. Sabrina Meister of the Johannes Gutenberg University, Mainz, Germany as described [68, 190].

Human blood plasma from 15 apparently healthy donors was collected at the Otorhinolaryngology, Head- and Necksurgery (ENT) department at the Medical University Mainz in EDTA-coated tubes to prevent blood clotting. The samples were anonymized in order to be untraceable back to a specific donor. Studies were performed according to the local ethics committee of the Medical University Mainz and in accordance with the Declaration of Helsinki.

For protein corona investigation, PLA nanoparticles were incubated with an equal volume of human plasma sample for a defined period of time (5, 15, 30 and 60 min). Afterwards, the mixture was loaded onto a sucrose cushion (0.7 M in PBS) and centrifuged through cushion (12,000 rpm, 20 min, 4 °C), thereby allowing a separation of plasma from the nanoparticle-protein complexes. After washing the nanoparticle-protein pellet three times with PBS, the proteins were eluted from the nanoparticles by adding an equal amount of sodium dodecyl sulfate (SDS) buffer (62.5 mM Tris-HCl pH 6.8; 2 % w/v SDS, 10 % glycerol, 50 mM DTT, 0.01 % w/v bromophenol blue) at 95 °C for 5 min (also see [68]).

The proteins were separated by gel electrophoresis on a 12 % SDS-polyacrylamide gel that was stained with Coomassie Brilliant Blue R-250. Quantitative analysis of proteins was performed by using a commercially available protein assay kit from Bio-Rad Laboratories. Qualitative analysis of proteins was performed by immunochemistry. Proteins from the nanoparticles' corona were relocated to polyvinylidene difluoride (PVDF) membranes, which were blocked with 5 % non-fat dry milk in tris-buffered saline (TBS) containing 0.01% Tween® 20, before performing primary antibody staining with anti-ApoA4 and anti-ApoE3 and a horseradish peroxidase-coupled secondary antibody (antibodies are listed in section 3.1, also see [68]).

3.2.8 Cellular binding studies

Different endothelial cell lines and primary cells were seeded on multi-well culture plates, previously coated with human collagen IV ($131 \mu\text{g}/\text{cm}^2$). Samples and controls were incubated for 4 hours at 37°C . Nanoparticulate formulations were added in a final concentration of $105.3 \mu\text{g}/\text{cm}^2$ growth surface. Fluorescence-labeled ApoE3 was added in a concentration of $1.053 \mu\text{g}/\text{cm}^2$ growth surface to simulate the approximate concentration of ApoE3 on ApoE3-modified nanoparticles ($10 \mu\text{g}$ ApoE3/ 1 mg nanoparticle). After incubation, the cells were washed twice with PBS, detached from the growth surface by trypsin-EDTA (0.5 %) incubation and transferred into FACS tubes. Cells were again washed two times with PBS and subsequently fixed with FACS-Fix solution. For flow cytometry analysis, at least 10,000 cells per sample were counted and evaluated with the aid of *CellQuest Pro* software. Untreated control cells were used for population gating (Figure 12). Lumogen® F Orange 240 labeled PLA nanoparticles were detected in fluorescence channel FL-1 (Ex 488/Em 530), PromoFluor-633 labeled ApoE3 was detected in FL-4 (Ex 633/Em 661).

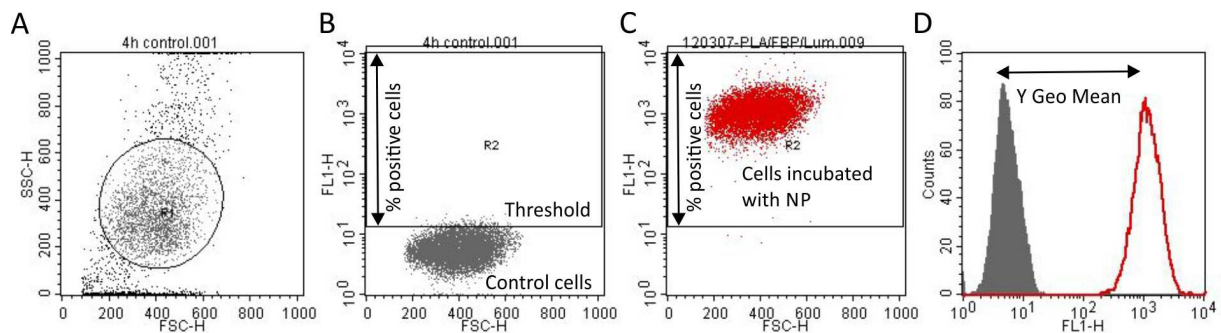


Figure 12: Exemplary analysis of flow cytometry data. (A) First, a cellular population is gated as control (Forward-scattered light (FSC) vs. sideward-scattered light (SSC)). (B) To quantify events, the threshold can be set by including approx. 1 % of the untreated control cells. (C) All fluorescence events above the threshold are counted as positive cells. (D) Alternatively, the parameter Y Geo Mean (reflects binding intensity) can be analyzed. It describes the shift of the histogram (represents signal intensity in the relevant fluorescence channel, here FL1-H).

3.2.9 Cellular uptake studies

Cellular uptake of nanoparticles can be monitored by confocal laser scanning microscopy (CLSM). For this purpose, primary pBCEC or the human BBB model cell line HBMEC were seeded on human collagen IV-coated glass cover slides and incubated with $105.3 \mu\text{g}/\text{cm}^2$ of nanoparticulate formulations for 37°C for 4 or 24 hours. After washing with PBS, cells were incubated with CellTracker™ Blue CMAC according to the manufacturer's instructions to stain the cytosol. Then, samples were fixed with 1 % paraformaldehyde for 10 minutes at room temperature, dried and embedded in VECTASHIELD® Hard Set™ mounting medium, which either contained DAPI or not. Microscopy analysis was performed with a Zeiss LSM 510 or a Leica TCS SP8 confocal microscope. PLA nanoparticles were labeled with Lumogen® F Orange 240 for detection at 524/539 nm wavelength.

3.2.10 Determination of cytotoxic potential of nanoparticles

Influence on transendothelial electrical resistance

Transendothelial electrical resistance (TER) alteration after nanoparticle exposure was taken as an indirect indicator for cellular integrity and viability. TER values directly before sample incubation were defined as “original TER” and normalized to 100 %. After 4 hours, TER measurements were stopped and the latest values recorded by the cellZscope[®] device were averages and converted to “% of original TER” of each Transwell[®] insert. If possible, controls and sample solutions were applied in equal droplet size to assure comparable influence on vibration shock induced TER alteration.

Influence on marker permeability

To investigate the nanoparticles' influence on barrier integrity, 0.35-0.67 μCi of ^{14}C -inulin was directly added to each Transwell[®] after nanoparticles and controls were applied. After 2 hours of incubation, the medium from each compartment was collected and transferred to 6 ml scintillation fluid for analysis with a liquid scintillation counter. The decay per minute (dpm) and counts per minute (cpm) data were calculated by the QuantaSmart software with program settings for a single dpm assay and a measured energy level from 0 to 156 keV.

Cellular viability

Cellular viability can be assessed by incubation of resazurin (the active compound of alamarBlue[®]), which is blue in color, practically non-fluorescent and crosses cell membranes. Viable cells reduce resazurin continuously to resorufin, which is red in color and highly fluorescent, whereas non-viable cells lose metabolic capacity necessary for resazurin reduction. Therefore, it can be used as an oxidation-reduction and proliferation indicator in cell viability assays in order to measure aerobic respiration [191]. In this study, the cytotoxic potential of nanoparticles and other samples was investigated. For this purpose, freshly prepared pBCEC were seeded in 96-well plates and cultivated for 4 days. Subsequently, cells were incubated with different concentrations of ApoE3, flurbiprofen or flurbiprofen-loaded nanoparticles. Ethanol incubation served as positive control for cellular toxicity. After 4 hours, a medium exchange was performed and alamarBlue[®] solution was added according to the manufacturer's instructions and incubated for another 4 hours. Fluorescence intensity was measured with a common plate reader at Ex/Em 560/610 nm. The intensity of the fluorescent signal is proportional to the number of vital cells; untreated cells were set as 100 % vital. The assay was controlled for effects of medium and flurbiprofen-loaded nanoparticles in order to exclude false positive responses. Intern replicas of experimental or no-cell control samples were performed to minimize experimental errors.

3.2.11 Nanoparticle-mediated drug transport experiments

For drug transport experiments across an advanced *in vitro* BBB model, the following setup was chosen: Primary porcine brain capillary endothelial cells (pBCEC) were prepared from fresh skulls and seeded on Transwell® inserts in a cellZscope® device to monitor TER development as a quality control (also see 3.2.1). Four days later, when TER reached a plateau phase or was still rising, pBCEC were incubated with nanoparticles and other samples for 4 hours (Figure 13A).

To assess the flurbiprofen-loaded nanoparticles' capacity of transporting the drug across the *in vitro* BBB model, the following experiments were subsequently performed (Figure 13A-D):

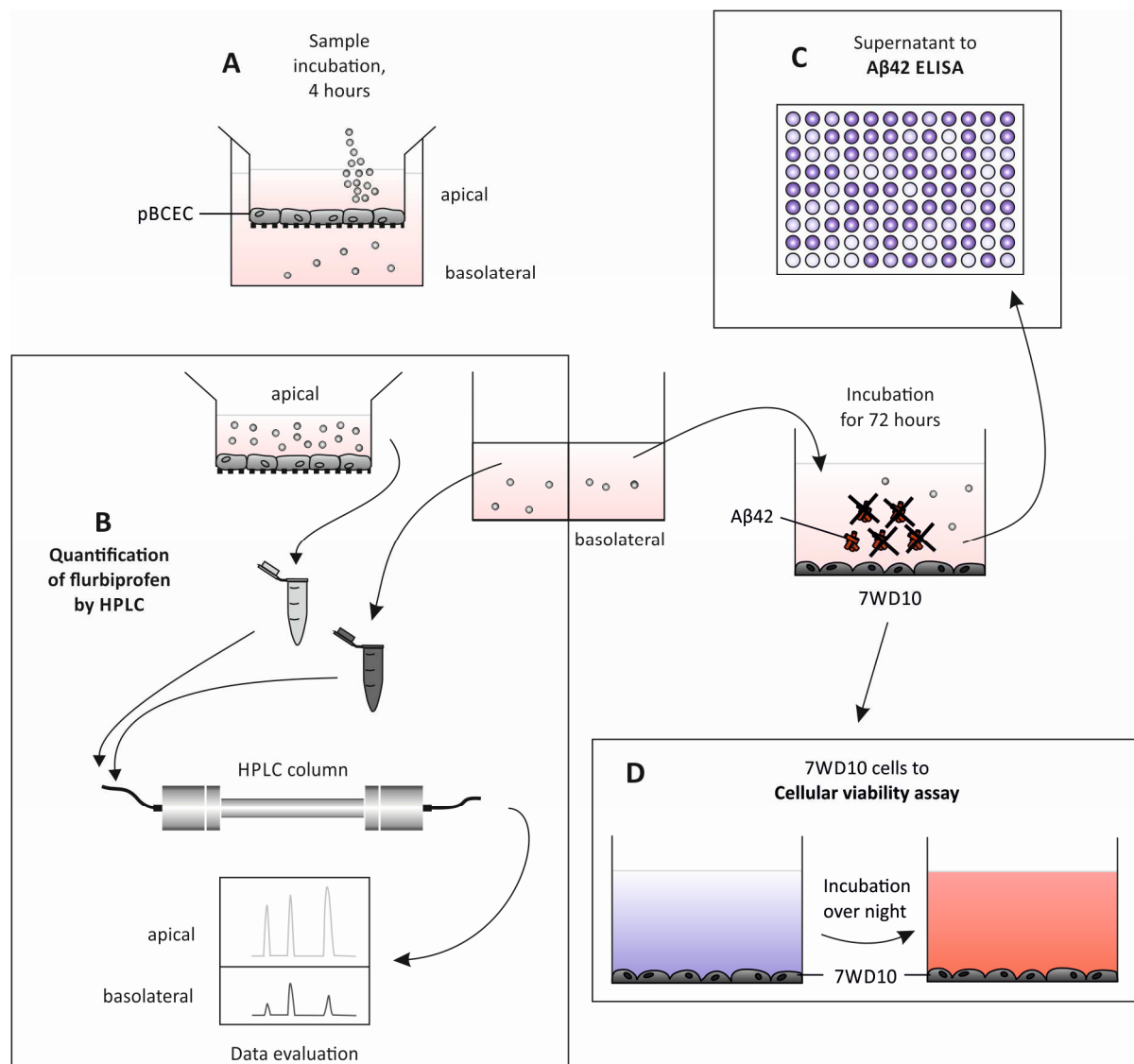


Figure 13: Overview of experimental setup for nanoparticle transport studies. (A) After isolation and cultivation, pBCEC were incubated with nanoparticles or control samples for 4 hours. Then, medium from the apical (blood-representing) and basolateral (brain-representing) compartment were either analyzed for flurbiprofen content in (B) HPLC analysis or (C) transferred to the Alzheimer's disease model cell line 7WD10 for 72 hours in order to perform an A β 42-detecting ELISA with the supernatants. (D) The cellular viability of the 7WD10 cells was afterwards checked for in a cellular viability (AlamarBlue) assay to exclude that an A β 42-reducing effect was caused by impaired viability.

Quantification of flurbiprofen by high performance liquid chromatography

For quantitative detection of flurbiprofen, cell culture samples from basolateral compartments were harvested after 4 hours of incubation in the pBCEC BBB model and transferred to high performance liquid chromatography (HPLC) analysis (Figure 13A, B). Medium from the apical compartment was harvested; mixed with 0.8 ml acetonitrile to precipitate proteins and disintegrate remaining nanoparticles [192]. After centrifugation (10,000 *g*, 10 min), 500 μ l of the supernatant was transferred to fresh vials and investigated in HPLC analysis.

Transwell® membranes were dissolved by adding 1 ml DMSO (also described to precipitate proteins[193]) and centrifuged (10,000 *g*, 10 min) to remove polycarbonate residues.

All supernatants were transferred to fresh vials for HPLC analysis, performed by either Dr Iavor Zlatev and Mr. Bastian Raudszus at IPTB at Münster University or at Fraunhofer IBMT (Table 2) with the aid of Ms. Linda Elberskirch. Calibration of flurbiprofen measurement was performed by DMSO-dissolved drug standard (IPTB: 1.5-150 μ g FBP, 7 concentrations or IBMT: 0.031-250 μ g FBP, 14 concentrations). Calculation of the calibration curve from standard served as reference for sample analysis.

Table 2: Parameters for flurbiprofen detection via HPLC analysis performed at IPTB in Münster, Germany or at IBMT in Sulzbach, Germany.

	IPTB	IBMT
HPLC device	Agilent 1200 Infinity	Agilent 1260 Infinity
Column	Gemini®-NX-C18	Poroshell 120EC-C18
Mobile phase	57.5 % acetonitrile	57.5 % acetonitrile
	42.5 % trifluoroacetic acid (0.1 % in H ₂ O)	42.5 % trifluoroacetic acid (0.1 % in H ₂ O)
Flow rate	1 ml/min	0.5 ml/min
Column compartment temperature	30 °C	40 °C
Detection	Diode array detector, 245 nm	Diode array detector, 247 nm
Injection volume	20 μ l	10 μ l
Runtime	8 min	8 min

Functional assay for detection of A β 42 species

A β 42 reducing potential of nanoparticles and control samples was assessed with a commercially available A β 42 detecting ELISA (Figure 13C). Again, pBCEC were incubated with samples for 4 hours in the apical, blood-representing compartment of the Transwell® model when TER was sufficient. Then, 800 μ l of the medium from the basolateral, brain-representing compartments was transferred to 24 well plates, previously seeded with 3×10^4 7WD10 cells/cm². 7WD10 are Chinese hamster ovary (CHO) cells that stably express APP751wt for the secretion of A β peptide [194]. After three more days without further medium exchange, the supernatant of the 7WD10 cells was analyzed in an A β 42 detecting ELISA according to the manufacturer's instructions. In the first step, standards of known A β 42 concentration (15.63 – 1,000.00 pg/ml), samples and controls were co-incubated with an antibody specific for the COOH terminus of the 1-42 A β sequence in a microtiter plate coated with an

antibody specific for the NH₂ terminus of the A β peptide. As recommended in the manufacturer's instructions, the protease inhibitor cocktail 4-(2-Aminoethyl)benzenesulfonyl fluoride hydrochloride (AEBSF) was added in a final concentration of 1 mM. Bound antibody was detected by adding a horseradish peroxidase (HRP)-labeled antibody that recognizes the species origin of the anti-A β 42 peptide antibody. Next, the HRP substrate (stabilized chromogen) was added and converted to a bluish color by HRP (directly proportional to the amount of A β 42). The reaction was stopped by a stop solution that changes color from blue to yellow and enabled detection at 450 nm with a common plate reader. Negative controls included chromogen blanks. All samples and standards were performed at least in duplex per assay. Untreated 7WD10 cell controls were set as 100 % A β 42 level.

Cellular Viability of the Alzheimer's disease model cells

In order to exclude cytotoxic effects on the Alzheimer's disease model cells that could falsify the outcome of A β 42 reduction, the cellular viability assay was performed after transport experiments across the pBCEC *in vitro* BBB model (Figure 13D) as described earlier. In brief, samples and controls were added to Transwell® inserts seeded with pBCEC as described earlier. After 4 hours of incubation, the basolateral medium was transferred to 7WD10 cells and after 72 hours, the supernatant was analyzed for A β 42 species and flurbiprofen content. The 7WD10 cells were washed with PBS and provided with fresh medium containing alamarBlue® overnight in an incubator and analyzed for fluorescence intensity (excitation 560 nm, emission 610 nm).

3.2.12 Experimental definitions and visual display of data

Unless otherwise stated, the term *independent experiment* was defined as the following: For primary cells, one preparation from one porcine brain, which was treated with nanoparticles from different lots (usually prepared on different days or in different batches). For cell lines, an *independent experiment* also was performed with different nanoparticle lots. Furthermore, cells from different passages were used.

Error bars represent the *standard error of the mean (SEM)* calculated with Microsoft Excel. Data was plotted with OriginPro 9.1 and the resulting graphs were customized and standardized with CorelDRAW® Graphics X6 without altering the original data. Fluorescent images were contrasted and modified in the same manner for all samples and controls.

4 RESULTS & DISCUSSION

This study investigates the transport capacity of poly(lactic acid) nanoparticles loaded with a potential anti-Alzheimer's disease drug across an advanced blood-brain barrier (BBB) model based on freshly isolated primary porcine brain capillary endothelial cells (pBCEC). It was examined whether application of flurbiprofen-loaded nanoparticles on the blood-representing compartment of the *in vitro* BBB model could reduce neurotoxic A β 42 peptide (expressed by 7WD10 cells) in the brain-representing compartment. Due to its physicochemical properties, flurbiprofen itself only poorly crosses the BBB *in vivo* and was therefore discontinued as an anti-Alzheimer's disease drug in clinical trials.

4.1 Characterization of the *in vitro* blood-brain barrier model*

In order to prove that the porcine *in vitro* blood-brain barrier model fulfils the expectations for drug transport studies, a number of quality tests were performed (Figure 14). After pBCEC isolation from primary material (also see 3.2.1), immunostaining for tight junction (TJ) proteins was performed as a first indicator for accurate barrier formation of the endothelial cell layer. Furthermore, the transendothelial electrical resistance (TER) of pBCEC cultured on Transwell® membranes was continuously monitored with the aid of a cellZscope® device, allowing impedance measurements across a cellular layer. Moreover, the permeability of ¹⁴C-labeled marker substances inulin and diazepam across the *in vitro* barrier was assessed by using a liquid scintillation counter (LSC).

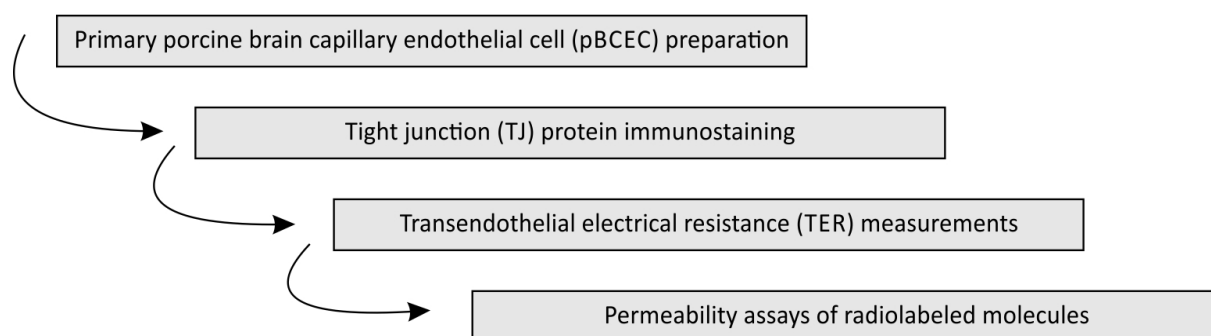


Figure 14: Flow chart of the experimental design. The blood-brain barrier model (pBCEC) was tested for its suitability as an appropriate model. After preparation and seeding of cells, tight junction (TJ) proteins were stained for. Next, transendothelial electrical resistance (TER) measurements were performed with the aid of a cellZscope® device that automatically monitors impedance. Furthermore, the permeability of radioactive tracers (¹⁴C-inulin and ¹⁴C-diazepam) was evaluated with the aid of a liquid scintillation counter (LSC).

* Parts of this section were published in [195].

4.1.1 Tight junction protein expression

Tight junction (TJ) proteins play a key role in maintaining barrier function in brain endothelial cells. Literally, they seal the gaps between the cellular monolayer (see Figure 2C). Without accurate tight junction protein expression, the cellular barrier lacks appropriate resistance and is permeable for various substances. To prove that pBCECs express the main TJ proteins, antibody staining was performed and evaluated by confocal laser scanning microscopy (CLSM). Claudin 5 (Cld-5) and claudin 3 (Cld-3), occludin (Occl) and zonula occludens (ZO-1) antibody staining (green) revealed a characteristic pericellular expression of tight junction proteins (Figure 15), implying that the connecting function between adjacent cells can be performed without restriction. Therefore, the pBCEC *in vitro* BBB model fulfils one of the fundamental requirements of a suitable barrier integrity.

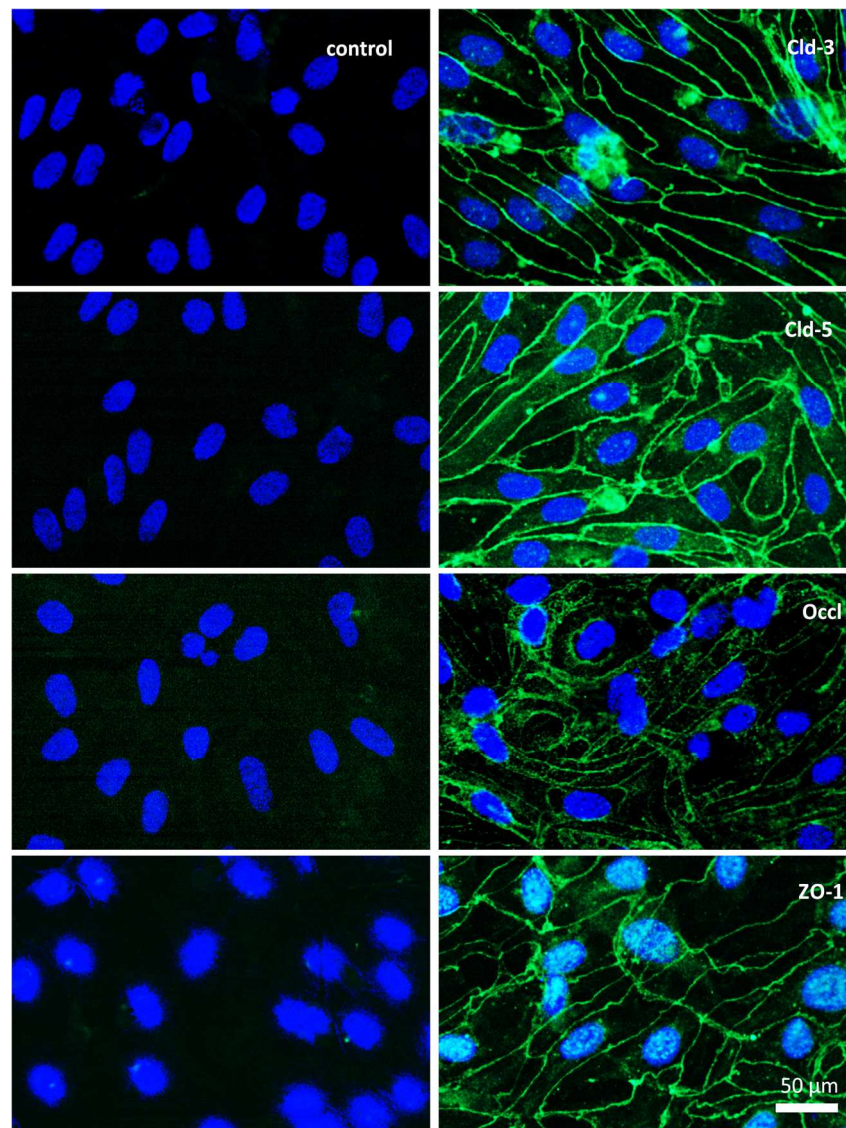


Figure 15: Tight junction protein expression in primary pBCEC. Claudin 5 (Cld-5) and claudin 3 (Cld-3), occludin (Occl) and zonula occludens (ZO-1) antibody staining displayed in green, DAPI-stained nuclei displayed in blue. Scale bar as indicated. Data published in [195].

4.1.2 Measurement of transendothelial electrical resistance

Different methods to determine endothelial barrier function exist. One convenient way is following barrier characteristics in real time with the automatized measurement of impedance (Figure 16A). For this purpose, pBCEC were isolated and seeded on Transwell® inserts in a cellZscope® device. Especially on small pore-sized membranes (0.4 μm polycarbonate membranes), transendothelial electrical resistance (TER) values are excellent and comparable to *in vivo* measurements of approximately 2,000 $\Omega \cdot \text{cm}^2$ (data not shown, compare Figure 36C). However, 0.4 μm sized pores might hamper the transport of nanoparticles, which in this study are approximately up to 0.25 μm in diameter. Consequently, for all transport experiments, pBCEC were cultured on polycarbonate membranes with larger pores (3 μm diameter). TER values are generally lower on larger pore sized membranes, but a hindrance for nanoparticle transport is less likely to occur.

An averaged example of TER development of pBCEC from one primary preparation displays that TER increased approximately two days after preparation and reached a plateau or slower escalating phase after four to five days (Figure 16B). During this phase in TER development, all further experiments were initialized, because it was assumed that TJ protein connections (disrupted during primary cell preparation) were reformed between endothelial cells. As a quality criterion, only pBCEC displaying $>300 \Omega \cdot \text{cm}^2$ were included. Transwell® controls, consisting of identically treated inserts without cells (“No cells” in Figure 16B) never displayed TER development, thereby ruling out that the polycarbonate membrane or collagen IV coating affected a barrier formation.

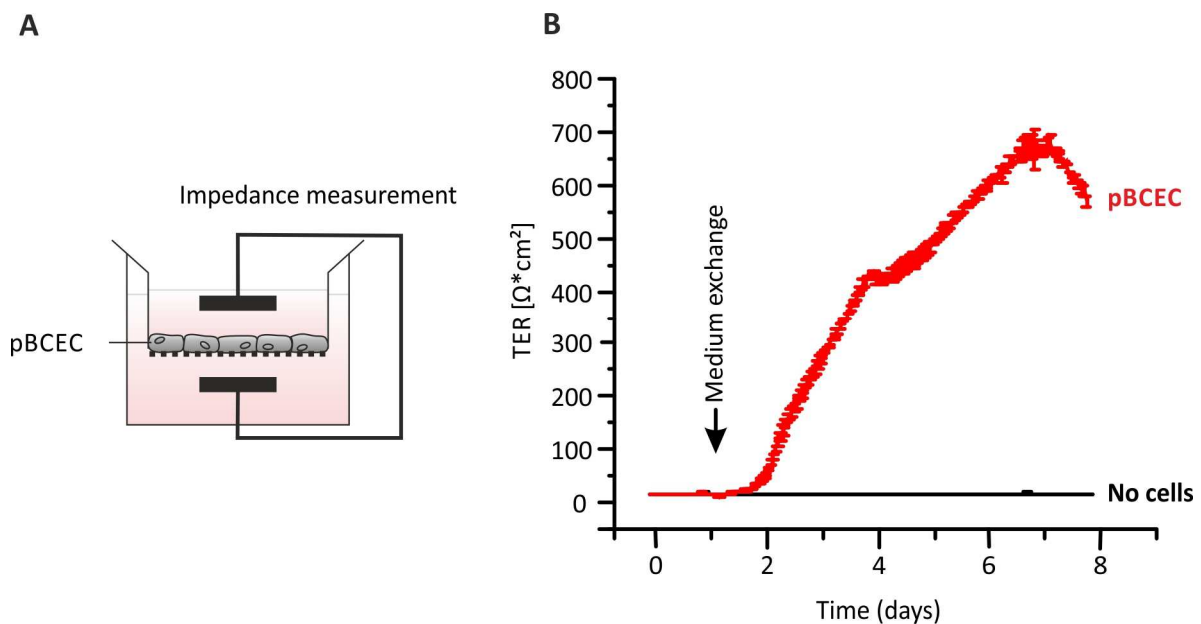


Figure 16: Transendothelial electrical resistance (TER) development of pBCEC on large pore-sized Transwell® membranes. (A) Schematic drawing of experimental design. **(B)** Transendothelial electrical resistance (TER) was measured in a Transwell® system and averaged by the cellZscope® software. Data from 3 independent Transwell® inserts, displayed with error bars.

4.1.3 Permeability of radiolabeled model substances

The quality of an *in vitro* blood-brain barrier model can also be described by the permeability of specific marker substances. Here, the pBCEC Transwell® model was incubated with radiolabeled ^{14}C -inulin, and radioactive decays were detected in the apical and in the basolateral compartment of the Transwell® insert (Figure 17A). The experiments were performed on 3 μm pore-sized membranes in order to validate barrier tightness, despite lower TER compared to smaller-pored membranes. For pBCEC grown on 3 μm pores, only about 0.2 % of the applied ^{14}C -inulin was detected in the basolateral compartment after two hours of incubation (Figure 17B). To validate that the low permeability is determined by the cellular barrier function (e.g. unrelated to inulin accumulation on the membrane), 20 % mannitol solution was added to prove for physiological function. Hyperosmolar mannitol is supposed to osmotically shrink the cells and therefore loosen the tightly packed endothelial cells. This technique is also used in patients *in vivo* for supporting drug transport across the blood-brain barrier. In the pBCEC model, mannitol application increased the low permeability for ^{14}C -inulin up to 3.5 % (Figure 17B). The physiological properties in terms of osmotic opening were therefore assumed to be confirmed. Next, the permeability of a transcellular marker was investigated. ^{14}C -diazepam is able to cross cellular membranes. Diazepam is a tranquilizing, anxiolytic (fear easing) and anti-epileptic drug that is highly lipophilic and works when applied orally for it crosses the blood-brain barrier *in vivo*. In the pBCEC Transwell® model, 6.1 % of the applied ^{14}C -diazepam was found in the basolateral compartment after 2 hours. As expected, the permeability for ^{14}C -diazepam rose drastically when mannitol addition forced the barrier to open. In this case 13.3 % of ^{14}C -diazepam was retrieved in the brain-representing, basolateral compartment.

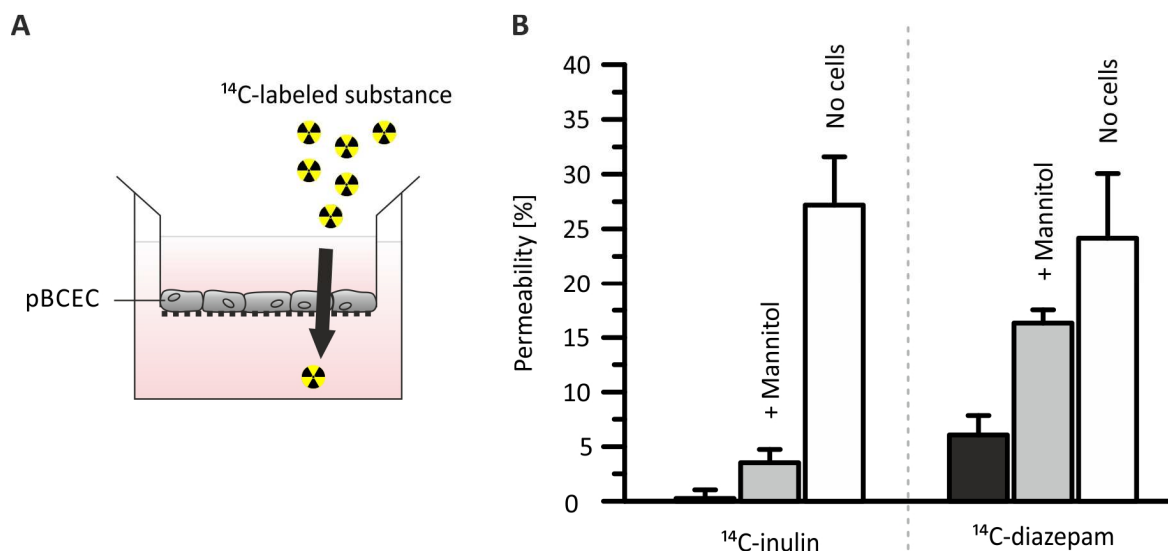


Figure 17: Verification of appropriate barrier characteristics *in vitro*. (A) Schematic drawing of experimental design. When TER was sufficiently high, ^{14}C -labeled markers were added to the pBCEC BBB model. (B) Permeability of radiolabeled marker substances ^{14}C -inulin and ^{14}C -diazepam in a pBCEC blood-brain barrier model was assessed by liquid scintillation counter (LSC) measurements. Hyperosmolar mannitol was applied to simulate an osmotic shock. For comparison, Transwell® inserts without pBCEC (No cells) were also measured for marker permeability. Data from at least 3 independent experiments with 3 internal replicas (=Transwell® inserts). Error bars indicate SEM. Data published in [195].

4.1.4 Concluding remarks on characterization of the *in vitro* blood-brain barrier model

All in all, this section closely characterized the quality of the *in vitro* primary pBCEC BBB model using various methods in order to verify the suitability of the pBCEC model for drug transport studies.

Firstly, tight junction (TJ) protein expression was analyzed. Tight junction proteins seal the intercellular gaps of the endothelial layer and therefore play a key role in blood-brain barrier integrity. The expression and right cellular localization of the most important tight junction proteins in pBCEC was confirmed by antibody staining and confocal laser scanning microscopy (CLSM) analysis. The pBCEC *in vitro* BBB model strongly expresses claudins 3 and 5, zonula occludens and occludin, being advantageous to commonly used cell lines that either do not express all of these TJ proteins or the expression level is very low [23].

Secondly, the development of transendothelial electrical resistance (TER) of the cellular layer was measured by impedance spectroscopy with the aid of a cellZscope® device. TER is a commonly used parameter for a non-invasive determination of a BBB model quality. Earlier studies showed that small pore sizes of 0.4 μm in diameter facilitate high TER values. However, the small pores might hamper nanoparticle transport. Hence, for transport experiments membranes with larger pores of 3 μm were used in this study. In general, a good model is expected to display TER values in the order of magnitude of hundreds $\Omega\cdot\text{cm}^2$ [19]. For comparison, *in vivo* fetal rats develop TER around 300 $\Omega\cdot\text{cm}^2$, adult rats up to 1,400 $\Omega\cdot\text{cm}^2$ [196]. In this study, pBCEC grown on 3 μm pore-sized membranes usually reached TER values up to 300 $\Omega\cdot\text{cm}^2$ and higher, thereby by far exceeding cell line-based BBB models like HBMEC (~25 $\Omega\cdot\text{cm}^2$) or bEnd3 (~40 $\Omega\cdot\text{cm}^2$) [19–21, 68].

Thirdly, to assure that the cells grown on 3 μm pore-sized membranes are also a suitable model with good barrier integrity, a permeability assay with transcellular and paracellular radiolabeled markers was established. The measurement of radioactive tracers is one of the most sensitive assays to monitor permeability today. A proper model should be impermeable for inulin, which is neither actively transported via the blood-brain barrier, nor diffuses to the brain *in vivo*. High permeability is therefore always a sign of a leaky model. ^{14}C -labeled inulin and diazepam were applied to the pBCEC model during the ascending phase of TER development. Only 0.2 % of the applied ^{14}C -inulin was detectable in the basolateral (brain-representing) compartment. This finding implies a strong barrier function of the cells. In contrast, when the BBB model was forced to open by mannitol addition, ^{14}C -inulin permeability drastically increased, which proves a good comparability to *in vivo* conditions, since mannitol-based opening of the BBB is also used in experimental animals and patients. Another indicator of physiological conditions is the good permeability for diazepam. This drug, also known by its trade name Valium®, easily crosses the BBB *in vivo*. The pBCEC models also is permeable for ^{14}C -labeled diazepam in *in vitro* experiments.

4.2 Nanoparticle preparation and characterization*

The first result and discussion section introduced a suitable in-house *in vitro* blood-brain barrier model usable for drug transport studies. This second section deals with preparation of nanoparticles for BBB crossing and their characterization. An overview of the experimental setup is shown in Figure 18. After preparation of different polymer-based flurbiprofen-loaded nanoparticles quality parameters like size, surface charge and poly dispersity index were determined with the aid of a Zetasizer® device. Flurbiprofen-loading of the nanoparticles was assessed by high-performance liquid chromatography (HPLC) analysis.

Usually, the pBCEC *in vitro* BBB model reacts very sensitively to external stimuli and consequently, several experiments were performed to further investigate the nanoparticles' cytotoxic potential. The cellular viability of the pBCEC BBB model was evaluated after nanoparticle incubation in a resazurin-based, color changing (alamarBlue®) assay. Furthermore, the influence of nanoparticles on the transendothelial electrical resistance (TER) in short- and long-term exposure was investigated in impedance measurements with the aid of a cellZscope® device. Finally, the influence on barrier integrity was assessed by determining the permeability of radiolabeled marker substances after nanoparticle incubation with the aid of a liquid scintillation counter (LSC).

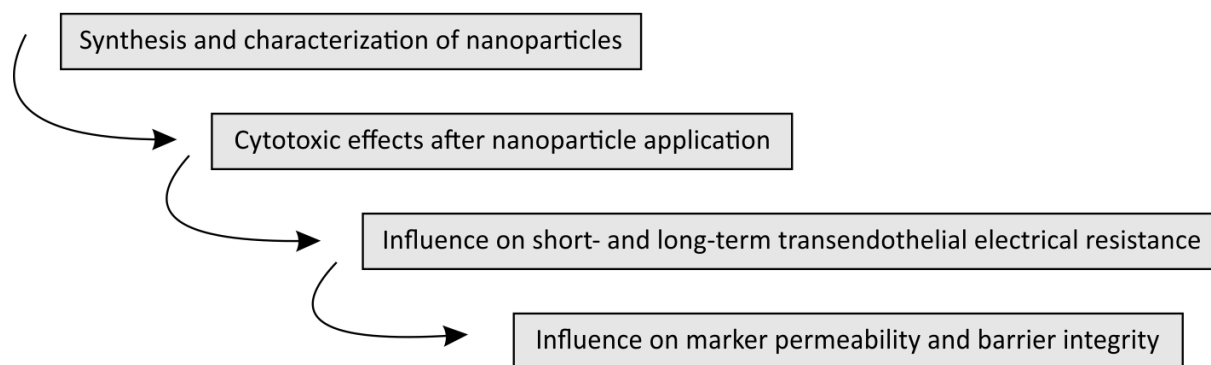


Figure 18: Flow chart of the experimental design. Nanoparticulate formulations based on different basis materials were prepared and investigated for various quality features. Also, they were tested for their cytotoxic potential regarding the BBB-forming pBCEC in a cellular viability assay. Furthermore, the nanoparticles' influence on transendothelial electrical resistance (TER) development after short- and long-term exposure was investigated in impedance measurements with a cellZscope® device. Intact barrier integrity after nanoparticle application was checked for in permeability studies with radiolabeled marker substances.

* Parts of this section were published in [68, 195, 197].

4.2.1 Choice of basis material, synthesis and characterization of nanoparticles

Different basis materials are possible to take into account when preparing nanoparticles capable of drug transport across the BBB. During the course of the project, various nanoparticulate formulations were prepared and tested for their drug transport capacity and interaction with BBB model cells (see [197]).

HSA-based nanoparticles were prepared by a well-established desolvation technique that allows ApoE3-modification [197], but requires chemical precipitation with ethanol. Flurbiprofen is hardly soluble in aqueous media and tends to dissolve in the alcohol that is dropped into the aqueous phase for nanoparticle formation. The loading consequently was too inefficient for further experiments [197]. For three different preparation techniques, more than 80 % of the originally used drug were redetected in washing supernatants and not incorporated in HSA nanoparticles [197].

PLGA-based nanoparticles loaded with flurbiprofen during the preparation process (PLGA-FBP NP) failed in *in vitro* experiments and did not lower A β 42 levels in the brain representing compartment of the pBCEC BBB model (data not shown). The drug was not detected in expected amounts in HPLC analysis after transport, and PLGA-FBP NP did not evoke cytotoxic effects (data not shown). Most of the flurbiprofen was likely released from the PLGA-FBP NP during further wash steps in the preparation protocol, and therefore the theoretical loading efficacy did not reflect the actual flurbiprofen content during the cell culture experiments. This effect is in accordance with other recent data, describing that PLGA-FBP NP very quickly release flurbiprofen [197]. Neither oil/water (O/W) emulsion diffusion nor water/oil/water (W/O/W) emulsion evaporation technique improved FBP-loading of PLGA NP if they were dissolved in media with pH >7, which is essential for biological applications. PLGA is consequently not suited for this application.

PLA-based nanoparticles were prepared by an emulsion-diffusion method as described in 3.2.5 and also a recent publication [68]. For PLA nanoparticle tracking in microscopy and flow cytometry experiments, an optional fluorescent substance (Lumogen[®] F Orange 240) was added for visualization (also see 3.2.5). During the preparation process, flurbiprofen was added and incorporated into the nanoparticles (PLA-FBP NP). The main characteristic features of PLA-FBP NP were determined with the aid of a Zetasizer Nano ZS and by HPLC analysis (Table 3).

Table 3: Characterization of flurbiprofen-loaded poly(lactic acid) (PLA) nanoparticles (PLA-FBP NP) and unloaded control nanoparticles (PLA NP). Table of NP characteristics according to data sheets provided by the Institute for Pharmaceutical Technology and Biopharmacy (IPTB) at Münster University. Diameter and dispersity index were measured with the aid of a Zetasizer Nano ZS. Flurbiprofen loading was determined by HPLC analysis.

	Lots (n)	Diameter (nm)	Poly dispersity index (PDI)	FBP loading ($\mu\text{g}/\text{mg NP}$)
PLA NP	6	250.0 (± 19.6)	0.089 (± 0.036)	
PLA-FBP NP	10	239.9 (± 11.2)	0.070 (± 0.026)	52.27 (± 11.3)

The mean nanoparticle diameter settled at < 250 nm for drug-loaded or control particles; the poly dispersity index of less than 0.1 indicates a monodisperse, meaning homogeneous particle population (Table 3). The mean loading of the drug into PLA-based nanoparticles leveled off at around $52 \mu\text{g}$ flurbiprofen per 1 mg nanoparticle formulation (Table 3). Reconstitution of the lyophilized PLA-FBP NP in saline resulted in a quick release of the drug. After 6 hours, more than three quarters of the initially incorporated flurbiprofen appeared in the supernatant of redispersed nanoparticles (Figure 19 and [68, 197]).

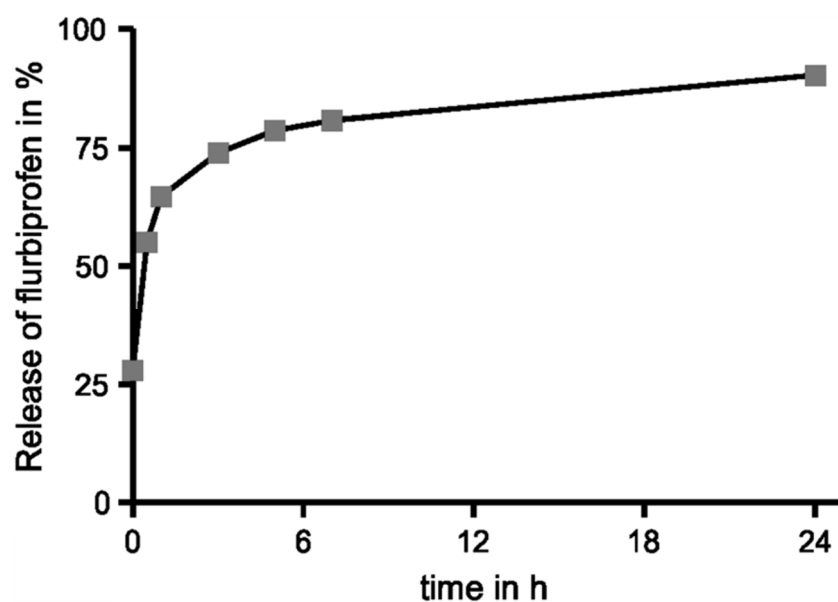


Figure 19: Flurbiprofen released from PLA-FBP NP over time. Nanoparticles were dissolved in aqueous solution at pH 7.5, before drug content was measured by HPLC analysis at different time points as indicated. Release of flurbiprofen is displayed as percent of the originally incorporated drug. Figure copied from [68].

4.2.2 Cellular viability of model cells after nanoparticle application

To test for nanoparticles' cytotoxic potential on the *in vitro* BBB cellular model, different viability tests are possible. Here, an alamarBlue® cellular viability assay was performed that quantifies the reduction from a non-fluorescent (resazurin) to a highly fluorescent dye (resofurin), which can only be performed by living cells (see 3.2.10). The pBCECs were incubated with increasing concentrations of DMSO-dissolved flurbiprofen (FBP) and a corresponding solvent control (DMSO) (Figure 20). In order to compare the cytotoxic potential of drug-loaded nanoparticles and the free drug, the equal concentration of flurbiprofen incorporated in flurbiprofen-loaded nanoparticles (PLA-FBP NP) was added to the cells.

FBP application strongly influenced cellular viability, reducing it to less than 50 % in higher concentrations, whereas (in equivalent concentrations) the solvent DMSO itself did not alter cellular viability, ruling out a solvent-mediated effect. FBP-incorporation in nanoparticles abolished the cytotoxic potential of the drug: PLA-FBP NP did not reduce cellular viability of pBCEC. On the contrary, especially higher concentrations seemed to slightly elevate resazurin conversion compared to control cells. For the PLA-FBP NP were intended for BBB crossing purposes and coatings with surfactants were shown to enable and enhance BBB transit [37, 49, 64–67], the nanoparticles were pre-incubated with 1 % Tween®80, which was reported to enable brain uptake of PLA-based nanoparticles before [88]. However, coating PLA-FBP NP with 1 % Tween®80 in this experimental setup reduced cellular viability and appeared to be toxic to pBCEC in high concentrations (Figure 20).

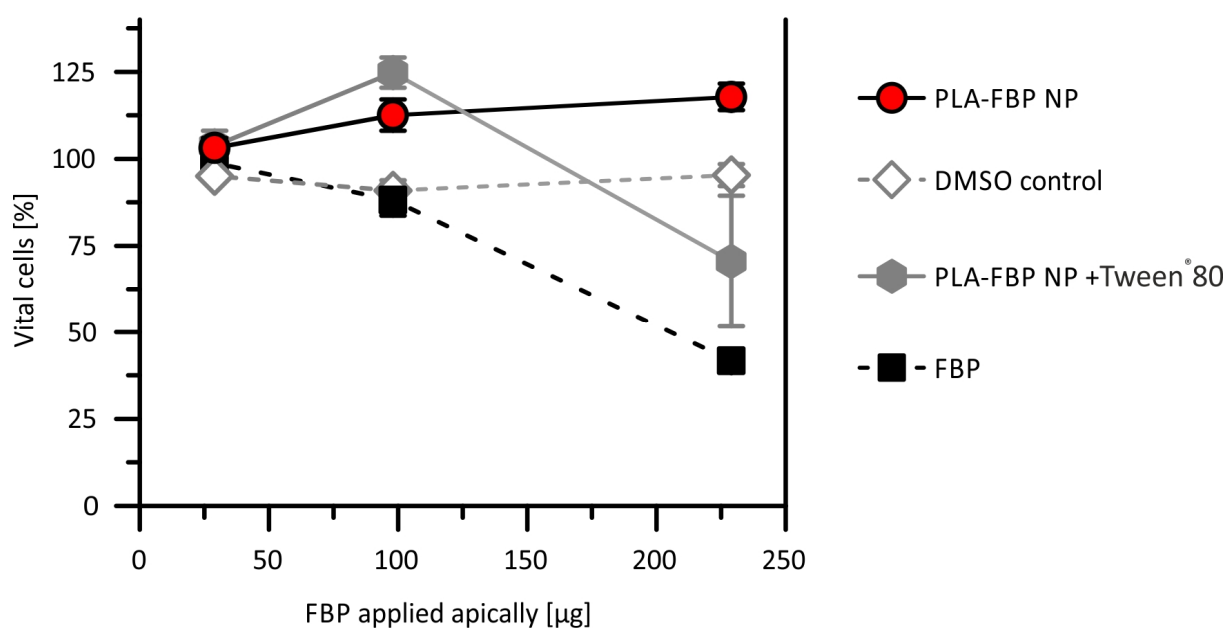


Figure 20: Cellular viability of *in vitro* blood-brain barrier model cells (pBCEC) after incubation of dissolved flurbiprofen (FBP) or flurbiprofen-loaded poly(lactic acid) nanoparticles (PLA-FBP NP). The pBCECs were incubated with increasing amounts of FBP or PLA-FBP NP and corresponding controls for 4 hours at 37 °C. Error bars as indicated, n is at least 3 from independent experiments with multiple internal replicas. Data partly published in [195].

4.2.3 Influence on transendothelial electrical resistance development

As transendothelial electrical resistance (TER) is a strong indicator for BBB integrity and pBCEC viability, the nanoparticles' influence on TER was checked for with the aid of a cellZscope® device.

Regarding short-term TER development, even low concentrations of the free drug FBP drastically decreased TER by more than 70 % in low concentrations, even by 90 % in high concentrations, therefore completely abolishing TER (Figure 21A, B). In contrast, PLA-FBP NP only caused minor, reversible drops in TER that rapidly recovered again. Although application of PLA-FBP NP forced a concentration dependent drop in TER, pBCEC nearly completely recovered during the following 4 hours. After PLA-FBP NP application, TER never dropped by more than 15 %, even in highest concentrations. Cells incubated with lower concentrations of PLA-FBP NP showed no major difference in further TER development (Figure 21A, B). The co-incubation of Tween®80 negatively impacted on TER development, but did not decrease TER by more than 50 % compared to original values. Control cells were treated with PBS to simulate the droplet-induced cellular stress.

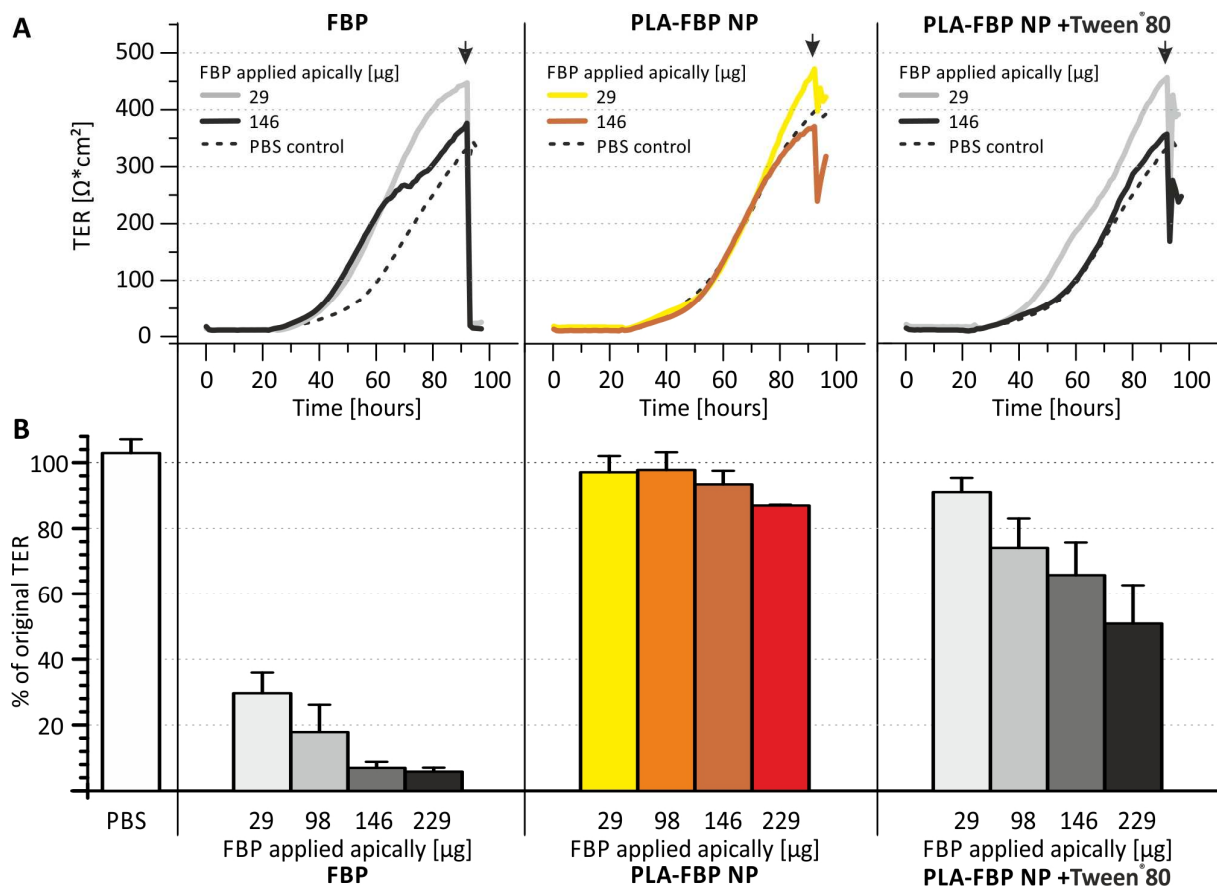


Figure 21: PLA-FBP NP influence on short-term development of transendothelial electrical resistance (TER). (A) After preparation, pBCEC were cultured on Transwell® inserts as described earlier and TER was monitored by a cellZscope® device. Nanoparticles (±Tween®80) or free drug were added (indicated by black arrow) when TER was still increasing. Lines represent representative measurements of pBCEC on Transwell® inserts treated with different drug concentrations or PBS as control. (B) Mean influence on TER after sample incubation is plotted for different concentrations of flurbiprofen, either applied as free drug or PLA-FBP NP (±Tween®80). Error bars represent SEM, n > 3. Data partly published in [195].

To investigate if nanoparticles influenced TER in the long term, PLA-FBP NP and the free drug FBP were applied to pBCEC and incubated for several weeks during which TER measurements were continuously performed automatically every hour in a cellZscope® device.

Cells treated with dissolved FBP reacted with a dramatic TER impairment that did not fully recover during the following weeks (Figure 22A). Furthermore, TER value development of FBP-treated cells did not compare to PBS-treated control cells (Figure 22A). In contrast, application of PLA-FBP NP barely affected the long-term development of TER in the *in vitro* pBCEC BBB model: although TER values did not always reach TER of the control cells during the next weeks, the general time course of TER development appeared similar for PLA-FBP NP-treated and PBS-treated control cells (Figure 22B). Pre-coating of nanoparticles with Tween®80 generally decreased TER values, but the time course of TER development appeared to be comparable to PLA-FBP NP-treated cells and controls (Figure 22B).

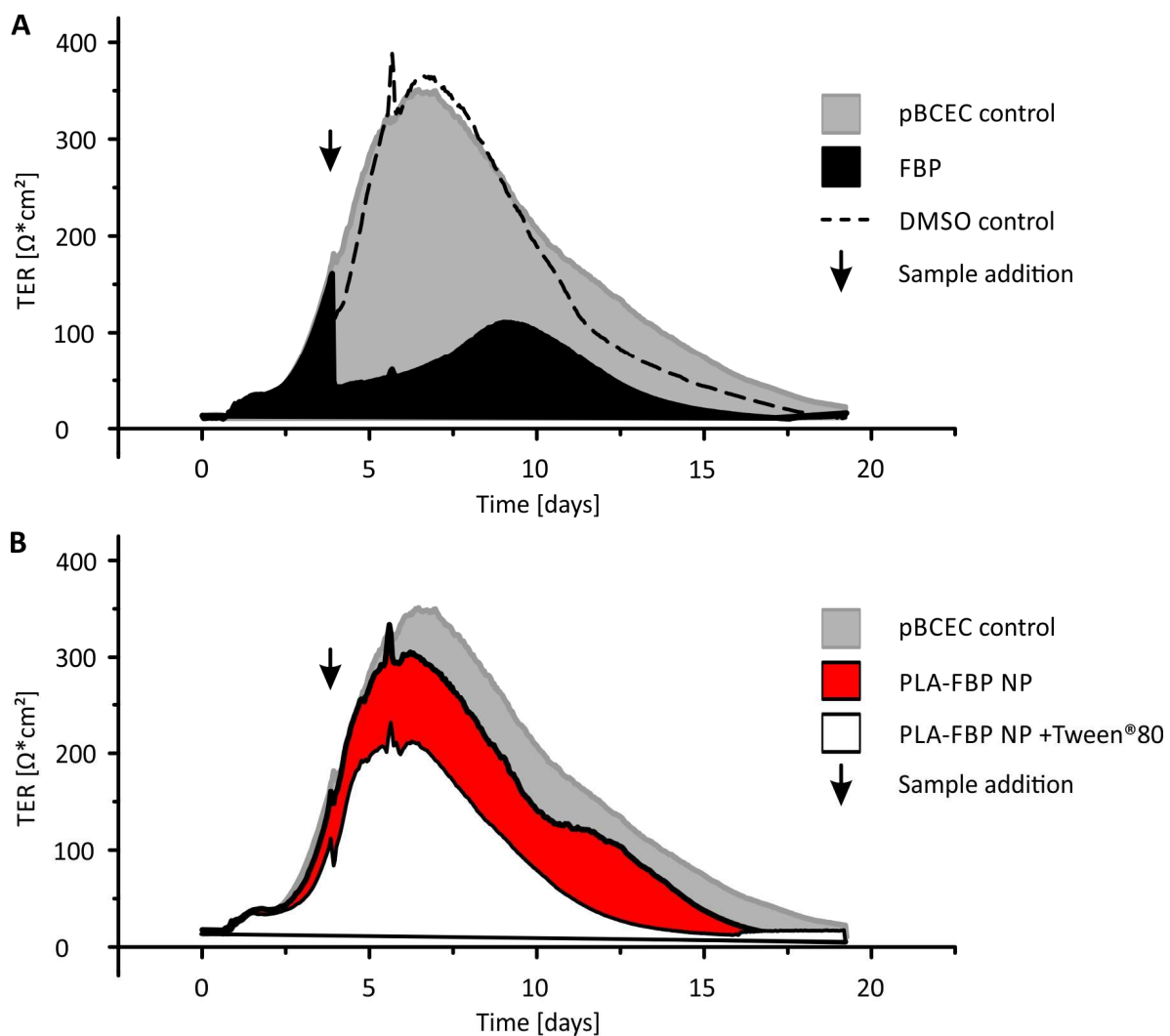


Figure 22: Influence of flurbiprofen (FBP), flurbiprofen-loaded nanoparticles (PLA-FBP NP) with or without Tween®80 on long-term transendothelial electrical resistance (TER). (A) Exemplary measurements of pBCEC treated with either 29 μg FBP (black filled curve) and corresponding DMSO control (dashed line). (B) Same experimental setup, this time 29 μg flurbiprofen from PLA-FBP NP with (white filled curve) or without (red filled curve) prior 1% Tween®80 coating of the nanoparticles was applied. Light grey filled curve represent control cells treated with PBS. Black arrows indicate time point of sample addition.

4.2.4 Influence on marker permeability and barrier integrity of the *in vitro* BBB model

The reversible decrease in TER (Figure 21) after PLA-FBP NP application might symptomize a short-term barrier disruption for pBCEC. This would be fatal, because it would mimic a transport process of PLA-FBP NP when actually the barrier became leaky.

To rule out a permeable barrier after nanoparticle application, freshly isolated pBCEC were grown on 3 μm pore Transwell® membranes as described in 3.2.1 and incubated with the free drug FBP and PLA-FBP NP (Figure 23A) while TER was still rising. In this experimental setup, the paracellular marker ^{14}C -inulin was simultaneously applied in order to identify fenestration or impairment of the pBCEC BBB model. As shown earlier in Figure 17, again pBCEC control cells were highly impermeable and only allowed less than 0.2 % of the apically applied ^{14}C -inulin to pass (Figure 23B). Increasing concentrations of flurbiprofen-loaded nanoparticles (PLA-FBP NP) did not increase permeability of ^{14}C -inulin, suggesting unaffected barrier integrity. Incubation with DMSO-dissolved flurbiprofen on the other hand had a drastic effect on barrier integrity (Figure 23B). Even the lowest concentrations of FBP increased ^{14}C -inulin permeability to more than 3.5 %, which compares to simultaneous mannitol application (see also Figure 17). Higher concentrations of FBP resulted in a drastic increase of ^{14}C -inulin permeability to over 15 %, indicating that the barrier function of the pBCECs was destroyed. The solvent DMSO itself negatively impacted ^{14}C -inulin permeability, but not as drastically as dissolved FBP (Figure 23B).

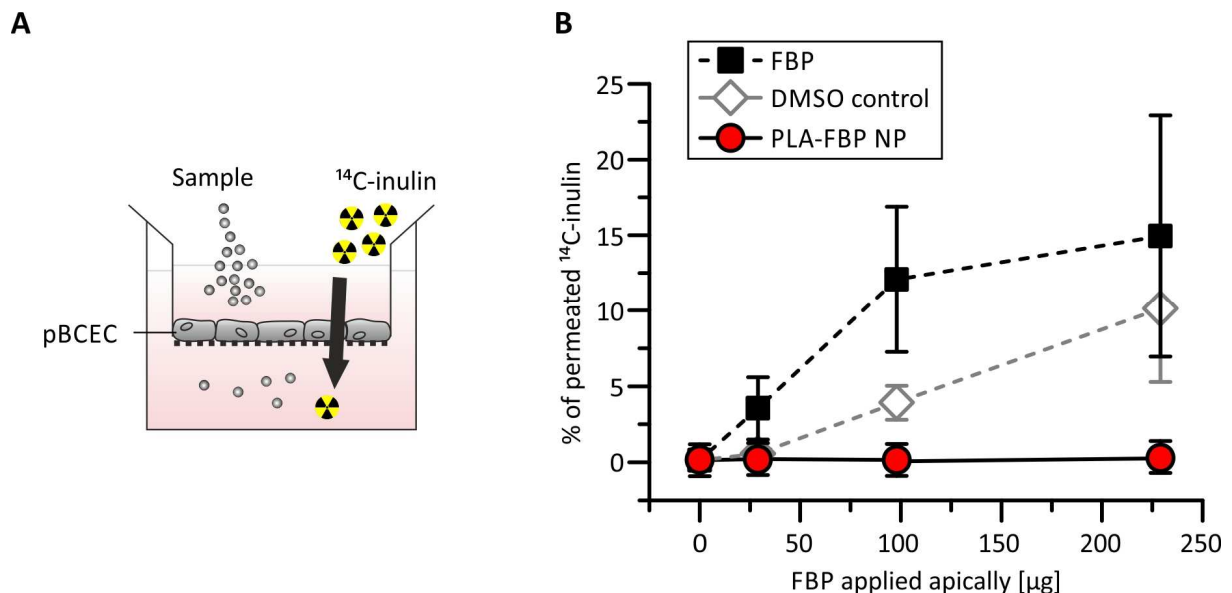


Figure 23: Influence of flurbiprofen and flurbiprofen-loaded nanoparticles on the permeability of the paracellular marker ^{14}C -inulin. (A) Schematic drawing of experimental design. Increasing concentrations of DMSO-dissolved flurbiprofen (FBP) or flurbiprofen-loaded PLA nanoparticles (PLA-FBP NP) were applied to pBCEC cultured in a cellZscope® device when transendothelial electrical resistance (TER) was sufficient. Simultaneously, the paracellular marker ^{14}C -inulin was added and incubated for 2 hours at 37°C. (B) Analysis of ^{14}C -inulin content in the basolateral compartment after sample addition, measured with the aid of a liquid scintillation counter (LSC). Error bars represent SEM, n is at least 3 from independent experiments with multiple internal controls. Data published in [195].

4.2.5 Concluding remarks on nanoparticle preparation and characterization

In this study, the basis material PLA was chosen for nanoparticle preparation for various reasons. Firstly, PLA itself is a common basis material used for nanoparticle preparation and displays excellent biocompatibility [55]. The human bodies' capability to degrade PLA was first described nearly 50 years ago [198] and explains why PLA was approved by the US Food and Drug Administration (FDA) for contact with biological fluids and a vast number of other applications, ranging from wrapping and catering material, agricultural use to medical technology, e.g. surgical implants.

Secondly, compared to HSA and PLGA, PLA in this study showed the most efficient flurbiprofen loading capacity. However, freeze-dried PLA-FBP NP quickly released the incorporated drug after redispersion. More than 75 % of flurbiprofen exits the nanoparticles during the first 6 hours in phosphate buffer [68, 197], which could be optimized in future preparation protocols.

Other basis matrices for nanoparticle preparation incorporating flurbiprofen could comprise alginate, gelatin or poly(butylcyanoacrylate) (PBCA) (for a review on nanoparticle preparation see [50]).

To investigate the nanoparticles' influence on the *in vitro* BBB model, several experiments were performed. Firstly, a cellular viability assay (alamarBlue[®]) revealed that pBCEC tolerated PLA-FBP NP application. In contrast, the free drug flurbiprofen (FBP) drastically decreased cellular viability in high concentrations. Coating the nanoparticles with Tween[®]80 reduced cellular viability in high concentrations. Secondly, the development of the pBCEC's transendothelial electrical resistance (TER), which represents an indicator for barrier function, was barely influenced by PLA-FBP NP application – neither in short-term, nor in long-term TER monitoring. Again, the free drug FBP drastically (and irreversibly) impaired TER, even in low concentrations. Coating the nanoparticles with Tween[®]80 negatively impacted on short- and long-term TER development, but not as drastically as the incubation of the free drug FBP. Thirdly, PLA FBP NP application did not increase ¹⁴C-inulin (a paracellular marker) permeability across the BBB model, which proves for an unimpaired barrier integrity. Application of free FBP caused a major increase of ¹⁴C-inulin permeability and therefore massively weakened the barrier function. All in all, the PLA-FBP NP used in this study are characterized by a very low cytotoxic potential and therefore suitable for further examination.

4.3 Nanoparticle-mediated drug transport across the *in vitro* barrier*

After characterizing the flurbiprofen-loaded, PLA-based nanoparticles (regarding physicochemical parameters and cytotoxic or barrier-disrupting potential) in the last section (see 4.2), this part of the study deals with the actual drug transport capacity of the nanoparticular formulation across the pBCEC *in vitro* BBB model, which displays excellent barrier characteristics (also see 4.1).

In brief, the following experiments were performed in order to investigate if the nanoparticles effectively convey the incorporated drug across the cellular barrier and if the transported drug is still biologically active and able to reduce A β 42 levels in the brain-representing compartment of the *in vitro* model (Figure 24). First, the cellular binding and uptake capacity of the drug-loaded nanoparticles was investigated in flow cytometry and confocal laser scanning microscopy (CLSM), for these processes are required for a successful transcytosis across the BBB. Next, the drug content in the different compartments of the *in vitro* pBCEC BBB model was analyzed by high-performance liquid chromatography (HPLC). The medium from the brain-representing compartment was subsequently transferred to a cellular *in vitro* Alzheimer's disease model (7WD10), which expresses a mutated amyloid precursor protein (APP) variant. A β 42 levels after incubation with the medium from nanoparticle-treated BBB model was assessed by an A β 42-recognizing enzyme-linked immunosorbent assay (ELISA). To rule out that a possible A β 42-reducing outcome was mediated by cytotoxic effects, the Alzheimer's disease *in vitro* model was investigated in a cellular viability assay (alamar[®]Blue) after application of nanoparticle-treated medium.

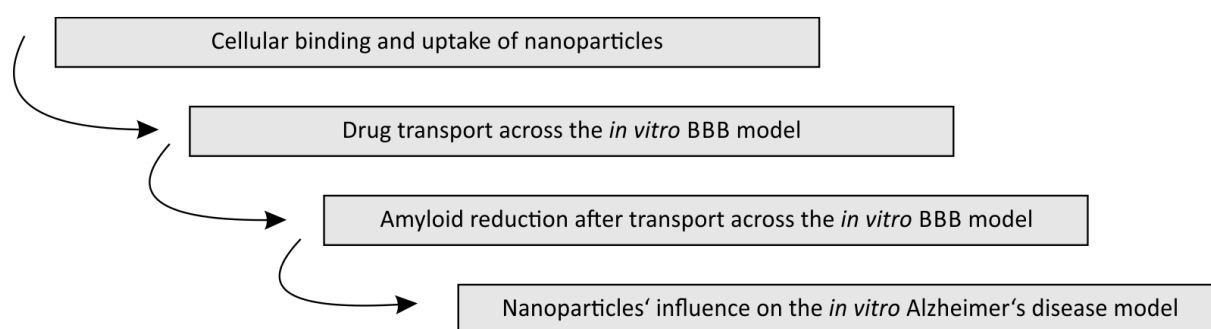


Figure 24: Flow chart of experimental design. Cellular binding and uptake of nanoparticles was checked for in flow cytometry and high resolution CLSM analysis. Drug transport capacity of the nanoparticles across the cellular barrier was assessed by HPLC analysis. Verification of preserved biological efficiency of the drug after nanoparticle packing was achieved by a functional A β 42 species ELISA. To ensure that a potential A β 42-lowering effect was not due to cytotoxicity, the Alzheimer's disease model cells were finally investigated in a cellular viability assay.

* Parts of this section were published in [68, 195].

4.3.1 Cellular binding of nanoparticles

When nanoparticles are intended to be used as carrier systems to overcome the blood-brain barrier by receptor-mediated transcytosis, the first step is binding to the cellular surface. Here, cell lines of different species (human HBMEC and murine bEnd3) as well as freshly isolated primary porcine brain capillary endothelial cells (pBCEC) were investigated for their ability to bind to drug-loaded poly(lactic acid) nanoparticles in flow cytometry analysis. For detection, a Lumogen® Orange label was introduced during the nanoparticle preparation process that allowed visualization at 539 nm. The fluorescent, flurbiprofen-loaded PLA nanoparticles (PLA-FBP-Lum NP) were applied to different blood-brain barrier model cells and incubated for 4 hours at 37 °C. Data was analyzed either by counting % *positive cells* or by measuring the binding intensity (displayed as *Y Geo Mean*) of nanoparticles. Nearly 100 % of the different endothelial model cells were positive in flow cytometry experiments after nanoparticle incubation, meaning that nearly all cells bound PLA-FBP-Lum NP (Figure 25A). This result was independent from the cellular model and equally true for HBMEC, bEnd3 or the primary pBCEC model systems. Binding intensity peaks (labeled as “Y Geo Mean”) shifted from cell type to cell type, whereas the human-derived BBB model cell line HBMEC most extensively bound PLA-FBP-Lum NP (Figure 25B). This data is in accordance with analysis concerning the expression of BBB relevant receptors (also see Table 4), revealing that (of the three cellular BBB models used in this study) HBMEC most extensively express receptors of the low density lipoprotein (LDL) receptor family. The LDL receptors (especially LRP1) were shown to play a key role in apolipoprotein-modified nanoparticle uptake in BBB model cells [81]. For PLA nanoparticles form a protein corona partially consisting of apolipoproteins [68] after incubation in plasma or serum-containing medium, the different LDL receptor expression of the various BBB model cell lines explains the altering binding capacity of the nanoparticles.

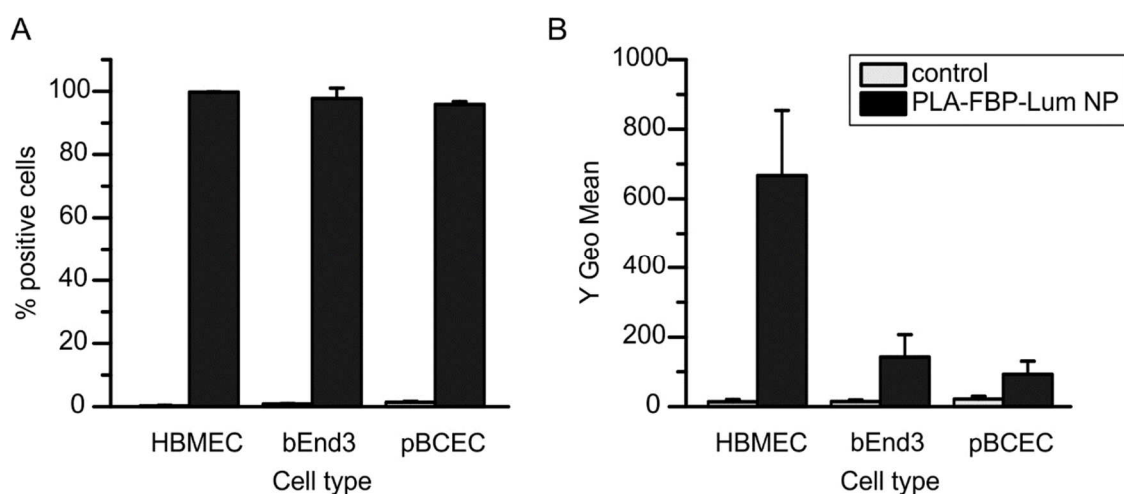


Figure 25: Binding capacity of PLA-FBP-Lum NP to different blood-brain barrier model cells in flow cytometry experiments. (A) Binding characteristics of PLA-FBP-Lum NP after 4 hours of incubation analyzed as “% positive cells”, displaying quantitative evaluation. Data partly published in [195]. (B) Same experiments analyzed by “Y Geo Mean”, representing the binding intensity of PLA-FBP-Lum NP to the different endothelial cells as indicated. Data was obtained in at least 3 independent experiments with multiple internal replicas.

4.3.2 Cellular uptake of nanoparticles

Cellular uptake of poly(lactic acid) nanoparticles was investigated in confocal laser scanning microscopy (CLSM). After incubating HBMEC with flurbiprofen-loaded, fluorescent poly(lactic acid) nanoparticles (PLA-FBP-Lum NP) and staining for the cytosol with CellTracker™ Blue afterwards, a correlation between the cytosolic staining (blue in Figure 26) and the signal for PLA-FBP-Lum NP (yellow) was detectable in effectively every cell. It appeared that the nuclei of the cells were not infiltrated with the fluorescent labeling molecules of the nanoparticles (Figure 26).

To strengthen this data, similar experiments were performed with primary porcine brain capillary endothelial cells (pBCEC) incubated with PLA-FBP-Lum NP. As shown for the cell line HBMEC, the cytosolic staining of pBCEC (blue in Figure 27) correlated with the fluorescent signal of the nanoparticles (yellow in Figure 27) when PLA-FBP-Lum NP were incubated for 4 hours at 37 °C.

In untreated control cells (upper panel in Figure 27), no nanoparticle signal was detected. Furthermore, nanoparticle incubation at 4 °C instead of 37 °C, completely abolished PLA-FBP-Lum NP uptake (lower panel in Figure 27).

Another experiment used confocal microscopy imaging to obtain pictures not only in x and y direction, but additionally in z coordinates (Figure 28) in order to reconstruct 3D images of PLA-FBP-Lum NP-treated pBCEC and rule out that scattered signals from the cellular surface might be mistaken for cellular uptake. Again, when incubation occurred at 4 °C, samples lacked cell associated nanoparticle signals (Figure 28A). In contrast, incubation at 37 °C provoked a correlation of the cytosol signal (blue) and the signal for the nanoparticles (yellow) (Figure 28B). The effect becomes particularly apparent when images are cropped (Figure 28C), underlining the cellular uptake of the nanoparticles by allowing insight into the cytosol (Figure 28C-F).

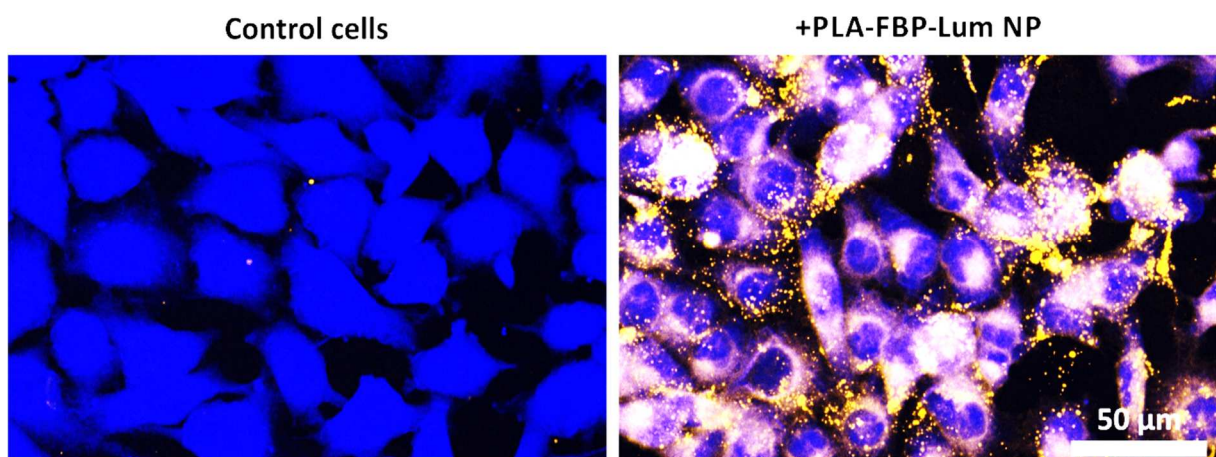


Figure 26: HBMEC uptake of fluorescent PLA-FBP NP. Confocal laser scanning microscopy (CLSM) revealed a clear correlation of the yellow fluorescent signals (nanoparticles) with the blue-stained cytosol of HBMEC cells (right image). In contrast, no yellow fluorescence signal was detected in control samples that were incubated with PBS instead of nanoparticles (left image) after 4 hours of incubation at 37 °C. Scale bar as indicated.

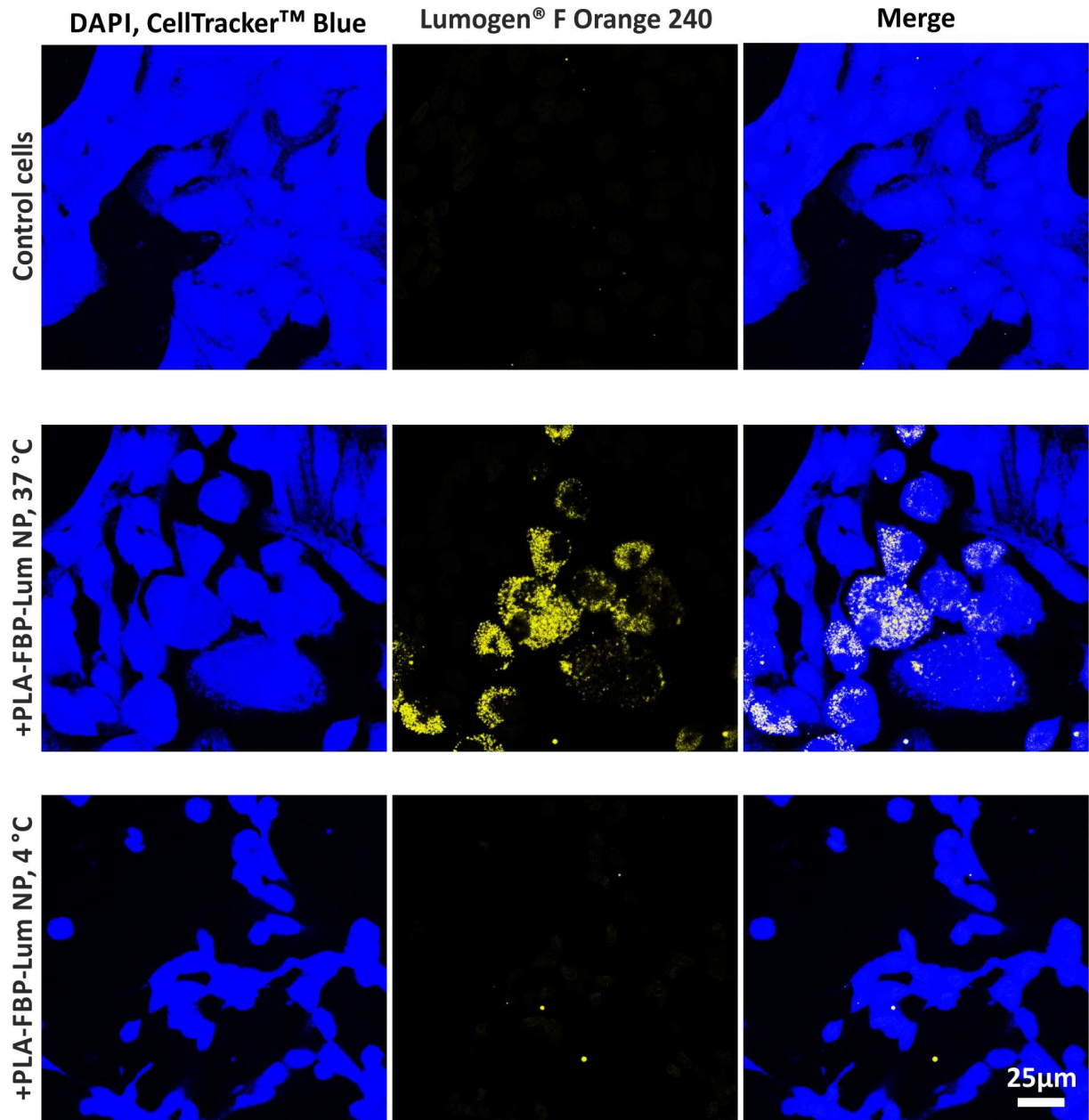


Figure 27: Primary pBCEC uptake of fluorescent PLA-FBP NP analyzed by confocal laser scanning microscopy (CLSM). Nanoparticles were incubated on pBCEC for 4 h either at 37 °C (middle panel) or 4 °C (lower panel). Cells without PLA-FBP-Lum NP incubation served as control (upper panel). After nanoparticle incubation, cells were stained with CellTracker™ Blue for 30 min; mounting medium for CLSM analysis contained DAPI. At 37 °C, PLA-FBP-Lum NP signals (yellow) correlated with the cytosol staining (blue), whereas for 4 °C incubation or control cells, no yellow signals were detectable in the cytosol. Scale bar as indicated.

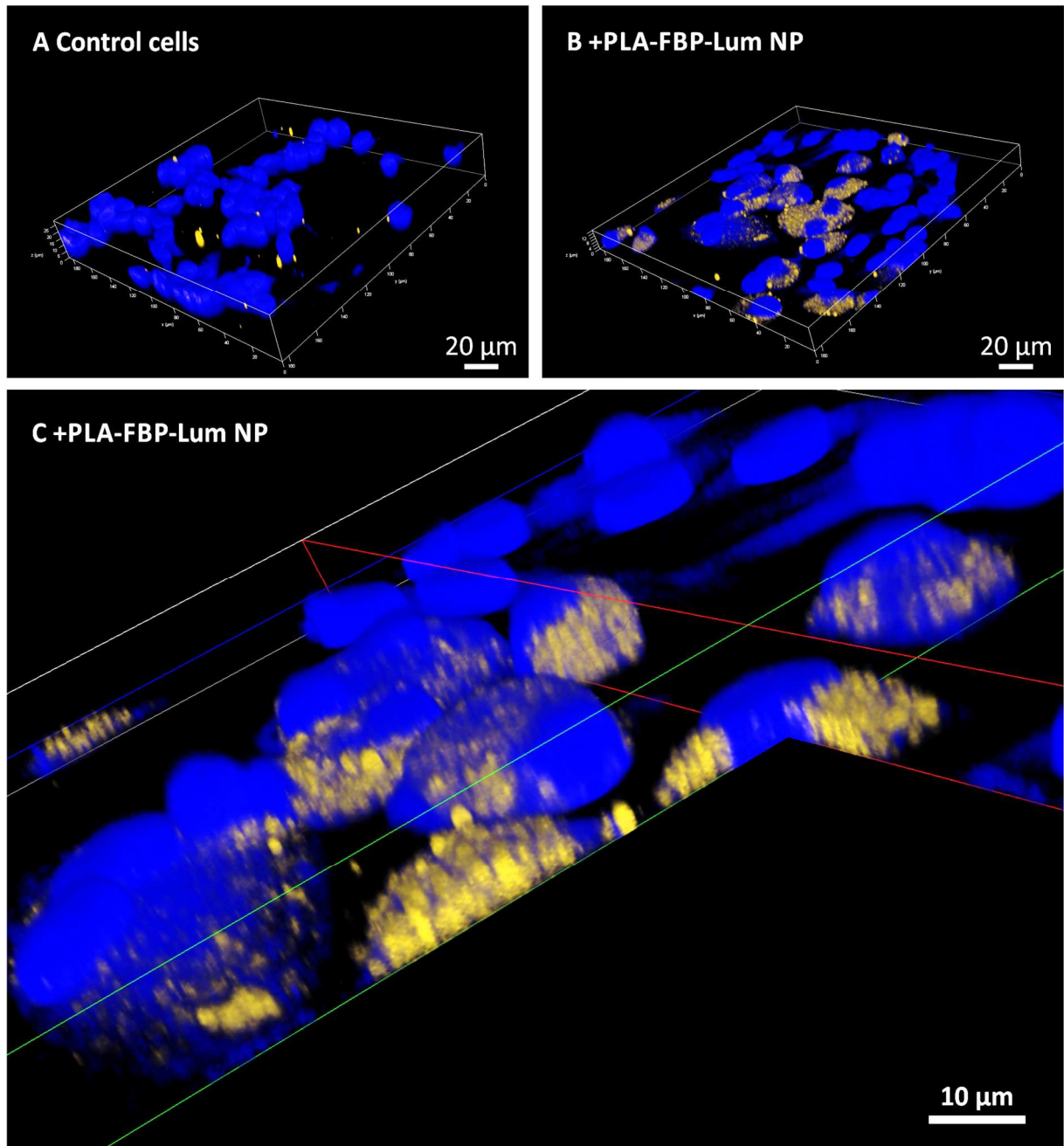


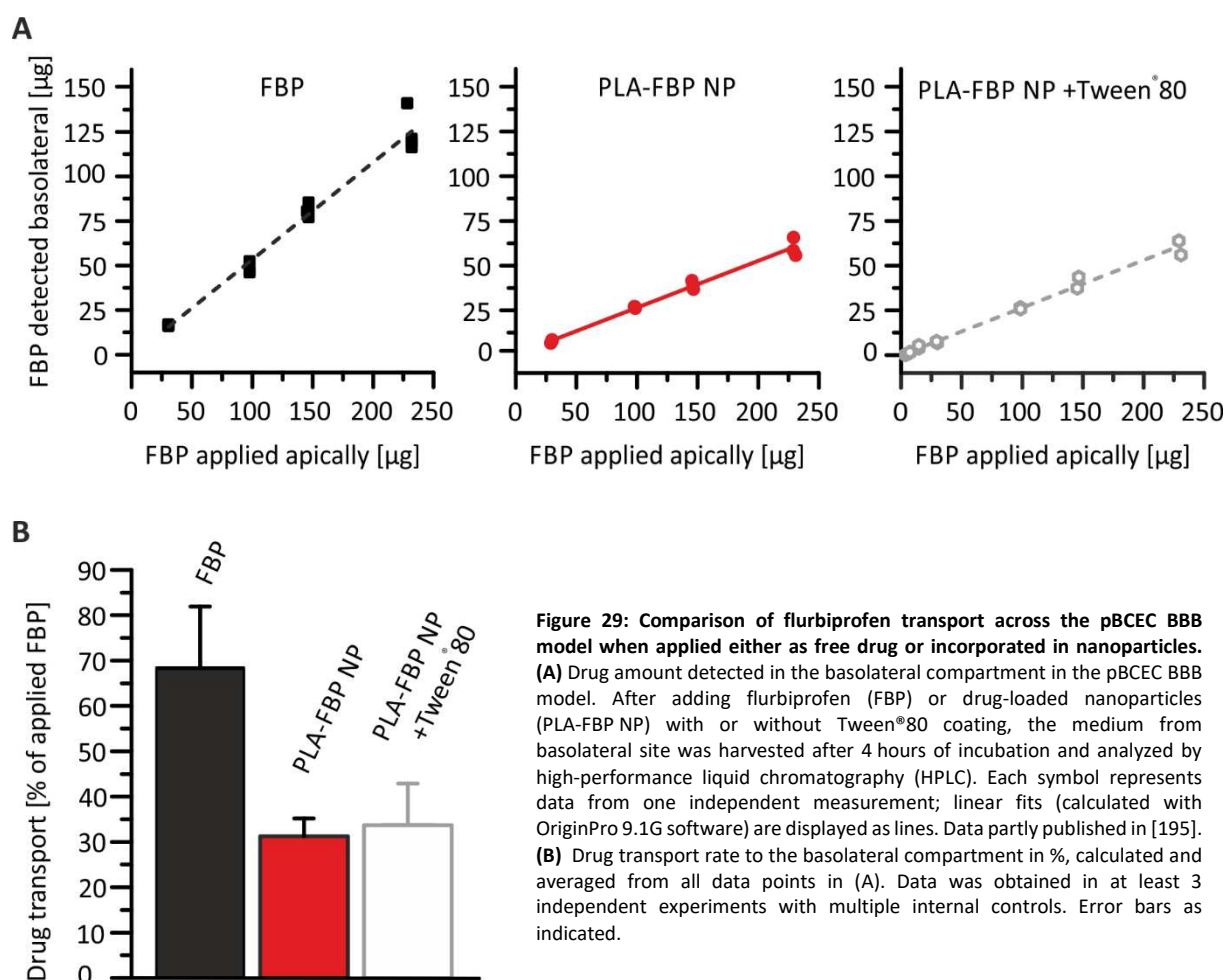
Figure 28: 3D projection of confocal laser scanning microscopy (CLSM) analysis of pBCEC after nanoparticle incubation. (A) Untreated control cells, cytosol was stained with CellTracker™ Blue, nuclei are DAPI stained. **(B)** Cells incubated at 37 °C with PLA FBP NP. Yellow signal for nanoparticles correlates with blue cytosol staining. **(C)** Magnification of cells positive for nanoparticle signals. Red and green line represent level for optical cutting in x and y direction. Front quarter was cropped to allow in insight into the cytoplasm. Nanoparticle signal seems to be distributed to the cytosol. Nuclei appear not to be infiltrated by nanoparticles. Scale bar as indicated. Data partly published in [195].

4.3.3 Drug transport studies

Total flurbiprofen transport across the barrier

To check if flurbiprofen-loaded nanoparticles release the incorporated drug on the brain-representing compartment of the *in vitro* BBB model, the basolateral media of pBCEC grown Transwell® inserts was collected after sample incubation and analyzed for flurbiprofen in high-performance liquid chromatography (HPLC).

Figure 29A displays single measurements for different concentrations of either the free drug or nanoparticle formulation and was used to calculate Figure 29B, which averages the transport rate of flurbiprofen across the barrier. More than 2/3 of apically applied flurbiprofen (FBP) was detectable in the basolateral (brain-representing) compartment (Figure 29A, B) after 4 hours of incubation in the *in vitro* pBCEC BBB model. When PLA-FBP NP were applied, less than 30 % of the incorporated drug passed the barrier, independent from Tween®80 coating of the nanoparticles. The large discrepancy between flurbiprofen transit when applied as free drug or incorporated in nanoparticles raised the question where PLA-FBP NP remained in the *in vitro* BBB model. Therefore, the model's compartments were analyzed separately in the next experiment.



Drug distribution within in the *in vitro* model

In order to localize the remaining PLA-FBP NP within the *in vitro* BBB model, the different compartments of the model were analyzed by HPLC separately:

To calculate the retrieval rate of the theoretically applied drug, medium from the apical, blood-representing compartment (grey in Figure 30) was incubated with acetonitrile in order to precipitate proteins from cell culture medium on the one hand, and disintegrate remaining nanoparticles to release the drug payload on the other hand. Transwell® inserts (white in Figure 30), seeded with pBCEC, were treated with DMSO to disintegrate the polycarbonate membrane and solubilize the cells, ideally dissolving the incorporated drug into the solvent matrix. Medium from basolateral, brain-representing compartment (black in Figure 30) was analyzed in HPLC without further treatment. Whereas for FBP the entire drug amount could be retrieved, retrieval rates for PLA-FBP NP were about less than 90 % (Figure 30A). For nanoparticles, about half of the calculated drug crossed the BBB model and was detected in the basolateral compartment (independent from Tween®80 coating) (Figure 30B), for the free drug FBP, basolateral values exceeded 60 %. When the total amount of the samples was set as 100 % (Figure 30B), nanoparticle samples had a higher retrieval rate (>6 %) in the Transwell® compartment than the free drug (<2 %). This data indicates that a proportion of PLA FBP NP could still be endocytosed inside the pBCEC and were not yet transcytosed across the *in vitro* BBB.

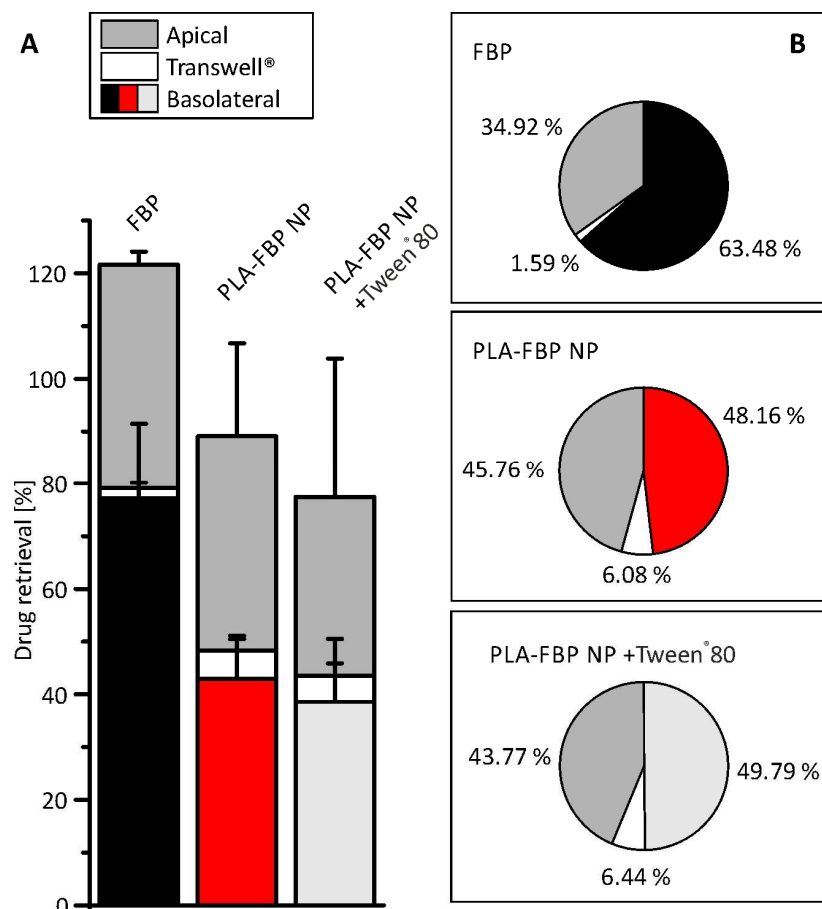


Figure 30: Drug retrieval in different compartments of the BBB model analysed by HPLC. (A) Percentage of drug retrieved in apical (grey), basolateral (black) or Transwell® (white) compartment of the BBB model when applying one exemplary concentration (146 µg FBP/TW) flurbiprofen. **(B)** Total retrieved drug values from (A) were set as 100 % in each sample, in order to quantitatively compare the different localizations of flurbiprofen. Data from at least 3 independent experiments with multiple internal controls. Error bars indicate SEM. Data partly published in [195].

4.3.4 A β 42 reduction by flurbiprofen-loaded poly(lactic acid) nanoparticles

Drugs should keep their biological efficacy after transport across the BBB. In order to assess if the incorporated flurbiprofen from nanoparticles can still reduce A β 42 levels *in vitro*, we designed an experimental setup with A β 42 overexpressing cells 7WD10 (Figure 31A).

After pBCEC (grown on Transwell® inserts as described) were incubated 4 hours with either flurbiprofen (FBP) or flurbiprofen-loaded nanoparticles (PLA-FBP NP), the basolateral medium was transferred to A β 42 overexpressing 7WD10 cells and left there for 72 hours (Figure 31A). The subsequent A β 42 ELISA revealed that the transported flurbiprofen from PLA-FBP NP can reduce the A β 42 levels to less than 70 % of the control level (Figure 31B). Nanoparticle coating with Tween®80 did not seem to enhance the effect. Similar concentrations of FBP reduced A β 42 to 30 % of the original level. The more pronounced A β 42 reducing effect of FBP was expected, because (as shown before in Figure 29) more drug was detected in the basolateral compartment after FBP incubation, compared to PLA-FBP NP application. However, FBP appeared to be toxic for pBCEC in higher concentration (shown in (Figure 20-23), indicating that the barrier became leaky after FBP application.

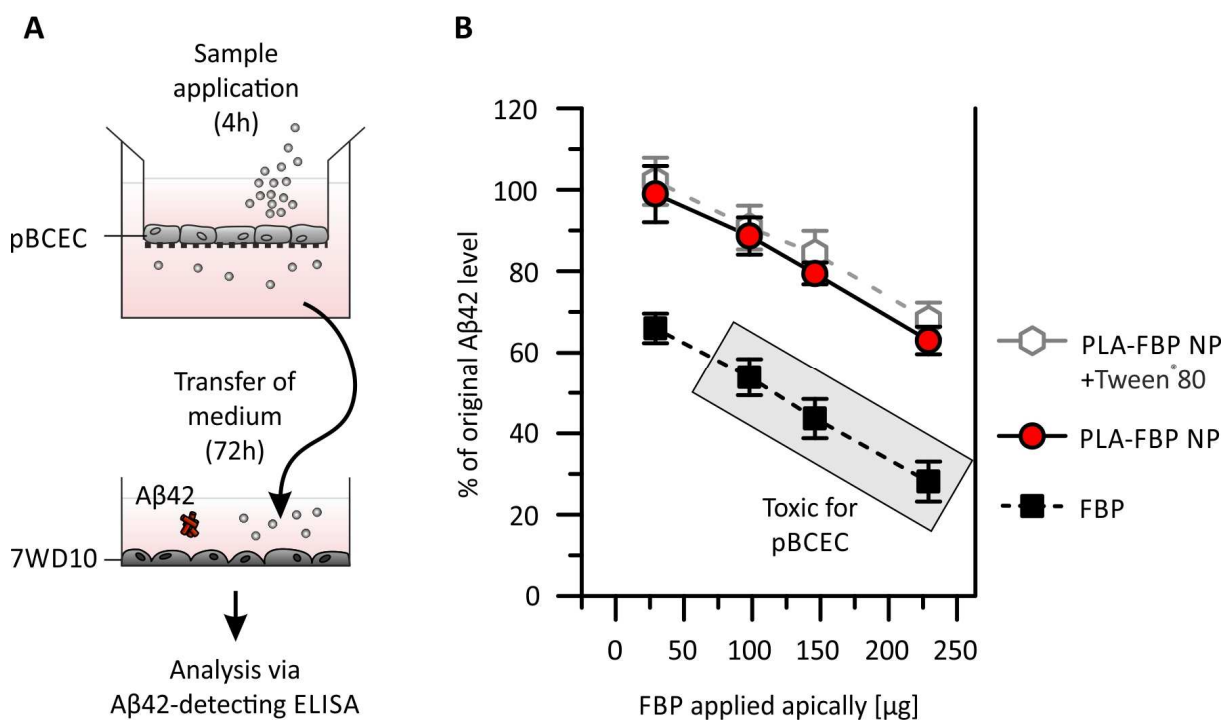


Figure 31: Flurbiprofen-loaded poly(lactic acid) nanoparticles (PLA-FBP NP) reduce A β 42 levels after transport across the *in vitro* blood-brain barrier (BBB) model. (A) Schematic drawing of experimental design: pBCEC were isolated and cultivated as described earlier. When transendothelial electrical resistance (TER) was adequate, samples were incubated for 4 hours. The apical compartment and pBCEC were then discarded and basolateral medium was transferred to culture plates seeded with A β 42 producing 7WD10 cells. After 72 hours, the supernatants were harvested and analyzed in a human A β 42-recognizing ELISA assay. **(B)** Increasing concentrations of applied flurbiprofen (FBP) gradually decrease A β 42 levels. PLA-FBP NP application achieves reduction of A β 42 levels to less than 70 % of the control samples, independent from Tween®80 pre-incubation. Grey rectangle indicates free FBP concentrations that showed a toxic effect on pBCEC in cellular Data from at least 3 independent experiments, error bars indicate SEM. Data partly published in [195].

4.3.5 Cellular viability of the Alzheimer's disease model cells 7WD10

In order to exclude that the transported flurbiprofen from apically applied drug-loaded nanoparticles may alter cellular viability of the Alzheimer's disease model cell line in the basolateral compartment, cytotoxicity assays after transport studies were performed. A decrease in cellular viability could cause false positive results for A β 42 reduction in the subsequent assay.

FBP or PLA-FBP NP (\pm Tween[®]80) were first applied to the apical compartment of the *in vitro* blood-brain barrier model for 4 hours. Then, the basolateral medium was transferred to the 7WD10 cells (Figure 32A). 7WD10 cells were not negatively affected by the samples. Even after 72 hours of incubation, all treated cells displayed viability values near 100 % compared to untreated control cells.

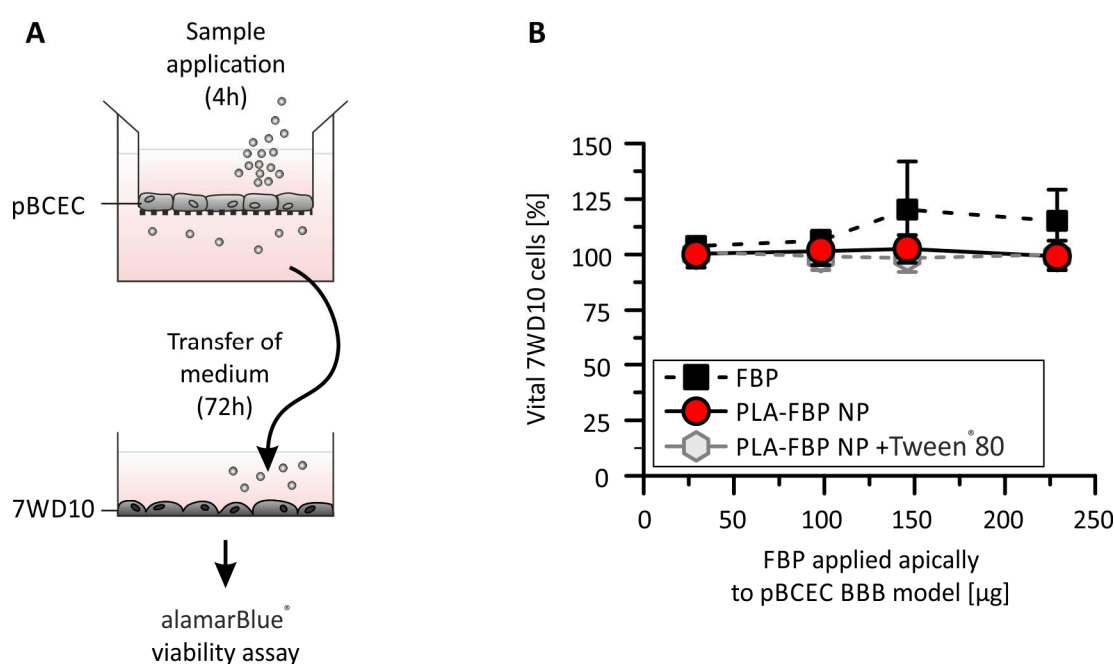


Figure 32: Nanoparticles' influence on the Alzheimer's disease model (7WD10) cells' viability after crossing the pBCEC BBB model. (A) Schematic drawing of experimental design: pBCEC were incubated with FBP or PLA-FBP NP (\pm Tween[®]80). After 4 hours, medium of the basolateral compartment was transferred to the 7WD10 cells for 3 days, before performing an alamarBlue[®] cell viability assay. **(B)** Data from cellular viability assay. 7WD10 cells treated with basolateral medium from control Transwell[®] inserts without drug application were set as 100 % vital. Data from at least 3 independent experiments, error bars indicate SEM. Data partly published in [195].

4.3.6 Summary drug transport

The first step in nanoparticle-mediated transcytosis for drug transport comprises binding of the particles to the cells' surfaces at the blood-representing site, followed by an uptake into the cytoplasm of the BBB model cells and finally a release process at the brain-representing site.

The binding characteristics of PLA-FBP NP were investigated by using the primary *in vitro* BBB model (pBCEC) as well as commonly used BBB model cell lines (bEnd3, HBMEC). Flow cytometry revealed that the nanoparticles strongly bound to the cells, although binding intensity differed from model to model, being strongest for the human-derived cell line HBMEC. However, flow cytometry data in this case

includes both surface-bound nanoparticle signal and intracellular signal, therefore confocal laser scanning microscopy (CLSM) was also performed to further investigate cellular uptake. CLSM analysis allowed optical sectioning by focusing on selected depths of samples and thereby provided insight access into the nanoparticle-treated cells. CLSM data revealed that the nanoparticle signal correlated with the cytosolic staining, verifying cellular uptake of PLA-FBP NP in endothelial cells.

Next, the drug transport capacity of PLA-FBP NP was investigated in HPLC analysis. Flurbiprofen from PLA-FBP NP was detected in the brain-representing compartment of the primary *in vitro* BBB model after 4 hours incubation in the blood-representing compartment, verifying that the nanoparticulate formulation and drug-loading efficacy is suitable for this purpose. In this study's experimental setup, transit of free FBP was about twice as high as for PLA-FBP NP. However, the BBB crossing of FBP is rather due to barrier disruption than active transport for several reasons: As stated earlier, FBP performed poorly regarding cellular viability of the pBCEC, also TER and C^{14} -inulin permeability were strongly influenced by FBP. Another disadvantage of FBP application was the low solubility of FBP in water, which required the use of solvents. In this study, FBP was dissolved in DMSO. However, DMSO is poorly compatible with the basis material (polycarbonate) of the Transwell® inserts, and can dissolve the actual membrane structure. Although a very low volume (>20 μ l) of DMSO was applied to a total volume of 2.5 ml, an effect of the DMSO became apparent in 14 C-inulin permeability assays, indicating that even the DMSO solvent destroys the barrier function of pBCEC grown on polycarbonate Transwell® membranes. FBP therefore is not a suitable control in drug transport experiments in this experimental setup.

Finally, this study's data verifies that drug transport from flurbiprofen-loaded poly(lactic acid) nanoparticles (PLA-FBP NP) is sufficient to evoke a biological effect and reduce A β 42 levels in the brain-representing compartment of the pBCEC model – most importantly, without impairing the barrier function of the barrier. HPLC analysis of flurbiprofen content in the brain-representing compartment verified this conclusion; supporting the promising binding and uptake experiments of the nanoparticles with endothelial cells.

In a recent publication [68], we could already underpin this study's data by showing that PLA-FBP NP successfully reduced A β 42 levels by more than 25 %. Nevertheless, using a simpler, murine cell line-based BBB model consisting of bEnd3, the study had one major limitation. bEnd3 cells only develop low TER values ($\sim 40 \Omega \cdot \text{cm}^2$), not comparable to the *in vivo* situation (e.g. in fetal rats around $300 \Omega \cdot \text{cm}^2$, in adult rats up to $1,400 \Omega \cdot \text{cm}^2$) [196]. Here, this gap was closed by using a more advanced, primary pBCEC-based model with higher TER values ($300\text{-}1,200 \Omega \cdot \text{cm}^2$). Additionally, intact barrier integrity was verified by checking for permeability of radiolabeled, non-transportable tracers to minimize false positive results in drug transport studies.

This promising *in vitro* data suggests that PLA-FBP NP could also be used to transport flurbiprofen to the brain *in vivo*. The approach shows major benefits compared to the application of the drug alone. Flurbiprofen is indeed capable of lowering A β 42 levels in an *in vitro* Alzheimer's disease model, consisting of 7WD10 cells that secrete A β peptides. However - in contrast to PLA-FBP NP - the application of the dissolved drug is toxic to pBCEC (verified in cellular viability assays) and drastically impairs the BBB integrity (shown in transendothelial electrical resistance measurements and permeability assays with radiolabeled ^{14}C -inulin). Since flurbiprofen destroys the barrier function of the *in vitro* BBB model, more drug crosses the pBCEC layer (verified in HPLC analysis and A β 42 ELISA). In the first study, flurbiprofen also evoked cytotoxic effects on bEnd3 cells prohibiting application of corresponding concentrations of dissolved drug compared to PLA-FBP NP [68]. Here again, a cytotoxic effect in viability assays was observed. In addition, DMSO-dissolved flurbiprofen increased ^{14}C -inulin permeability (even low concentrations) (Figure 23), making the dissolved drug an unsuitable control for drug transport studies.

Furthermore, it was investigated if the pre-coating of nanoparticles with the surfactant Tween[®]80 increased drug transport capacity across the *in vitro* pBCEC BBB model. Surfactants generally lower the surface tension between two liquids or between a liquid and a solid. For nanoparticles, it was widely proposed that surfactant (like Tween[®]80) coating of nanoparticles facilitates brain transport in *in vivo* experiments. Hypothetically, Tween[®]80 coating is expected to anchor lipoproteins from sera or plasma, thereby enhancing endocytosis processes at the BBB, because the bound proteins (like ApoE) from the blood or cell culture medium promote uptake by BBB specific receptors (for review see [47]). Other (less likely) hypotheses state that Tween[®]80 coatings could act either by inhibiting efflux pumps (especially P-glycoprotein) or by a general effect characterized by endothelial membrane fluidization and enhanced permeability (for review see [47]).

Many brain targeting nanoparticles coated with Tween[®]80 show promising study outcomes (Table 1). For PLA-based nanoparticles, evidence exists that Tween[®]80 enhances brain uptake. For example, Sun *et al.* reported that for BBB crossing of their FITC-loaded PLA nanoparticles, Tween[®]80 coating was actually required in their *in vivo* experimental setup [88]. Interestingly, in this study's experimental setup, the pre-incubation of PLA-FBP NP with Tween[®]80 did not enhance BBB crossing, indicated by unaltered A β 42 reduction in the following functional experiments. This is in accordance with the HPLC data showing that Tween[®]80 coating of PLA-FBP NP did not enhance flurbiprofen concentration in the brain-representing compartment after application to the blood-representing compartment.

Kreuter recently reviewed that for some nanoparticular formulations (like PLGA-based nanoparticles) Tween[®]80 coating was not as efficient for BBB transit than other surfactants [47]. Therefore, other surfactant coatings that were shown to enhance crossing of the BBB (like Pluronic-F68[®]) could be tested

for PLA-FBP NP in the future. However, Meister *et al.* used the same PLA-FBP NP that were used in this study and applied them to a simpler BBB model consisting of bEnd3 cells [68]. The sodium dodecyl sulphate polyacrylamide gel electrophoresis (SDS-PAGE) and Western blot data (Figure 33A, B) showed that a protein corona appeared on the surface of the nanoparticles – notably without prior surfactant coating of the nanoparticles. So, the PLA-FBP NP obviously adsorbed to apolipoproteins, regardless of surfactant coating. The protein corona appeared already after 5 min of plasma incubation (Figure 33A) and increased over time, rather quantitatively than qualitatively. Notably, the protein corona partially consisted of ApoE3 (Figure 33B). Apolipoproteins enable receptor-mediated uptake by lipoprotein receptors at the BBB, and ApoE-coupling to nanoparticles allows active endocytosis of the nanoparticles via the low density lipoprotein receptor-related protein 1 (LRP1) [81]. Here, it seems that in the case of PLA-FBP NP, Tween®80 coating does not seem to play a major role for drug transport *in vitro* (but should nevertheless be taken into account for possible *in vivo* studies). Alternatively, direct coupling of relevant ligands to the nanoparticles' surface could be applied. Consequently, the next section of this thesis concentrates on further describing a potential ligand for PLA-FBP NP to improve BBB crossing.

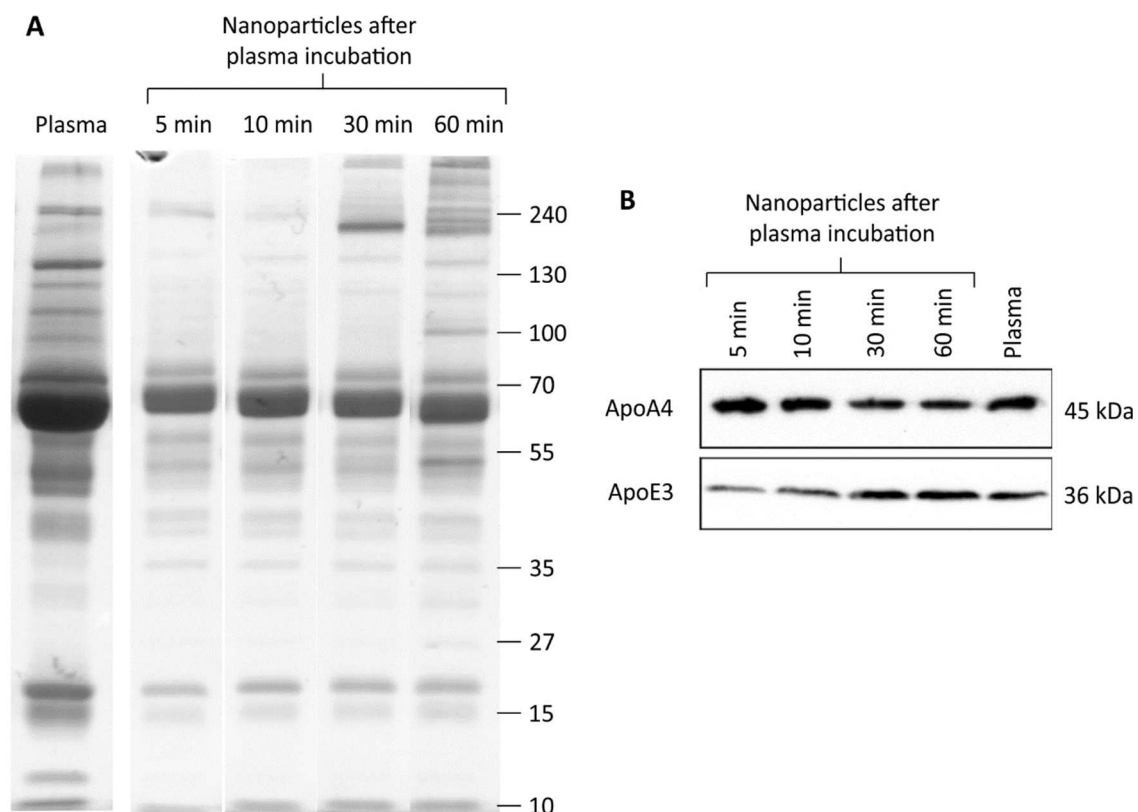


Figure 33: Protein corona of PLA-FBP NP after plasma incubation without surfactant coating. (A) Coomassie Blue-stained SDS-PAGE of nanoparticles incubated with human plasma for different periods as indicated. The nanoparticle-plasma protein complexes were separated from human plasma by sucrose cushion centrifugation before gel electrophoresis. Protein corona formation on nanoparticles is already visible after 5 min of plasma incubation and the amount of bound protein seems to increase over time. (B) Western blot data of the nanoparticle-protein complexes stained for Apolipoprotein A4 (α -ApoA4) and E (α -ApoE). Image copied and modified from [68].

4.4 A suitable ligand for *in vivo* application: Apolipoprotein E3*

For this study's *in vitro* transport experiments (see 4.3), flurbiprofen-loaded nanoparticles without a surface modification were used. However, for *in vivo* application, a specific ligand modulation would be desirable to specifically target receptor-mediated transport across the blood-brain barrier.

Coupling apolipoprotein E3 (ApoE3) to the nanoparticles' surface targets the low density lipoprotein receptor (LDLR) family, in particular the low density lipoprotein receptor-related protein 1 (LRP1), for specific transport. This next section summarizes the preliminary experiments for specific ligand coupling.

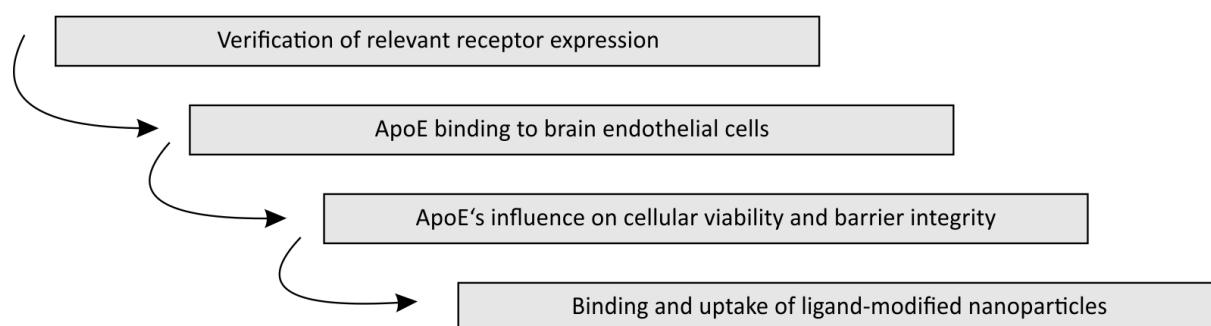


Figure 34: Flow chart of the experimental design. Different model cells (pBCEC, bEnd3, HBMEC) were tested for the expression of relevant blood-brain barrier receptors in flow cytometry after antibody staining. Next, cells were incubated with fluorescent ApoE3 or ApoE3-modified nanoparticles and analyzed in flow cytometry or confocal laser scanning (CLSM) experiments. The cytotoxic potential of ApoE3 was investigated considering permeability, viability and influence on transendothelial electrical resistance (TER).

4.4.1 Verification of receptor expression

The different *in vitro* BBB model cells (pBCEC, HBMEC and bEnd3) robustly express the surface receptors LDLR, LRP1 and LRP2 (also known as Megalin) (Table 4). The human-derived cell line HBMEC most extensively expresses the receptors compared to bEnd3 and pBCEC. Cells were stained with specific primary antibodies and fluorescent secondary antibodies and subsequently analyzed in flow cytometry measurements. The signal increased in a concentration-dependent manner when compared to control cells (incubated without the primary antibody). For clarity, only one antibody concentration per sample is displayed.

* Parts of this section were published in [195].

Table 4: Expression low density lipoprotein receptor protein receptor (LDLR) family members. Different endothelial cells were antibody-stained for receptors expressed at the BBB *in vivo* and analyzed in flow cytometry experiments. Data from at least 3 independent experiments with multiple replicas of >10,000 cells. Symbols represent proportion of % positive cells: (-) <10 %; (+) 11-49 %; (++) 49-90 %; (+++) >90 %

	pBCEC	bEnd3	HBMEC
LDLR	++	+++	+++
LRP1	++	++	+++
LRP2	++	++	+++

4.4.2 ApoE binding to blood-brain barrier model cells

To address the question if the planned ligand binds to *in vitro* BBB model cells, ApoE3 was fluorescently labeled with a commercially available kit (also see 3.2.8) and investigated in flow cytometry experiments. For this screening experiment, the human BBB model cell line HBMEC was used to avoid time and cost-consuming primary cell preparation of pBCEC. As shown in Table 4, HBMEC expresses the relevant receptors required for lipoprotein binding.

Fluorescent ApoE3 (ApoE-633) in a concentration of 1 $\mu\text{g}/\text{cm}^2$ showed excellent binding that was reduced by about 40 % when unlabeled ApoE3 (in a 10-fold excess) was applied for competitive displacement at the LRP1 receptor (Figure 35). A random protein of comparable molecular weight (ovalbumin) that was not expected to be specifically transported via the LRP1 receptor served as a negative control and was simultaneously fluorescently labeled. As expected, the basal binding of the fluorescent ovalbumin (Ov-633) was unaltered by co-incubation with 10-fold excess of free, unlabeled ApoE3 (Figure 35). The binding of ApoE3 therefore is assumed to be specific.

Similar binding experiments were performed in a 4 °C environment, instead of 37 °C (Figure 35). As Wagner *et al.* showed in 2012 for ApoE3-modified nanoparticles, it was confirmed that also the uptake of free, fluorescently labeled ApoE3 is an active process that cannot be performed if the cell's metabolism is reduced to a minimum. Values for the mean fluorescence intensity dropped by >95 % when cells were incubated at 4 °C instead of 37 °C for four hours.

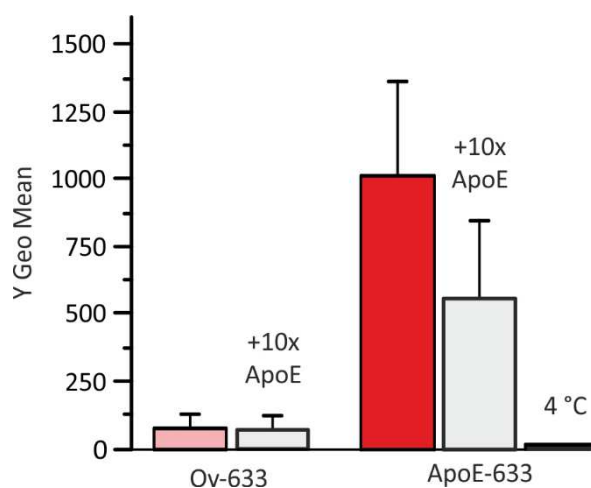


Figure 35: ApoE binding to brain endothelial cells. The human cell line HBMEC was incubated with fluorescence-labeled ApoE3 (ApoE-633) or ovalbumin (Ov-633) for 4 hours at 37 °C or 4 °C before analyzing binding intensity (described as Y Geo Mean) by flow cytometry. Untreated pBCEC served as control and threshold setting. Unlabeled ApoE3 in a 10-fold excess was added as indicated to check for competitive displacement at the specific receptors. Data from at least 3 independent experiments with multiple replicas of >10.000 cells.

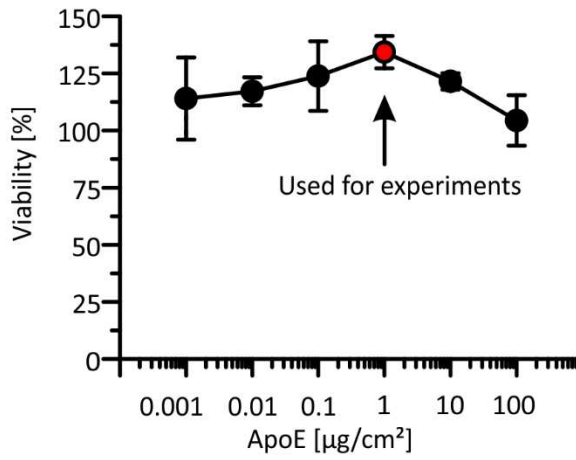
4.4.3 ApoE influence on barrier integrity and viability of primary BBB model cells

ApoE3 was tested for its potency to reduce cellular viability *in vitro*. ApoE3 showed no relevant reduction in viability when applied in concentrations up to 100 µg/cm² (Figure 36A). After excluding a cytotoxic effect, ApoE3 was also investigated for its potential to alter the permeability of radiolabeled marker substances in the primary pBCEC BBB model. As described earlier, pBCEC were isolated from freshly slaughtered pig brains and cultivated in a cellZscope[®] device to monitor their barrier qualities. When the transendothelial resistance (TER) was still rising, permeability experiments with radiolabeled ¹⁴C-inulin were performed.

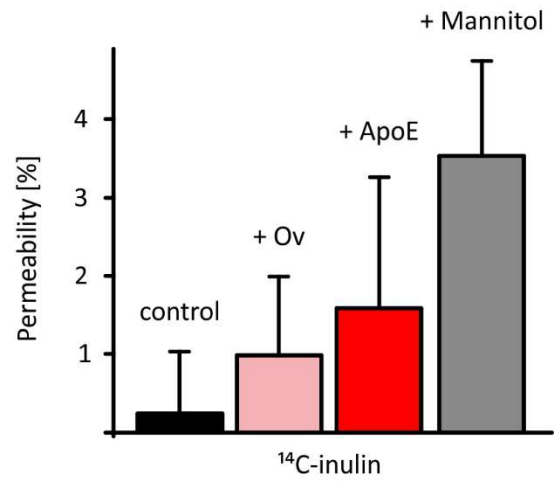
After exposure of ¹⁴C-inulin (0.4 µCi/ml) to the apical compartment, only about 0.2 % of the originally applied substance was detectable in the basolateral compartment - indicating good barrier integrity of the primary model system (see also 4.1.3). In contrast, addition of 1 µg ApoE3/cm² growth surface promoted permeability of ¹⁴C-inulin, although data can only be interpreted as a trend, because statistical significance was not achieved. As a further control, hyperosmotic mannitol solution was applied together with the ¹⁴C-inulin. As expected, the permeability of the radiolabeled marker rose drastically (Figure 36B), implying physiological characteristics.

Next, ApoE3 was tested for its influences barrier integrity by application to pBCECs during TER measurements in a concentration of 1 µg ApoE3/cm² growth surface. While the TER values of control cells still increased after a comparable droplet of PBS was applied to the Transwell[®], the TER of samples incubated with ApoE3 decreased (Figure 36C). The concentration was equivalent to the amount of the ApoE3 coupled to the nanoparticles when applied in the standard concentration of 100 µg NP/cm² growth surface. However, in terms of experiments with nanoparticles, these concentrations will not be attained at the cellular level, because the ApoE3 is coupled to the surface of the assumed spherical structure. The surface of a sphere is defined as $S = 4\pi r^2 = \pi d^2$. If the diameter of the nanoparticle is approximately 200 nm, surface area totals to 125250 nm². This results in a very low actual concentration of ApoE3 at the cellular surface. In accordance with this assumption, ApoE3-modified nanoparticles show substantial milder effects on TER in the equivalent ApoE3 concentration per incubation surface: Wagner *et al.* reported in a study investigating uptake mechanisms for ApoE-modified HSA-based nanoparticles a rapid, reversible drop in TER after incubation that appeared to be less drastic than the free ApoE3 in this study's experiments [81]. Overall, ApoE3 appears to alter barrier integrity without being toxic to the primary *in vitro* BBB model pBCEC.

A



B



C

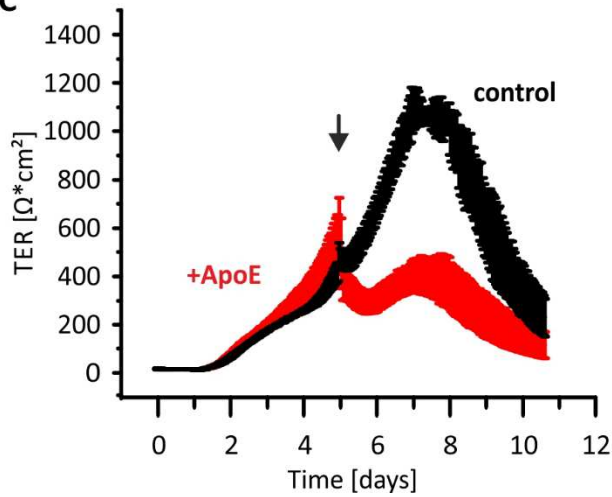


Figure 36: Cell – ligand interactions of ApoE3 and pBCEC. (A) Influence of ApoE3 on cellular viability of pBCEC was assessed in a cellular viability assay after cells were incubated with different concentrations of ApoE3. PBS-treated cells served as negative control and were assumed to be 100 % vital. (B) Influence of ApoE and ovalbumin (Ov) on barrier integrity of primary pBCEC. Mannitol was added to test for physiological characteristics of the BBB model. (C) Influence of ApoE3 on transendothelial resistance (TER) of pBCEC grown on 0.4 µm Transwell® membranes. One exemplary experiment out of at least 3, PBS-treated cells served as control. Data from >3 independent experiments with multiple internal controls.

4.4.4 Binding and uptake of ligand-modified nanoparticles

The previously described drug transport experiments in section 4.3 were performed by using unmodified, drug-loaded nanoparticles. It was shown that, after human plasma incubation, these nanoparticles form a protein corona consisting of apolipoproteins [68]. For coupling of apolipoproteins to nanoparticles can increase BBB translocation [59, 66, 81, 199], the next step in this study comprised ligand modification of poly(lactic acid)-based nanoparticles.

A PEGylation of the nanoparticles surface allowed coupling of the ligand ApoE3 (PLA-PEG-ApoE NP) or the control protein ovalbumin (PLA-PEG-Ov NP). The amount of covalently bound ApoE to the nanoparticles was 14.8 μg protein/mg NP, comparable to the amount of bound ovalbumin (11.48 μg /mg NP) (Table 5). The diameter of unmodified PLA NP was 244.1 nm, confirming previous data (see Table 3). Ligand-modification slightly increased the nanoparticles' diameter to 266.9 nm for PLA-PEG-ApoE NP and 263.1 nm for PLA-PEG-Ov NP. Next, the preparation procedure of the PLA-PEG-ApoE NP was slightly changed and lacked NaOH in the buffer composition (PLA-PEG-ApoE NP w/o NaOH). Thereby the ApoE3 binding reaction is expected to be diminished, representing a further control to verify specific, ApoE3-mediated uptake of the nanoparticles. The diameter of these control PLA-PEG-ApoE NP w/o NaOH was unexpectedly larger (285 nm) compared to PLA-PEG-ApoE or Ov NP. Similar to experiments in section 4.3.1 and 4.3.2, cellular binding and uptake of ligand-modified nanoparticles was checked for. Flow cytometry experiments revealed that incubating different endothelial cells (HBMEC, pBCEC) with PLA-PEG-ApoE NP drastically enlarged binding capacity, compared to unmodified control nanoparticles (PLA NP) (Figure 37A, B). Binding of PLA-PEG-ApoE NP w/o NaOH was similar to PLA NP. Coupling of the random protein ovalbumin (resulting in PLA-PEG-OV NP) also scaled down binding to pBCEC.

CLSM analysis indicated that PLA-PEG-ApoE NP entered primary endothelial cells (Figure 36C, D). Primary pBCEC were incubated either with ApoE3-modified PLA nanoparticles for 24 hours at 37 °C. The blue signals for DAPI-stained nuclei and yellow nanoparticle fluorescence did not overlap indicating a cytosolic distribution. Untreated control cells lacked cell specific nanoparticle signals.

Table 5: Characterization of ligand-modified poly(lactic acid) (PLA) nanoparticles and control nanoparticles. Table of NP characteristics. Diameter and dispersity index were measured with the aid of a Zetasizer Nano ZS. The amount of bound protein was calculated indirectly by detection of unbound protein in the supernatant after NP purification by gel permeation chromatography (GPC) analysis. For visualization, all NP were labeled with 1.5 μg Lumogen® F Orange 240/mg NP.

	Diameter (nm)	Poly dispersity index (PDI)	Bound protein ($\mu\text{g}/\text{mg}$ NP)
PLA NP	244.1	0.064	-
PLA-PEG-ApoE NP	266.9	0.075	14.8
PLA-PEG-ApoE NP w/o NaOH	285.0	0.106	-
PLA-PEG-Ov NP	263.1	0.132	11.5

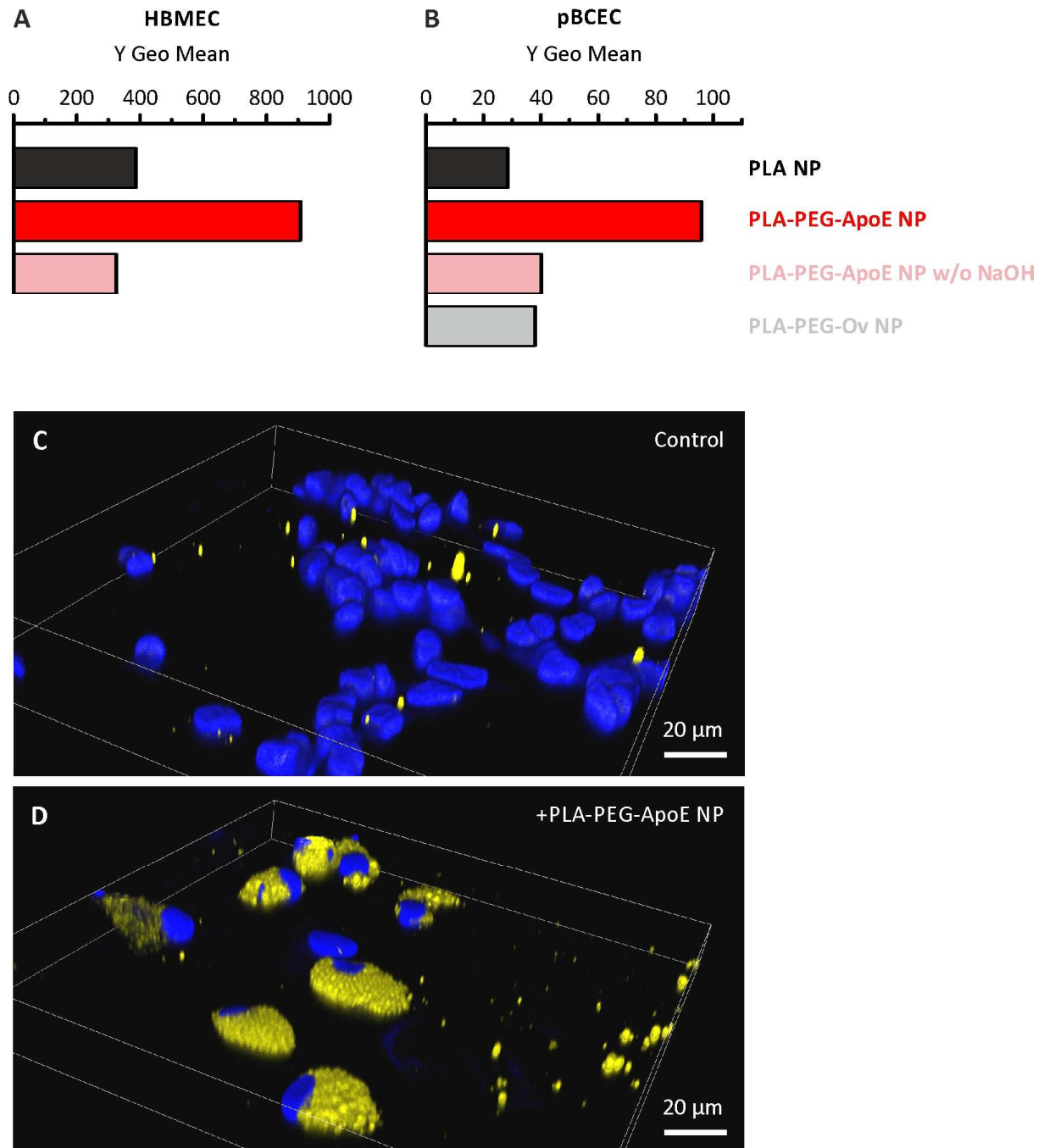


Figure 37: Influence of ApoE3 modification on nanoparticles' binding and uptake characteristics in endothelial cells. In pilot flow cytometry experiments, (A) HBMEC or (B) pBCEC cells were incubated with 105.3 μg NP/cm² growth surface for 4 hours at 37 °C. ApoE3-modified nanoparticles (PLA-PEG-ApoE NP) strongly increased binding intensity, compared to unmodified control nanoparticles (PLA NP). If the preparation procedure of PLA-PEG-ApoE NP was modified and lacked NaOH in the buffer (PLA-PEG-ApoE NP w/o NaOH), binding capacity dropped drastically again. Nanoparticle modification with the control protein ovalbumin (PLA-PEG-Ov NP) did not seem to strongly alter binding compared to unmodified nanoparticles (PLA NP). The effect was also observed for other concentrations and incubations times (data not shown). n=1. Note different y axis increment. Data from (B) was published in [195]. Cellular uptake of PLA-PEG-ApoE NP was checked for in primary pBCEC analyzed by confocal laser scanning microscopy (CLSM): (C) In control samples, no cell specific nanoparticle signal was detectable; (D) after 24 h of incubation with PLA-PEG-ApoE NP, nanoparticulate accumulation in the cytoplasm appears (yellow) was apparent. Pilot experiment, n=1. Nuclei are DAPI stained (blue). Scale bar as indicated.

4.4.5 Concluding remarks on ligand modification

Previous studies demonstrated that modification of nanoparticles with apolipoproteins facilitates the transport across the BBB *in vitro* and *in vivo* [26, 59, 66, 77, 81, 200]. This effect was already reported for human serum albumin (HSA)-based nanoparticles and is especially important for *in vivo* application to promote targeted transport across the BBB in the body. Examples for successful brain targeting formulations are loperamide-loaded [78, 90, 91] and obidoxime-loaded [26] ApoE3-modified nanoparticles. Loperamide, for example, an opioid drug used against diarrhea, does not cross the BBB *in vivo* and consequently does not reduce pain. However, it shows analgesic effects if it is injected directly into the brain or loaded into ApoE3-modified HSA nanoparticles that are intravenously injected into mice. These animals react less sensitive in a tail-flick test, vividly demonstrating the elegant potential of nanoparticle-mediated drug transport to the brain [77].

Here, nanoparticles that were coupled to apolipoprotein E3 or control ligands were used. Pilot experiments with these nanoparticles suggest that pBCEC take up ApoE3-modified PLA nanoparticles (PLA-PEG-ApoE NP). Furthermore, PLA-PEG-ApoE NP bind stronger to brain capillary endothelial cells than control nanoparticles. Elegantly, the control nanoparticles are in this case not just PEGylated nanoparticles, but particles that are prepared by the exact same procedure except for the lack of NaOH during the coupling phase (preventing the functionalization of free OH groups for coupling ligands). All in all, it is therefore likely that ApoE3-modification of flurbiprofen-loaded nanoparticles (PLA-FBP NP) also will enhance brain transport capacity of the incorporated drug *in vivo*.

5 OUTLOOK & SCIENTIFIC CONTEXT

5.1 Optimization of nanoparticles for flurbiprofen transport

Drug-loading capacity, release profile and surface modification

Although flurbiprofen-loaded poly(lactic acid) nanoparticles (PLA-FBP NP) used in this *in vitro* study displayed very promising results in terms of low cytotoxic potential, crossing of the *in vitro* BBB model and capability to reduce amyloid burden in a subsequent *in vitro* Alzheimer's disease model, many ways of further improving them exist.

Firstly, the drug release profile of PLA-FBP NP used in this study is rather quick, meaning that the complete drug loading is released within a few hours after redispersing the freeze-dried nanoparticles. For the *in vitro* study, the release profile was sufficient, but for *in vivo* experiments, a retarded drug release profile of PLA-FBP NP is more desirable. *In vivo*, nanoparticles can be transported to the brain as fast as 15 min after intravenous injection [59], but a sustained drug release in the brain parenchyma would prolong treatment intervals for humans. Possibilities to produce "retard nanoparticles" in the future comprise coating with different guarding substances, such as chitosan or PEG (for review see [201]). It is also possible to produce multilayer nanoparticles that bear a PLA-based, FBP-loaded core with shells of different material in order to keep the drug inside the particle for a longer time.

Secondly, the nanoparticle formulation for flurbiprofen transport should further be improved to allow a ligand-modification on the one hand, and an optimal drug-loading efficacy on the other hand. In this study, PLA served as a nanoparticle basis material due to its advantageous flurbiprofen-loading capacity (compared to HSA- or PLGA-based nanoparticles). Furthermore, coupling of the surface ligand ApoE3 to unloaded PLA nanoparticles was achieved (PLA-PEG-ApoE NP). In summary, one nanoparticle species with a ligand modification without drug loading (PLA-PEG-ApoE NP) and another nanoparticle without ligand, but with drug loading (PLA-FBP NP) were available for *in vitro* testing. In the future, one nanoparticle must possess these two critical key attributes: it must be capable of selectively crossing the blood-brain barrier (due to a surface modification) and must bear a sufficient amount of the drug flurbiprofen to evoke biological effects.

Nanoparticle trafficking and tracking in vitro and in vivo

The question arises if the *in vitro* BBB model depicts realistic local *in vivo* concentrations. The pBCEC BBB model is based on a simple Transwell® system, meaning the endothelial cells grow horizontally on a porous membrane. Also, the system lacks any fluidic movements and is therefore a static system. This does not portray the realistic circumstances at the neurovascular unit since in human brains more than 600 ml of blood passes the capillaries per minute with a mean flow velocity of 1 mm/s [202]. Without question, the local concentration of nanoparticles that can interact with the BBB surface *in vivo* will be considerably lower. Therefore, the data obtained in this *in vitro* study cannot predict an outcome in humans, but rather serves as a proof of concept for future experiments. The data obtained from the pBCEC BBB model is less prone to be false positive results compared to weaker *in vitro* BBB models and confirms PLA-FBP NP as appropriate technology for transporting drugs to the brain.

This study only indirectly suggests that drug-loaded nanoparticles crossed the *in vitro* BBB model, because detection occurred via analyzing the released drug at the brain-representing site by HPLC and biological efficacy of the released drug via an A β 42-detecting ELISA assay and not the actual nanoparticles themselves. It would therefore additionally be interesting to track the nanoparticles in *in vitro* and *in vivo* experiments. Different strategies exist to label nanoparticles with radioactive tracer molecules since either incorporated or bound proteins can be labeled [203] or the nanoparticles' basis material (e.g. PLGA) [204] can bear radioactive molecules.

If nanoparticles consist of or bear proteins or peptides, iodination strategies [205] are a convenient way to add a radioactive tracer (depending on the amino acid that becomes labeled). Commonly, the Bolton-Hunter reagent (^{125}I , ^{131}I) is used for iodination of proteins. It can be applied directly to peptide or protein samples and conjugates to terminal amino groups effectively introducing radioactive iodine. This technique is non-oxidative and less harsh to proteins than alternative methods. One disadvantage is that iodine isotopes have relatively short half-lives (60 days for ^{125}I and 8 days for ^{131}I) and need to be used very soon after labeling. Here, Bolton-Hunter iodination could be used to label either HSA-based nanoparticles or ApoE3-modified PLA-based nanoparticles in order to monitor transport across the *in vitro* BBB model. Another way to achieve radiolabeled nanoparticles is to label one of the nanoparticles components before the actual nanoparticle preparation process. Various methods and isotopes exist that allow traceable nanoparticle formulations. Tritium (^3H) (a radioactive isotope of hydrogen) can be used to label peptides [206]. The low energy β emitter has a half-life of 12.32 years, making it convenient for laboratories. Peptides can be easily tritium labeled by catalytic exchange, e.g. it would be possible to ^3H -label the ApoE3 ligand before or after nanoparticle modification. Using *N*-succinimidyl [2,3- ^3H]propionate (^3H NSP), the reaction is similar to using Bolton-Hunter reagent and labels free amino groups with less alteration of the protein structure, though with lower specific

activity compared to Bolton-Hunter reagent. Also, it is possible to tritium label the basis material as companies offer custom synthesized ^3H -PLGA formulations [204] that can be further used to prepare nanoparticles respectively.

Peptide labeling can also be achieved by ^{14}C [207]. Theoretically, ^{14}C -labeled amino acids can be incorporated in peptides or ^{14}C can be added to the N-terminus of peptides by acetylation of free amino groups with ^{14}C acetic acid. However, compared to tritium labeling, this approach is rather expensive and reduced in specific activity [208].

A further step to investigate nanoparticulate trafficking routes in the body is to follow *in vivo* routes by high resolution imaging techniques, such as magnetic resonance imaging (MRI). For this purpose, the ferrimagnetic compound magnetite (Fe_3O_4) can be introduced to nanoparticles. We already showed that magnetite-labeled HSA nanoparticles can be detected in rats with clinical MRI scanners with limited sensitivity, although further investigations with ligand-modified, magnetite-labeled HSA nanoparticles are needed to reliably visualize brain uptake [209]. A magnetite labeling of PLA-based nanoparticles that carry a flurbiprofen loading would also be desirable to test in *in vivo* MRI trafficking experiments. Different groups already demonstrated that it is possible to prepare magnetic nanoparticles that consist of, or carry PLA [210, 211]. Further elucidation the potential of PLA-FBP NP as anti-Alzheimer's disease drug would be possible by adapting the preparation protocol to produce magnetic PLA-FBP NP for MRI analysis.

Nevertheless, past experiments have shown that even the best *in vitro* data cannot accurately reflect the *in vivo* situation, especially not for brain delivery. Since flurbiprofen already failed in clinical trials, the *in vitro* data of this study needs to be critically regarded and confirmed with great care, requiring verification *in vivo*. The study outcome is not yet confirmed in animal models, which would be essential to further promote PLA-FBP NP in anti-Alzheimer's disease drug development. The body distribution of this nanoparticulate formulation would be of utmost importance to correlate the *in vitro* data with *in vivo* trafficking and suitability as a brain drug.

5.2 Improving models: Can *in vitro* data predict *in vivo* outcome?

“Animal experiments will remain necessary in biomedical research for the foreseeable future” [212] states the Basel Declaration, a document signed by scientists from Switzerland, Germany, the United Kingdom, France and Sweden to promote alternatives to working with laboratory animals. The basic 3R principle (replace, reduce, refine) aims at avoiding and reducing animal tests and suffering of laboratory animals. One important cornerstone to achieve this goal are *in vitro* models.

In drug development research, *in vitro* models are commonly used before testing promising formulations in *in vivo* animal studies or in clinical trials with healthy humans or diseased patients (strictly regulated by official institutions such as the US Food and Drug Administration (FDA) or the European Medicines Agency (EMA)). Especially advanced (close to *in vivo*) models can reduce false positive study outcomes and limit the number of candidates suited for *in vivo* studies and clinical trials – saving research money and decreasing ethical concerns.

Alzheimer’s disease models

In this study, 7WD10 cells (a widely reported cell line heterogeneously overexpressing amyloid precursor protein 751WT (APP751WT) prone to peptide aggregation) were used as an *in vitro* Alzheimer’s disease model. As for all simplified *in vitro* models, this cell line cannot replicate all characteristics of Alzheimer’s disease, but is rather used to explore the pharmacological efficacy in targeting the amyloid cascade in a controlled experimental setup.

Generally, great effort has been made to improve *in vitro* cellular Alzheimer’s disease models. Israel *et al.* reprogrammed primary cells from patients suffering from either the familial or sporadic Alzheimer’s disease by using induced pluripotent stem cell (iPSC) technology [213]. They further characterized their model for pathological markers like amyloid- β levels and phosphorylated τ and treated purified neurons with β - and γ -secretase inhibitors to investigate phenotypes relevant to Alzheimer’s disease. In a recent *Nature* publication, Choi *et al.* introduced familial Alzheimer’s disease mutations (in APP and PSEN1) in a neural stem-cell-derived model cultured in a three-dimensional setup [214]. These cells produced amyloid- β (and also amyloid- β plaques) and aggregated phosphorylated and filamentous τ . Application of β - and γ -secretase inhibitors reduced amyloid- β pathology and also tauopathy [214].

A further step in testing anti-Alzheimer’s disease drug candidates are *in vivo* models, but the situation is complicated. As the most common animal model *Mus musculus* does not suffer from dementia itself and so far no neurotoxin has been discovered that induces Alzheimer’s disease in mice (as the compound 1-methyl-4-phenyl-1,2,3,6-tetrahydropyridine (MPTP) does for a Parkinson’s disease phenotype). Nevertheless, generation of genetically modified mouse models drastically increased the

understanding of Alzheimer's disease pathology and improved preclinical testing of potential therapeutics [215]. However, it is vital to keep in mind that alterations in these transgenic animals can lead to potential confounding factors due to overexpression of A β or τ . Models based on the amyloid hypothesis (used to test A β reducing strategies) are, for example, Tg2576 [216]. These mice overexpress a mutant APP and show A β plaques comparable to those observed in humans, even though these animals lack neuronal tangles or neuronal loss. Analogously, τ transgenic models (e.g. Tg4510 [217]) overexpress a mutant τ form and display neurofibrillary tangles, functional deficits and brain atrophy. Furthermore, the elegant 3xTg Alzheimer's disease mouse model combines three gene mutations (tauP301L, APPK670N/M671L and PS1M146V) and displays three of the Alzheimer's-associated characteristics: amyloid aggregation, fibrillary tangles and deficiencies in synaptic transmission.

A very recent model uses *Octodon degus*, a rodent native to South America, as a sporadic Alzheimer's disease model: apparently, these animals spontaneously develop pathological hallmarks associated with Alzheimer's disease, such as amyloid- β plaques and τ deposits; also, they develop a decline in cognition with age [218]. All in all, the *Octodon degu* model seems to fulfil a plethora of Alzheimer's characteristics found in humans, including molecular, cellular and even behavioral aspects, making it a unique natural rodent model for neurodegeneration.

Still, no currently established disease model can display all aspects that are reported for Alzheimer's disease in humans. Therefore, it will always be necessary to reconfirm *in vitro* and *in vivo* animal data in clinical trials to prove efficacy in Alzheimer's disease therapy in humans.

Blood-brain barrier models

Overall, this study suggests that the monoculture of the primary porcine *in vitro* model based on pBCEC represents a strong, physiologically comparable fort. This conclusion was also recently underpinned in [219]. Also, using swine primary material closely resembles human conditions regarding genome, anatomy and physiology [220] (unlike many other experimental animal species), but lacks ethical concerns compared to using primary primate cells. Nevertheless, there is a plethora of possibilities to further improve.

As cells never grow isolated in a physiological system, advanced *in vitro* models focus on multiple cell type cultures and three dimensional setups. Literature bursts of studies concerning co-cultures of endothelial cells with astrocytes, pericytes and neurons or even aforementioned triple-cultures. Especially astrocytes, which *in vivo* cover more than 90 % of the endothelial cells' surface, seem to play a major role. Many reports claim an increased blood-brain barrier integrity of model cells if astrocytes (or even astrocytoma cell lines like 1321N1) are cultured on the opposite side of the Transwell®

membranes, or if astrocyte-covered membrane disks or if sole astrocyte-conditioned media are added to endothelial cell cultures [19, 221–223].

Other innovative *in vitro* cell culture models try to remodel the natural blood flow of the *in vivo* situation by expanding to a third dimension (3D models) or introducing dynamics and fluidics, because the lack of shear stress in static models (like Transwell® inserts) can influence barrier characteristics, like the expression of TJ proteins and BBB-relevant ion channels and transporters. Inducing shear stress at the endothelial cells' surface alone can induce a convergence to *in vivo* situations and can improve barrier integrity, as well as the separation into compartments allowing co-culturing of different cell types (endothelial and neuronal cells, astrocytes, pericytes). Current microfluidic models that allow multiple cell cultures in different compartments comprise, for example, NDIV-BBB [28, 29], μ BBB [30] and SyM-BBB [31]. These systems mimic a blood flow through a vessel that is better suited for drug transport studies than the static, horizontal Transwell® system. In a 3D blood vessel model, sedimentation of substances is not possible and detection of the substances at the other side of the barrier is more likely due to active transport processes. This allows a better predictability for the transport of a drug *in vivo*. Nevertheless, in all three models the culture surface is rather small (e.g. in [30]: 10 x 10 mm²); making detection of substances with a low permeability *in vivo* rather difficult (due to detection range).

Additionally, the increase in complexity in an *in vitro* BBB model makes it more and more difficult for pharmaceutical industries to transit the model to a high through-put variant for large scale research and development, and eventually for preclinical testing of promising drug candidates. Overall, simple BBB models that still display excellent barrier characteristics and moreover can be upgraded to high through-put techniques are most desirable for pharmaceutical drug development.

Impairment of the blood-brain barrier in Alzheimer's disease

A further complicating factor for BBB modelling in the context of neurodegenerative disorders is the existing BBB dysfunction in Alzheimer's disease. It was postulated that neurotoxic A β crosses an impaired BBB and induces neurodegeneration; the process of A β accumulation in the brain and BBB impairment are also believed to interact and reinforce each other, eventually promoting neurodegeneration [224–226].

5.3 Further strategies and candidates profiting from nanotechnology

This study proves that nanoparticle-mediated drug transport allows transit across an advanced *in vitro* blood-brain barrier model and therefore may be an excellent tool to treat life-threatening brain diseases, like brain tumors (glioblastoma multiforme) or others. The etiology and pathological processes associated with neurodegenerative disorders, like Alzheimer's disease, are confusingly complex. Often it remains unclear if a certain hallmark is reason or cause of the disease development and progression, prohibiting reliable prognosis of effective drug treatment options in the future.

Prevention or acute treatment?

Experts on the Alzheimer's disease topic are consent that the disease is not currently treatable and therapy will, if anything, only halt or slow down the disease's progression. Of very large concern is the timing of the intervention, because by the time amyloid deposits and neurofibrillary tangles are present, treatment is expected to be past the point of efficacy [104]. However, imaging data suggests that amyloid plaques appear even before clinical decay [227]. The diagnosis of a very early stage Alzheimer's disease is therefore essential - and justifies the great efforts in molecular biomarker development [228–230]. When the first symptoms become noticeable, patients have already lost a big part of the neural signaling capacity, meaning a large proportion of neurons already perished, and the remaining neurons tire while compensating the loss of the other neurons. The rigorous exhaustion again causes neural death and even more neurons perish. Furthermore, the lack of synaptic stimulation causes neurons to draw back their dendrites and reduce themselves to mainly soma. These altered, "sleeping" neurons fall into a passive condition and lose their capability in signal passing.

Screening for Alzheimer's disease biomarkers in certain cases, like when tangible risk factors (such as familial Alzheimer's disease history or APOE4 genotype) are given, therefore would be a step towards early intervention possibilities. From current research, anti-amyloid treatment can only be preventive and this must be taken into account when developing nanoparticle formulations. Advantages of nanoparticulate formulations compared to conventional drug development comprise low doses and less side effects due to targeted transport (Figure 38). However, a long-term prevention of diseases by drug therapy should ideally be orally applied, cheap and should aim at good compliance and low side effects for the patients. A common example is secondary prevention of cardiovascular diseases with the antithrombotic drug acetylsalicylic acid (ASA, Aspirin™): a daily oral dose of >100 mg/day is sufficient for antithrombotic prevention [231, 232] (whereas for pain relief 500–1,500 mg are required) and people only suffer from an acceptable rate of side effects.

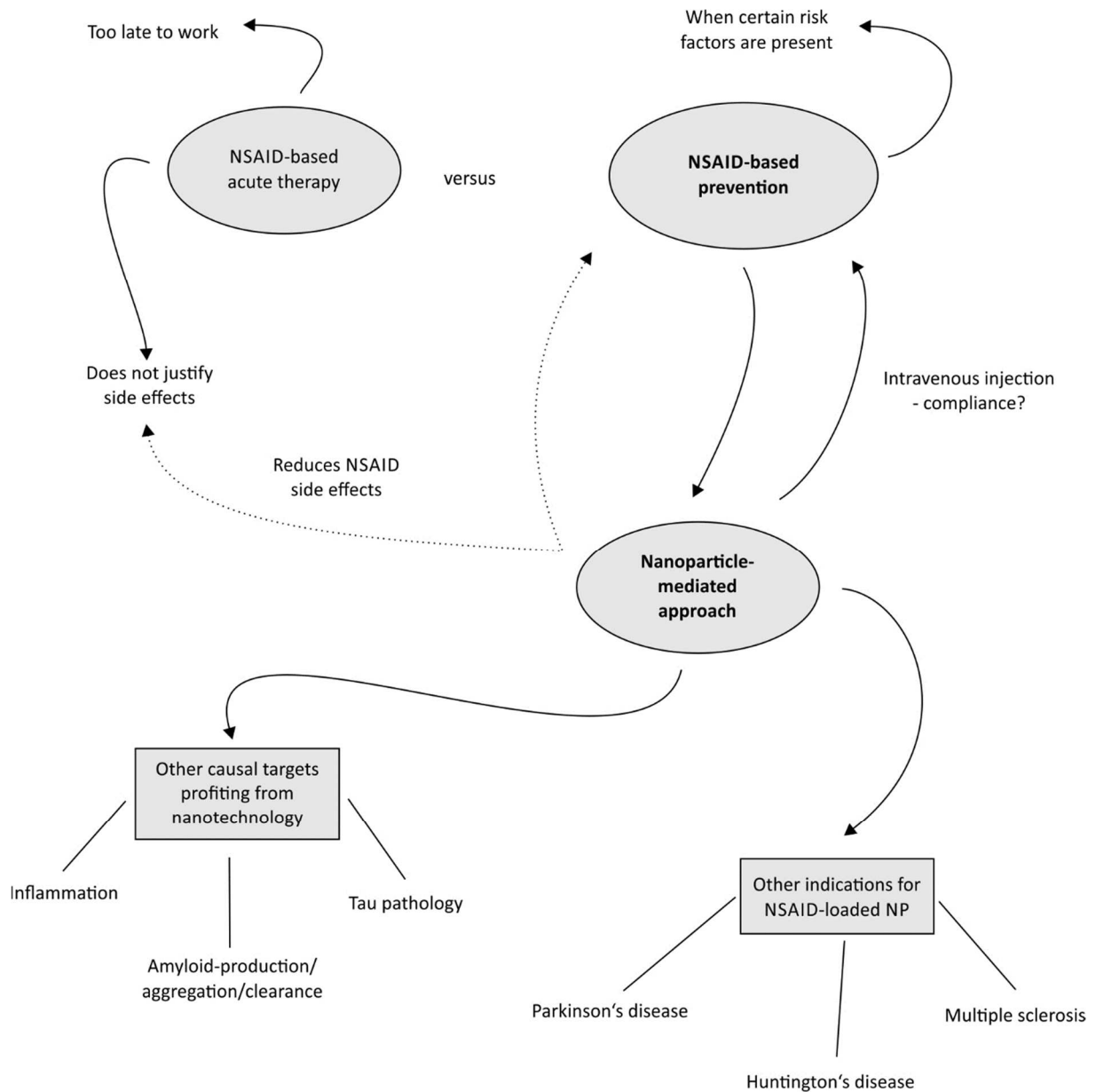


Figure 38: Overview of nanoparticle-mediated benefits and concerns for Alzheimer’s disease and other neurodegenerative disorders regarding NSAID- and other potential drug-loading for preventive approaches. NSAID-based drug application is only expected to work against Alzheimer’s disease if given at very early stage. But high doses required relevant in AD outcome do not justify NSAID-prevention therapy without further indications. Nanoparticles can be used to target NSAIDs to the brain to reduce peripheral side effects and enhance local drug concentrations, but at the moment, only intravenous injection of brain-targeted nanoparticles is feasible, raising ethical concerns and questions about patients’ compliance. Nevertheless, NSAID-loaded nanoparticles could not only be beneficial for Alzheimer’s disease patients, but also in context of other neurodegenerative diseases (like Parkinson’s or Huntington’s disease). Other disease modifying strategies in the battle against Alzheimer’s disease could comprise nanoparticles targeting causal mechanisms (like inflammation or amyloid production). Often these substances are not able to cross the blood-brain barrier themselves, which could be allowed by effectively using nanotechnology.

In the case of flurbiprofen, long-term high dose NSAIDs application for Alzheimer's disease risk reduction (as shown in patients with rheumatoid arthritis) is not justifiable, because of the severe adverse side effects in these doses. Therefore, packing flurbiprofen into nanoparticles as Trojan horses in order to target transport to the brain is an elegant approach to reduce side effects by lower doses in the periphery.

However, at present, nanoparticles that are intended to be given orally and to treat brain diseases are years away from tangible development. Examples exist for nanoparticles that are given orally and reach their target site in the gastrointestinal (GI) tract [233–235]. However, if the nanoparticles are supposed to exit the GI tract and enter the blood stream numerous problems exist. Mainly, the nanoparticles are very unlikely to cross the mucosa of the intestine. This can be beneficial if a high local concentration is sought (e.g., when the nanoparticles should be degraded in the mucus), but mucus crossing of un-degraded nanoparticles to be further transported to the blood stream is very unlikely to happen. In addition, the natural route would take them to the portal vein directly to the liver where they are likely to accumulate.

Therefore, the nanoparticle formulations discussed in this study are only applicable to intravenous injection (Figure 38). The ethical concern is that it is not justifiable to treat people, especially the elderly (that are more prone to infections and critical immune responses) with a prevention that needs to be intravenously applied. In addition, the patients' compliance is expected to be very low. One possibility makes an intravenous preventive treatment more palatable for potential patients would be to increase the time span between recurrent applications. If it was possible to prepare a retard nanoparticle that consistently releases the drug in an e.g. monthly period, it would be conceivable that people would use it as prevention regimen.

A common example for an injected prevention strategy is vitamin B12 supplementation for vegans. Vitamin B12 is only present in animal products (and its oral availability is generally low), but it is essential for neural development and memory performance. Therefore, vegans (and also non-vegans) often perform a vitamin B12 treatment where the drug hydroxocobalamin or cyanocobalamin (which is metabolized to vitamin B12 in the body) is intramuscularly injected monthly or weekly over a certain period of time.

Analogously, certain risk factors for Alzheimer's disease would justify a long-term intravenous drug therapy or prevention approach using nanotechnology. Indications could consist of predisposition of a familial variant of Alzheimer's disease, caused by gene mutation in the APP or γ secretase-encoding gene. All current mouse models of Alzheimer's disease make use of these mutations to mimic Alzheimer's disease, where the proportion of the familial variant only covers 5-10 % of all Alzheimer's disease cases. However, for the people suffering from the gene mutation, it would be legitimate to

intervene with e.g. NSAIDs that were repeatedly shown to modulate γ -secretase activity and are expected to be beneficial if they can reach brain parenchyma.

Another indication for nanoparticle-based NSAID prevention could be a peculiar Alzheimer's disease biomarker. Researchers and clinicians put a lot of effort into establishing an early diagnosis of Alzheimer's disease. Particularly useful is the analysis of cerebrospinal fluid (CSF) for total τ (T- τ), phosphorylated τ (P- τ) and β -amyloid peptide ($A\beta_{42}$) [236–238]. Hinting at neurofibrillary tangle formation and amyloid pathologies, these analyses can therefore identify patients at early Alzheimer's disease stages that did not yet develop dementia (it also serves as differential diagnosis between Alzheimer's disease and other dementias). These patients could actually benefit from nanoparticle-mediated drug therapy in the early stage of the disease, justifying the perceived burden of a recurrent intravenous prevention approach.

Ideally, the drug release profile of the nanoparticles should then be optimized to a retard profile, minimizing the frequency of injections. This could be achieved by a combination of basis material for the nanoparticles: e.g. if PLGA-based nanoparticles were used, the proportion of PLA and PGA in the PLGA composition varies the release profile of the drug. An injection could therefore include nanoparticles with increasing amounts of PLA in the PLGA composite to delay drug release. Furthermore, a subpopulation of the nanoparticles could be coated with protectants, such as chitosan, that would further delay degradation in the human body.

Intervention possibilities profiting from nanotechnology

The progression of Alzheimer's disease creates the largest unmet medical need in neurology. A hindrance is that the etiology hypotheses are not elucidated up to today and that it seems likely that more than one pathogenic pathway causes the disease state. This section discusses the current disease-modifying and prevention strategies that could profit from using nanotechnology, focusing in detail on $A\beta$ -related approaches and neuro-inflammation (other current approaches comprise targeting τ pathology, altered ApoE genotypes and metabolic dysfunction).

In his review from 2010, Citron outlines different causal intervention strategies [122] focusing on the reduction of $A\beta_{42}$ formation and $A\beta_{42}$ plaque pathology (summarized in Figure 39). A lot of these strategies could profit from nanotechnology, because many of the substances worth considering as anti-Alzheimer's disease drug candidate are not currently suited for blood-brain barrier crossing themselves - making nanoparticle-mediated drug transport a promising approach.

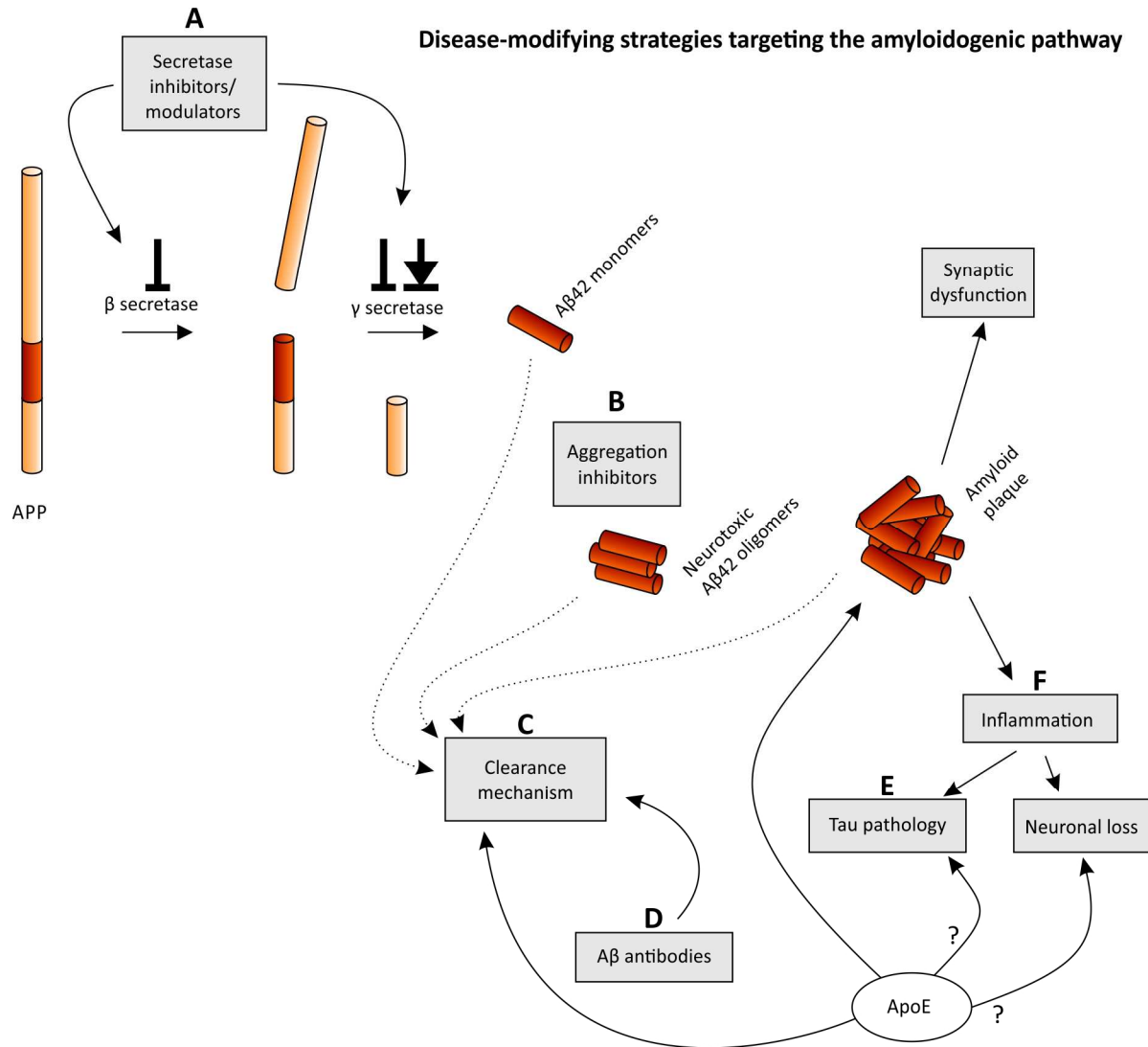


Figure 39: Disease modifying strategies against Alzheimer’s disease. The amyloid precursor protein (APP) is cleaved by β - and γ -secretase during the amyloidogenic pathway, resulting in aggregation-prone A β 42 peptide that forms neurotoxic oligomers and amyloid plaques, which may cause neuroinflammation. The amyloid cascade may trigger downstream τ pathology. ApoE can affect A β deposition and/or clearance. Various approaches for possible disease-modifying strategies that causally target the proposed pathology processes are shown: **(A)** Secretase inhibitors and modulators alter the proteolytic cleavage outcome, thereby reducing A β 42 levels. **(B)** Aggregation inhibitors target plaque formation by decreasing A β -A β interaction. **(C)** Clearance mechanisms comprise degrading A β peptides e.g. by proteases. **(D)** Alternatively, A β -recognizing antibodies can be used to mark neurotoxic A β peptides for degradation by the immune system. **(E)** Independent from A β pathway, τ pathology can be interfered with by decreasing either τ aggregation or τ hyperphosphorylation. **(F)** As neuroinflammation is linked to Alzheimer’s disease, targeting inflammation processes is another causal tool. However, it is still unclear to what extent inflammatory responses are harmful or beneficial in Alzheimer’s disease pathology. Image adapted and modified from Citron [122].

The amyloid hypothesis blames pathologic amyloid plaque accumulation in the brain due to an imbalance of A β 42 production and clearance as the origin for Alzheimer's disease development. Consequently, drugs that influence the amyloidogenic outcome of APP cleaving and resulting in less A β production are a cornerstone in anti-Alzheimer's disease drug development (Figure 39A). Despite some critical voices started to question the amyloid hypothesis in recent years, there is strong pathological and genetic evidence that A β peptide, especially the least soluble isoform A β 42 plays a key role in all types of Alzheimer's disease [239, 240]. However, in the last years, several therapeutics that were developed on behalf of the amyloid hypothesis failed in clinical tests. The next section summarizes recent efforts that failed, but might be revisited in nanoparticulate formulations.

The first target in A β 42 reduction was γ -secretase. **γ -secretase inhibitors** (Figure 39A) decrease A β 42 burden by altering progressive proteolytic cleavage of APP. Concerns towards γ -secretase inhibition arose when scientists found that deleting the γ -secretase component *PSEN* lead to lethal phenotype (comparable to a *Notch1* knock out) and that inhibiting Notch 1 cleaving interferes with thrombocyte differentiation and B-cell maturation [241, 242]. Nevertheless, companies developed γ -secretase inhibitors like semagacestat and avagacestat that were believed to be beneficial for Alzheimer's patients [243–246]. Unfortunately, cognitive decline did not significantly improve with semagacestat and avagacestat therapy, but rather it worsened. However, since γ -secretase has many substrates, the outcome of these trials is hard to interpret and the negative effect might be due to other altered pathways affected by γ -secretase inhibitors [247–249]. To avoid safety issues, circumventing an effect on the Notch pathway was aimed for and led to the development of **γ -secretase modulators** (not inhibitors). Some NSAIDs are able to decrease neurotoxic A β 42 species (Figure 39A), whereas other A β isoforms increase [250], without affecting Notch [251]. This effect is not mediated by the classical COX inhibition, but by direct γ -secretase interaction [173] or the corresponding substrates [252]. This study used the γ -secretase modulator flurbiprofen. R-flurbiprofen (tarenflurbil) failed in an Alzheimer's disease clinical trial, due to its poor transport capacity across the blood-brain barrier. Delivery of NSAIDs to the CNS is often inefficient, likely evoked by binding to plasma proteins [185–188, 253]. The incorporation of the drug within nanoparticles evoked an A β 42 reducing effect in the *in vitro* BBB/Alzheimer's disease model. Achieving targeted transport to the brain *in vivo* by surface modification of the flurbiprofen-loaded nanoparticles, may improve the prospects of disease modification in animal models or patients. Another explanation for the failure of R-flurbiprofen in clinical trials might have been the reduced impact on COX activity. Patients treated with high-dose, long-term NSAIDs were less likely to develop Alzheimer's disease, but this effect was also believed to be due to anti-inflammatory reactions. Another strategy to avert the amyloidogenic pathway [254] is targeting β -secretase (BACE1), which is ubiquitously expressed but elevated in the brain and its

biological role is still not clear. In sporadic Alzheimer's patients, *BACE1* is not mutated, but β -secretase activity is still enhanced (not clear if this is the cause of the pathology or a late-stage consequence). Generally, β -secretase inhibitors are a promising anti-Alzheimer's disease drug, but the development seems to be challenging as most of the candidates are large and hydrophilic peptides [255], prohibiting blood-brain barrier crossing. In these cases, nanoparticles could be an excellent approach to deliver these substances to the brain parenchyma since nanoparticles loaded with peptides or proteins have been successfully prepared in the past. Another (theoretically possible) approach is stimulation of α -secretase (e.g. through cell surface receptors [256]) providing less APP substrate for the amyloidogenic pathway. Nevertheless, far more APP enters the non-amyloidogenic pathway and for a measurable effect, α -secretase activity would need to markedly increase, changing not only APP but also various other membrane protein metabolism. The possible side effects are unknown and no α -secretase activator has entered clinical trials so far [122].

It is also possible to target **A β aggregation** for AD intervention (Figure 39B). In the brain, different A β isoforms are generated, of which A β 42 tends to aggregate in oligomers. Scientists originally assumed that only large fibrils would be neurotoxic, but later it was shown that even smaller A β oligomers can lead to synaptic dysfunction (for review see [240]). Consequently, one approach was developing substances that inhibit A β -A β interaction (Figure 39B), but not many of these drugs entered clinical trials. A prominent candidate, tramiprosate, keeps A β monomers in a non-fibrillary state [257] and reduced A β 42 in the cerebrospinal fluid in a phase II trial. It was not effective in a phase III trial, and it is still unclear if the drug blocked A β 42 in the brain. Nanoparticles could be used to try and enhance tramiprosate (Alzhemed™) transport to the brain.

Furthermore, enhancing **A β clearance** can be aimed for (Figure 39C) by involving two key structures: A β -degrading proteases and A β -targeting antibodies. Proteases (also called peptidases or proteinases) *ipso facto* cleave proteins (or peptides) by hydrolysis of peptide bonds. For A β peptide cleavage, the most important proteases identified are neprilysin, insulin-degrading enzyme and plasmin [258]. Plasmin degrades A β peptides *in vitro*, but is inhibited *in vivo* by plasminogen activator inhibitor 1 (PAI-1) (which prevents generation of plasmin from plasminogen). Consequently, blocking the PAI-1 leads to activated A β -degrading plasmin and also more A β clearance (Figure 39C). PAI-1 inhibitors reduced A β burden in transgenic mice [258, 259], but the brain transport of PAI-1 inhibitors is expected to be problematic in patients due to the blood-brain barrier. Proteins can be incorporated into nanoparticulate formulations. So, an interesting approach to target A β -degrading proteases to the brain could be packing the enzymes into nanoparticles of suited basis materials (e.g., PLGA) and using surfactant coating or direct coupling of surface ligands (e.g., ApoE3) to allow blood-brain barrier crossing and enhance protease concentration in the brain.

Concerning **immunotherapy** (Figure 39D), two pathways are assumed to support A β clearance (for review see [104]). Either a peripheral sink effect appears when antibody binding in the blood plasma causes a gradient that drives A β removal from the brain, or antibodies might tag A β species present in the brain making them recognizable for microglia (capable of phagocytosis). In active immunization, the A β 42 antigen itself is injected; in passive immunization whereby, patients receive A β 42-recognizing antibodies. However promising, up to today this stagey failed in terms of slowing cognitive decline and in some cases was even harmful to patients that developed a severe immune response [122]. Antibodies targeting the amyloid- β peptide repeatedly failed to slow cognitive declines in Alzheimer's patients during clinical trials and raised questions about the effectiveness of A β 42 reduction. In 2012, the *Nature news blog* reported that Bapineuzumab, a humanized monoclonal antibody, did not cause cognitive improvement in patients during two trials, even though Alzheimer's disease biomarkers (amyloid brain plaque and phosphorylated τ protein) in the cerebrospinal fluid (CSF) were decreased after Bapineuzumab treatment. In response, the developing company *Johnson & Johnson* therefore wanted to discontinue the development. In two global, randomized phase III clinical trials, the lack of efficacy of Bapineuzumab was recently confirmed [112]. *Eli Lilly and Company* also failed with a similar antibody (Solanezumab) in two phase III clinical trials. However, as previously mentioned, maybe study designs should be adapted to try to treat asymptomatic patients that already show the including criteria in biomarkers, but do not yet suffer from cognitive decline or dementia.

Another target in anti-AD drug development is reducing **hyperphosphorylated τ** (Figure 39E). The protein τ is a soluble and binds to and stabilizes microtubules in axons, thereby contributing to cytoskeleton functions and axonal transport. In Alzheimer's disease, hyperphosphorylated, insoluble, aggregated τ tangles (one of the two hallmarks of AD) appear, which either directly cause neuronal toxicity or contribute to the degeneration by reduced axonal transport (for review see [260]). The burden of τ in specific brain areas correlates with the degree of cognitive decline [261]. Furthermore, τ mutations can lead to other forms of dementia [262]. Strategies to counteract τ pathology comprise inhibiting either τ aggregation or hyperphosphorylation [263, 264]. Anti- τ aggregators seem appealing, because it is generally believed that τ aggregates are harmful and a lot of effort is made in quest for a suitable substance, LMTXTM (proposed trade name: Rember) from TauRx Therapeutics, for example, showed positive results in phase II clinical trials and entered phase III recently [265–267]. Generally, nanoparticles could be used to maximize transport capacity across the brain. Inhibition of kinases (enzymes that transfer a phosphate group from phosphate-donors to substrates), is the logical consequence to avoid hyperphosphorylation. However, the main pathologic kinase for Alzheimer's disease development is not yet identified. Nevertheless, for development of kinase inhibitors as anti-Alzheimer's disease drugs, nanoparticles could be advantageous to reduce the severe side effects that

follow chronic kinase inhibition by dose reduction and allow organ-specific targeting, thereby widening the number of potential substances and facilitating approval and regulating processes.

Moreover, a link between **inflammation** and Alzheimer’s disease exists– as numerous studies have shown until today – making it a causal target in anti-Alzheimer’s disease drug therapy development (Figure 39F). However, from the recent literature, it is still confusing if inflammation initiates Alzheimer’s disease, if it is just a natural bystander or if it might be an advantageous response (for review see [215]). Therefore, the question remains: should neuro-inflammation be targeted in Alzheimer’s disease therapy or not?

One the one hand, the early activation of the immune system can be beneficial in clearing A β species [215]. A β species themselves, for example, can activate innate immune responses to recruit activated microglia that are capable of phagocytosis, thereby counteracting Alzheimer’s disease pathology (Figure 40). One the other hand, neuro-inflammation processes are assumed to be harmful and directly related to Alzheimer’s disease development (Figure 40). Especially interesting is the interaction between astroglia, microglia and neurons. Astrocytes and microglia can recognize damage or injury to the brain (like trauma, infections or fibrillary A β) and consequently release pro-inflammatory signals (such as chemokines, interleukines, cytokines, prostaglandins, pentraxins, complement components and reactive oxygen species) that are up regulated in the affected brain areas [268–272]. If this secondary response is triggered constantly (e.g. by increased A β 42 generation), the activated neuro-inflammatory process leads to neuronal death [273]. Furthermore, activated microglia are correlated with senile plaques and it is believed that activated microglia cannot phagocytize A β in the presence of inflammatory cytokines, therefore promoting plaque formation [274].

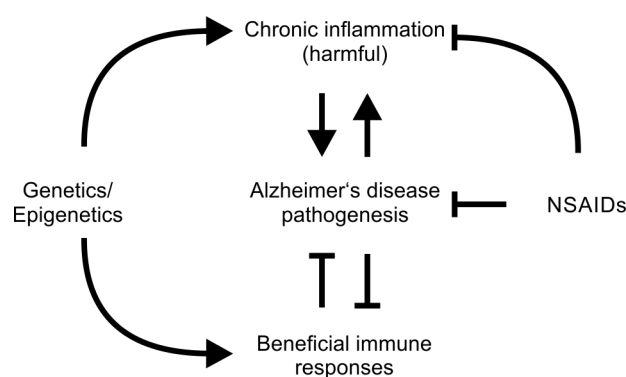


Figure 40: Inflammation in Alzheimer’s disease (Alzheimer’s disease). In Alzheimer’s disease, a chronic inflammation in certain brain regions appears that is supposed to be harmful and can further promote Alzheimer’s disease (up and down arrows). Other immune responses can be beneficial to suppress pathogenesis (inhibitory arrows), such as microglial phagocytosis of A β species. Genetics or epigenetics (like traumatic injury, infections or inherited diseases) can influence both beneficial and harmful immune responses (curved arrows). NSAIDs affect disease progression or development, for example by reducing A β generation or suppressing inflammation (curved inhibitory arrows). Schema adapted and modified from Wyss-Coray [215].

Therefore, anti-inflammatory therapy has been proposed as an anti-Alzheimer's disease therapy (Figure 40). As described earlier, the efficacy of chronic NSAIDs use regarding Alzheimer's disease risk reduction is undeniable and supported by animal model and epidemiological data [120, 156, 170, 215, 275]. However, the mechanism behind this beneficial effect is still not completely understood, because NSAIDs have multiple targets and modes of action that – apart from their potency to reduce A β 42 species - could be beneficial in the battle against Alzheimer's disease:

NSAIDs - Panacea or pharmacological sledgehammer?

The original NSAID, Aspirin (first synthesized and patented in the 1890s), was described to mainly target COX-1 and COX-2, thus inhibiting prostaglandin synthesis (Figure 41A). Today, many other NSAIDs exist with various selectivity for COX-1 or -2. In the context of epidemiological studies with rheumatic patients, NSAIDs were proposed as anti-Alzheimer's disease drugs, but largely failed in clinical trials (examples are celecoxib and rofecoxib (COX-2 selective) or naproxen [120] (mixed COX-1/COX-2 inhibitor)). Interestingly, people affected with arthritis that used long-term high-dose NSAIDs showed a drastic decrease of major histocompatibility complex (MHC) class II-positive activated microglia (compared to people without arthritis or without NSAID consumption) [276], suggesting that NSAIDs can reduce microglia activation. Even more interesting, neither NSAID-use nor arthritis changed the proportion of A β deposits and neurofibrillary tangles in the study. The A β 42-decreasing mechanism of NSAIDs is based on modulation or inhibition of γ -secretase (Figure 41B). Another target of certain NSAIDs is the small GTP-binding protein Rho and its kinase Rock (Figure 41C). Inhibition of Rho eventually leads to reduced A β production. Some NSAIDs (like R-flurbiprofen) seem to be capable of translocating NF κ B to the nucleus leading to reduced COX-2 expression (Figure 41D), which could be relevant for a beneficial effect in Alzheimer's disease patients. Activation of PPAR- γ by NSAIDs (Figure 41E) may lower the expression of β -secretase by repressing β -secretase cleaving enzyme 1 (*BACE1*) promoter [277], however, clinical trials with PPAR- γ agonists were rather sobering.

The NSAID failure in clinical trials regarding Alzheimer's disease may be due to various reasons: Firstly, it is consistent that anti-inflammatory approaches (as well as A β targeting strategies) would rather work as Alzheimer's disease prevention, but not Alzheimer's disease treatment when clinical features became obvious. Secondly, it appears that celecoxib and rofecoxib were targeting the wrong enzymes. Both being COX-2 selective, both drugs are associated with less gastrointestinal side effects, but COX-1 (not COX-2) is upregulated in activated microglia. Flurbiprofen, on the other hand is COX-1/-2 unselective, but might not have reached relevant concentrations in the brain, again underlining nanotechnologies' potential for enhanced drug transport.

Possible pathways of NSAID action in Alzheimer's disease

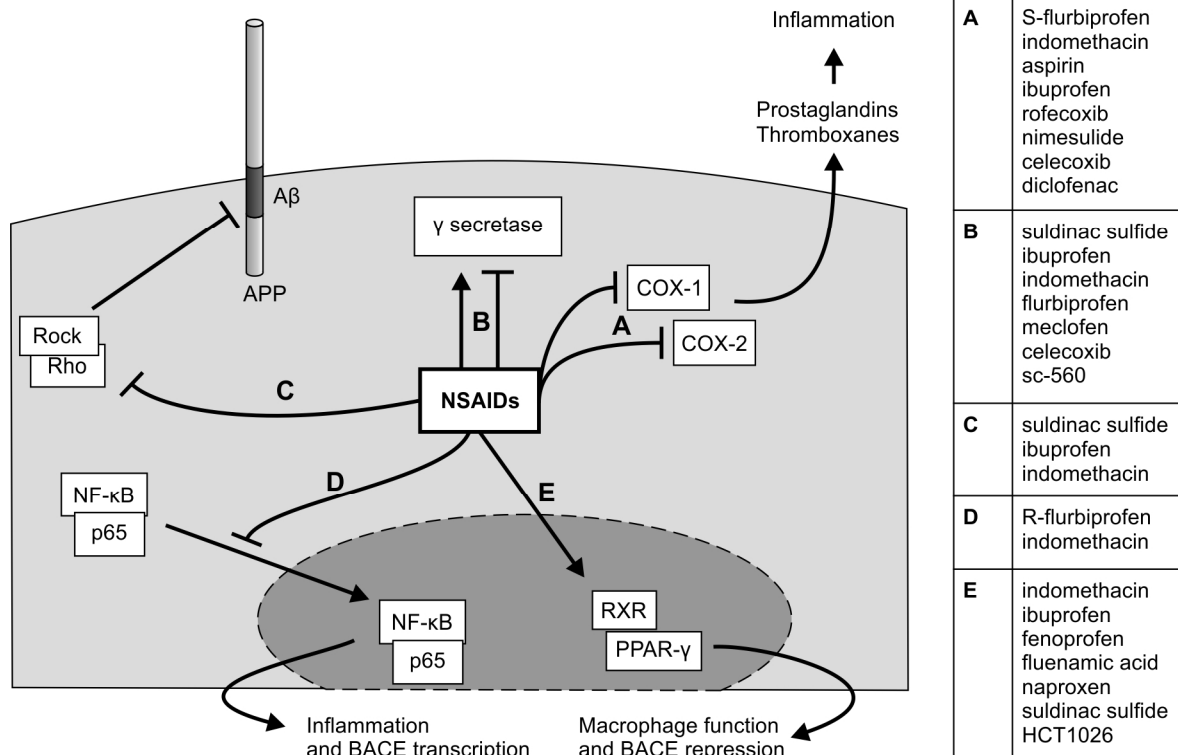


Figure 41: NSAIDs have multiple effects in Alzheimer's disease. (A) The classical role of NSAIDs is (selective or non-selective) cyclooxygenase (COX) inhibition, which inhibits prostaglandin and thromboxane synthesis thereby evoking anti-inflammatory effects (B) Other effects relevant in Alzheimer's disease are modulation or inhibition of γ -secretase (lowering $A\beta_{42}$), (C) inhibition of Rho and Rock, (D) inhibition of NF κ B translocation to the nucleus (reduces inflammation and BACE expression) and (E) activating PPAR- γ and the retinoid X receptor (RXR) (increases macrophage function and represses BACE expression). Schema adapted and modified from [215], examples for NSAIDs from [176, 177, 251, 278–286].

Furthermore, inflammatory processes are also discussed in various other diseases; therefore, NSAID-loaded nanoparticles could also be indicated not only against Alzheimer's disease. Neuro-inflammation does indeed appear to play a major role in other neurodegenerative disorders, such as multiple sclerosis [287], Huntington's disease [288] or Parkinson's disease [289, 290], where NSAID treatment was already reported to show beneficial effects in disease models [291]. Therefore, NSAID-loaded, brain-targeted nanoparticles could be used to enhance the drug transport to the brain to treat other disorders apart from Alzheimer's disease. Furthermore, a multiple ligand coupling could be used to target brain-nanoparticles to substructures, such as the *substantia nigra*, targeting tissue specific receptors (dopamine receptor 2, short splice variant (D2Rs), the dopamine autoreceptor exclusively expressed in dopaminergic neuron presynapses).

As a closing remark, it should be noted that also life style factors such as the organization of leisure time and fitness [292, 293] and nutrition are debated to play a role in neurodegenerative disease development and outcome. Especially, the beneficial impact of food intake for Alzheimer's disease prevention or therapy is a large research field today. For example, some studies pay high regard to high-dose B vitamin supplements (like folate, vitamin B6 and B12). Yet, in a randomized controlled trial patients with mild to moderate Alzheimer's disease did not profit from the vitamins and cognitive decline was not slowed down [294]. Analogously, meta-analysis and systematic reviews controversy discuss caffeine intake to be beneficial for Alzheimer's disease risk reduction [295, 296]

Other studies focused on fats: Ω 3 fatty acids and Ω 3 fatty acid-rich fish. These acids are suspected to be neuroprotective during development and aging and numerous epidemiologic studies and clinical trials have appeared on this topic during the last decade. Although data from animal models and cell culture studies wa promising [297–301], the results in humans are inconsistent and difficult to interpret [164, 166, 302–308]. Especially docosahexaenoic acid (DHA) was proposed to be beneficial in dementia. At the moment, it seems that high Ω 3 fatty acid intake prevents Alzheimer's disease development rather than eases symptoms in the manifested disease state [309]. The protective mechanism is not understood yet, but anti-inflammatory effects are conceivable [166] as well as the ratio of Ω 3 to Ω 6 fatty acids in erythrocyte membranes [165]. It could be beneficial to provide more Ω 3 fatty acids in the brain parenchyma, especially in individuals that have an increased risk for Alzheimer's disease (biomarkers) without established symptoms. This would be problematic with usual oral intake because the amount of DHA would be too large. An option would be to prepare fatty acid nanoparticles as described in the literature [310], consisting of DHA and modifying the surface with brain targeting ligands such as ApoE3 and transferrin. The increased amount of DHA in the brain parenchyma might evoke neuroprotection and slow cognitive decline in very early stages of Alzheimer's disease.

6 CONCLUSION

Today, people achieve a remarkably prolonged lifespan compared with past decades and centuries, thanks to increasing wealth, less heavy physical labor, improved hygiene standards, healthier lifestyles, the development of new life-saving drugs and interventions, and better health care systems.

However, the longevity accompanies a drastically increased prevalence for neurodegenerative disorders, like Alzheimer's disease. For the etiology of Alzheimer's disease is not yet completely understood, causal interventions or cures are currently still lacking, but desperately needed. In the search for potent anti-Alzheimer's disease drugs, various promising substances were identified. However, hope often crumbled when it came to clinical trials. One example is the non-steroidal anti-inflammatory drug (NSAID) flurbiprofen that was an anti-Alzheimer's disease candidate. After promising phase II clinical trials, flurbiprofen eventually failed in a phase III clinical trial, probably due to its low penetration capacity to the brain.

Here, flurbiprofen was revisited as an anti-Alzheimer's disease drug by trying to enhance brain transport with the aid of molecular Trojan horses. The drug was incorporated in poly(lactic acid) nanoparticles in order to mask the original physico-chemical properties of flurbiprofen that hinder blood-brain barrier crossing.

The appeal of flurbiprofen-loaded PLA-nanoparticles for anti-Alzheimer's disease drug development lies in the excellent biocompatibility and the already existing approval of the separate components - both flurbiprofen and poly(lactic acid) were approved by regulatory authorities (like the FDA). Furthermore, incorporating flurbiprofen in drug-loaded nanoparticles is expected to impede flurbiprofen binding to plasma proteins, which was proposed as the main reason for flurbiprofen's low blood-brain brain penetration capacity. As discussed in this study, flurbiprofen-loaded nanoparticles also bind to plasma proteins. However, in this case, the formation of a protein corona (partly consisting of apolipoproteins) on the nanoparticles surface after plasma incubation allows receptor-mediated transcytosis across the blood-brain barrier, rather than retention in the bloodstream. Enhancing the transport rate of flurbiprofen across the blood-brain barrier by nanotechnology is consequently expected to succeed. For NSAIDs, only less than 5 % of the originally applied drug amount reach the brain or the cerebrospinal fluid (CSF), resulting in less than 1.5 μM flurbiprofen at normal plasma concentrations *in vivo* [177, 185, 187, 188]. For an amyloid reducing effect in cellular Alzheimer's disease models, about 50 μM flurbiprofen are needed [68, 172]. Increasing the transport rate of flurbiprofen to the brain by more than 30 fold with the aid of nanoparticles seems feasible when using a suitable nanoparticulate formulation. For example, Chen *et al.* could increase loperamide permeability

across an *in vitro* BBB model by more than 20 fold when using a specific nanoparticle formulation [76]. Even more drastic effects for nanoparticle-mediated BBB crossing of loperamide were shown in *in vivo* nociceptive experiments, in which animals treated with loperamide-loaded nanoparticle reacted less sensitive to pain after nanoparticle-treatment than loperamide-treated control animals [49, 90].

However, the question remains at which time point a nanoparticle-based anti-Alzheimer's disease therapy or prevention strategy would be indicated. Would flurbiprofen still show beneficial effects in Alzheimer's disease patients when symptoms were already apparent? It is more likely that an intervention would be too late in this disease state. Rather, predisposed patients could profit from an early, marker- or genotype-indicated prevention approach. It seems conceivable that e.g. an existing familial variant of Alzheimer's disease or an accumulation of genetic risk factors - recognized before symptom occurrence – justifies nanoparticle-mediated NSAID or flurbiprofen prevention.

Future steps resulting from this study's data consist of optimizing nanoparticle preparation to combine drug-loading and ligand-modification in one formulation. Ideally, these nanoparticles should be traceable *in vitro* and *in vivo* e.g. by the inclusion of marker molecules. Furthermore, the aim should be to develop a retarded flurbiprofen-release profile to allow maximal effect in *in vivo* application. Other drugs (e.g. other non-steroidal anti-inflammatory drugs) that reduce A β 42 burden or positively affect neuro-inflammation in Alzheimer's disease could be incorporated in similar nanoparticles to enhance brain transport capacity *in vivo*.

For pre-screening, better *in vitro* blood-brain barrier models for drug transport studies can be achieved by co-culturing brain endothelial cells together with other cells of the neurovascular unit (providing biochemical support) and introducing shear stress in three-dimensional model structures (mimicking blood flow to improve barrier integrity and achieving more realistic local drug concentrations than in a static *in vitro* model). Nevertheless, even by refining the already very promising *in vitro* results presented in this study, a success in *in vivo* experiments is still not guaranteed.

Overall, it might seem like grasping at straws when reinvestigating drugs that already failed once. However, in the battle against Alzheimer's disease, the fast-emerging field of nanotechnology offers the possibility to enlarge the pool of substances that may have a positive impact - giving us hope that development of effective pharmacological tools will become more realistic in the near future.

7 REFERENCES

1. Wittchen HU, Jacobi F, Rehm J, Gustavsson A, Svensson M, Jönsson B, Olesen J, Allgulander C, Alonso J, Faravelli C, Fratiglioni L, Jennum P, Lieb R, Maercker A, van Os J, Preisig M, Salvador-Carulla L, Simon R, Steinhausen H-C: **The size and burden of mental disorders and other disorders of the brain in Europe 2010.** *European Neuropsychopharmacology* 2011, **21**:655–679.
2. Pardridge WM: **The blood-brain barrier: bottleneck in brain drug development.** *NeuroRx : the journal of the American Society for Experimental NeuroTherapeutics* 2005, **2**:3–14.
3. Antinori A, Cingolani A, Giancola ML, Forbici F, De Luca A, Perno CF: **Clinical implications of HIV-1 drug resistance in the neurological compartment.** *Scandinavian journal of infectious diseases Supplementum* 2003, **106**:41–4.
4. Kandaneeratchi A, Williams B, Everall IP: **Assessing the efficacy of highly active antiretroviral therapy in the brain.** *Brain pathology (Zurich, Switzerland)* 2003, **13**:104–10.
5. Pardridge WM: **Blood-brain barrier drug targeting: the future of brain drug development.** *Mol Interv.* 2003, **3**(2):90-105, 51.
6. Ehrlich P: **Beiträge zur Kenntniss der Anilinfärbungen und ihre Verwendung in der mikroskopischen Technik.** *Archiv für mikroskopische Anatomie* 1877, **Bd.13 187**:263–277.
7. Bentivoglio M, Kristensson K: **Tryps and trips: Cell trafficking across the 100-year-old blood-brain barrier.** *Trends in Neurosciences* 2014, **37**:325–333.
8. Goldmann E: **Die äussere und innere Sekretion des gesunden und kranken Organismus im Lichte der “vitalen Färbung”.** *Beitr Klin Chir* 1909, **64**:192–265.
9. Goldmann E: **Vitalfärbungen am Zentralnervensystem. Beitrag zur Physio-Pathologie des Plexus Chorioideus und der Hirnhäute.** *Abh Preuss Akad Wiss Physik -Math* 1913, **1**:1–60.
10. Reese TS, Karnovsky MJ: **Fine structural localization of a blood-brain barrier to exogenous peroxidase.** *The Journal of cell biology* 1967, **34**:207–17.
11. Abbott NJ, Rönnbäck L, Hansson E: **Astrocyte-endothelial interactions at the blood-brain barrier.** *Nature reviews Neuroscience* 2006, **7**:41–53.
12. Brightman MW, Reese TS: **Junctions between intimately apposed cell membranes in the vertebrate brain.** *The Journal of cell biology* 1969, **40**:648–77.
13. Furuse M, Hirase T, Itoh M, Nagafuchi A, Yonemura S, Tsukita S: **Occludin: a novel integral membrane protein localizing at tight junctions.** *The Journal of cell biology* 1993, **123**(6 Pt 2):1777–88.
14. Furuse M, Fujita K, Hiiragi T, Fujimoto K, Tsukita S: **Claudin-1 and -2: novel integral membrane proteins localizing at tight junctions with no sequence similarity to occludin.** *The Journal of cell biology* 1998, **141**:1539–50.
15. el-Bacha RS, Minn A: **Drug metabolizing enzymes in cerebrovascular endothelial cells afford a metabolic protection to the brain.** *Cellular and molecular biology (Noisy-le-Grand, France)* 1999, **45**:15–23.
16. Fagerholm U: **The highly permeable blood-brain barrier: an evaluation of current opinions about brain uptake capacity.** *Drug discovery today* 2007, **12**:1076–82.
17. Chiou WL, Barve A: **Linear correlation of the fraction of oral dose absorbed of 64 drugs between humans and rats.** *Pharmaceutical research* 1998, **15**:1792–5.
18. Goodwin JT, Clark DE: **In silico predictions of blood-brain barrier penetration: considerations to “keep in mind”.** *The Journal of pharmacology and experimental therapeutics* 2005, **315**:477–83.
19. Wilhelm I, Fazakas C, Krizbai IA: **In vitro models of the blood-brain barrier.** *Acta neurobiologiae experimentalis* 2011, **71**:113–28.

20. Deli MA, Ábrahám CS, Kataoka Y, Niwa M: **Permeability studies on in vitro blood-brain barrier models: physiology, pathology, and pharmacology.** *Cellular and Molecular Neurobiology* 2005, **25**:59–127.
21. Gumbleton M, Audus KL: **Progress and Limitations in the Use of In Vitro Cell Cultures to Serve as a Permeability Screen for the Blood-Brain Barrier.** *Journal of Pharmaceutical Sciences* 2001, **90**:1681–1698.
22. Williams RL, Risau W, Zerwes HG, Drexler H, Aguzzi A, Wagner EF: **Endothelioma cells expressing the polyoma middle T oncogene induce hemangiomas by host cell recruitment.** *Cell* 1989, **57**:1053–63.
23. Eigenmann DE, Xue G, Kim KS, Moses A V, Hamburger M, Oufir M: **Comparative study of four immortalized human brain capillary endothelial cell lines, hCMEC/D3, hBMEC, TY10, and BB19, and optimization of culture conditions, for an in vitro blood-brain barrier model for drug permeability studies.** *Fluids and barriers of the CNS* 2013, **10**:33.
24. Bowman PD, Ennis SR, Rarey KE, Betz a L, Goldstein GW: **Brain microvessel endothelial cells in tissue culture: a model for study of blood-brain barrier permeability.** *Annals of neurology* 1983, **14**:396–402.
25. Franke H, Galla HJ, Beuckmann CT: **An improved low-permeability in vitro-model of the blood-brain barrier: transport studies on retinoids, sucrose, haloperidol, caffeine and mannitol.** *Brain research* 1999, **818**:65–71.
26. Wagner S, Kufleitner J, Zensi A, Dadparvar M, Wien S, Bungert J, Vogel T, Worek F, Kreuter J, von Briesen H: **Nanoparticulate transport of oximes over an in vitro blood-brain barrier model.** *PloS one* 2010, **5**:e14213.
27. Linz U, Hupert M, Santiago-Schübel B, Wien S, Stab J, Wagner S: **Transport of treosulfan and temozolomide across an in-vitro blood-brain barrier model.** *Anti-cancer drugs* 2015, **26**(7):728-36
28. Cucullo L, McAllister MS, Kight K, Krizanac-Bengez L, Marroni M, Mayberg MR, Stanness KA, Janigro D: **A new dynamic in vitro model for the multidimensional study of astrocyte-endothelial cell interactions at the blood-brain barrier.** *Brain research* 2002, **951**:243–54.
29. Cucullo L, Marchi N, Hossain M, Janigro D: **A dynamic in vitro BBB model for the study of immune cell trafficking into the central nervous system.** *Journal of cerebral blood flow and metabolism* 2011, **31**:767–77.
30. Booth R, Kim H: **Characterization of a microfluidic in vitro model of the blood-brain barrier (μ BBB).** *Lab on a chip* 2012, **12**:1784–92.
31. Prabhakarandian B, Shen M-C, Nichols JB, Mills IR, Sidoryk-Wegrzynowicz M, Aschner M, Pant K: **SyM-BBB: a microfluidic Blood Brain Barrier model.** *Lab on a chip* 2013, **13**:1093–101.
32. Konofagou EE, Tung Y-S, Choi J, Deffieux T, Baseri B, Vlachos F: **Ultrasound-induced blood-brain barrier opening.** *Current pharmaceutical biotechnology* 2012, **13**:1332–45.
33. Lossinsky AS, Vorbrodt AW, Wisniewski HM: **Scanning and transmission electron microscopic studies of microvascular pathology in the osmotically impaired blood-brain barrier.** *Journal of neurocytology* 1995, **24**:795–806.
34. Salahuddin TS, Johansson BB, Kalimo H, Olsson Y: **Structural changes in the rat brain after carotid infusions of hyperosmolar solutions. An electron microscopic study.** *Acta neuropathologica* 1988, **77**:5–13.
35. Neuwelt EA, Rapoport SI: **Modification of the blood-brain barrier in the chemotherapy of malignant brain tumors.** *Federation proceedings* 1984, **43**:214–9.
36. Doolittle ND, Petrillo A, Bell S, Cummings P, Eriksen S: **Blood-brain barrier disruption for the treatment of malignant brain tumors: The National Program.** *The Journal of neuroscience nursing* 1998, **30**:81–90.
37. Jain KK: **Nanobiotechnology-based strategies for crossing the blood-brain barrier.** *Nanomedicine (London, England)* 2012, **7**:1225–33.
38. Schlegel U, Pels H, Glasmacher A, Kleinschmidt R, Schmidt-Wolf I, Helmstaedter C, Fließbach K, Deckert M, Van Roost D, Fimmers R, Bode U, Klockgether T: **Combined systemic and intraventricular chemotherapy in primary CNS lymphoma: a pilot study.** *Journal of neurology, neurosurgery, and psychiatry* 2001, **71**:118–22.

39. Wohlfart S, Gelperina S, Kreuter J: **Transport of drugs across the blood-brain barrier by nanoparticles.** *Journal of controlled release* 2012, **161**:264–73.
40. Fung LK, Shin M, Tyler B, Brem H, Saltzman WM: **Chemotherapeutic drugs released from polymers: distribution of 1,3-bis(2-chloroethyl)-1-nitrosourea in the rat brain.** *Pharmaceutical research* 1996, **13**:671–82.
41. Blasberg RG, Patlak C, Fenstermacher JD: **Intrathecal chemotherapy: brain tissue profiles after ventriculocisternal perfusion.** *The Journal of pharmacology and experimental therapeutics* 1975, **195**:73–83.
42. Illum L: **Is nose-to-brain transport of drugs in man a reality?** *Journal of Pharmacy and Pharmacology* 2004, **56**:3–17.
43. Weiss J, Dormann S-MG, Martin-Facklam M, Kerpen CJ, Ketabi-Kiyanvash N, Haefeli WE: **Inhibition of P-glycoprotein by newer antidepressants.** *The Journal of pharmacology and experimental therapeutics* 2003, **305**:197–204.
44. Pardridge WM: **Drug and gene targeting to the brain with molecular Trojan horses.** *Nature reviews Drug discovery* 2002, **1**:131–9.
45. Lesniak MS, Brem H: **Targeted therapy for brain tumors.** *Nature Reviews Drug Discovery* 2004, **3**:499–508.
46. Mehta GU, Heiss JD, Park JK, Asthagiri AR, Lonser RR: **Neurological Surgery at the National Institutes of Health.** *World Neurosurg.* 2010, **74**:49–59.
47. Kreuter J: **Drug delivery to the central nervous system by polymeric nanoparticles: what do we know?** *Advanced drug delivery reviews* 2014, **71**:2–14.
48. Kreuter J: **Drug targeting with nanoparticles.** *European journal of drug metabolism and pharmacokinetics* 1994, **19**:253–6.
49. Kreuter J: **Nanoparticulate systems for brain delivery of drugs.** *Advanced drug delivery reviews* 2001, **47**:65–81.
50. Lai P, Daeer W, Löbenberg R, Prenner EJ: **Overview of the preparation of organic polymeric nanoparticles for drug delivery based on gelatine, chitosan, poly(D,L-lactide-co-glycolic acid) and polyalkylcyanoacrylate.** *Colloids and surfaces B, Biointerfaces* 2014, **118**:154–63.
51. Rieger J, Freichels H, Imberty A, Putaux J-L, Delair T, Jérôme C, Auzély-Velty R: **Polyester nanoparticles presenting mannose residues: toward the development of new vaccine delivery systems combining biodegradability and targeting properties.** *Biomacromolecules* 2009, **10**:651–7.
52. Mukherjee B, Santra K, Pattnaik G, Ghosh S: **Preparation, characterization and in-vitro evaluation of sustained release protein-loaded nanoparticles based on biodegradable polymers.** *International journal of nanomedicine* 2008, **3**:487–96.
53. Cheng FY, Wang SPH, Su CH, Tsai TL, Wu PC, Shieh D Bin, Chen JH, Hsieh PCH, Yeh CS: **Stabilizer-free poly(lactide-co-glycolide) nanoparticles for multimodal biomedical probes.** *Biomaterials* 2008, **29**:2104–2112.
54. Hines DJ, Kaplan DL: **Poly(lactic-co-glycolic) acid-controlled-release systems: experimental and modeling insights.** *Critical reviews in therapeutic drug carrier systems* 2013, **30**:257–76.
55. Kumari A, Yadav SK, Yadav SC: **Biodegradable polymeric nanoparticles based drug delivery systems.** *Colloids and surfaces B, Biointerfaces* 2010, **75**:1–18.
56. Geiges G, Schapperer E, Thyroff-Friesinger U, Engert ZV, Gravel P: **Clinical development of two innovative pharmaceutical forms of leuprorelin acetate.** *Therapeutic advances in urology* 2013, **5**:3–10.
57. Wischke C, Neffe AT, Lendlein A: **Controlled Drug Release from Biodegradable Shape-Memory Polymers.** *Advances in Polymer Science* 2009, **226**:177–205.
58. Re F, Gregori M, Masserini M: **Nanotechnology for neurodegenerative disorders.** *Nanomedicine* 2012, **8 Suppl 1**:S51–8.
59. Zensi A, Begley D, Pontikis C, Legros C, Mihoreanu L, Wagner S, Büchel C, von Briesen H, Kreuter J: **Albumin nanoparticles targeted with Apo E enter the CNS by transcytosis and are delivered to neurones.** *Journal of controlled release* 2009, **137**:78–86.

60. Kreuter J: **Influence of the surface properties on nanoparticle-mediated transport of drugs to the brain.** *Journal of nanoscience and nanotechnology* 2004, **4**:484–8.
61. Kreuter J, Alyautdin RN, Kharkevich DA, Ivanov AA: **Passage of peptides through the blood-brain barrier with colloidal polymer particles (nanoparticles).** *Brain Research* 1995, **674**:171–174.
62. Schroeder U, Sommerfeld P, Ulrich S, Sabel BA: **Nanoparticle technology for delivery of drugs across the blood-brain barrier.** *Journal of pharmaceutical sciences* 1998, **87**:1305–7.
63. Schroeder U, Sommerfeld P, Sabel BA: **Efficacy of oral dalargin-loaded nanoparticle delivery across the blood-brain barrier.** *Peptides* 1998, **19**:777–80.
64. Lück M: **Plasmaproteinadsorption als möglicher Schlüsselfaktor für eine kontrollierte Arzneistoffapplikation mit partikulären Trägern, Dissertation.** Freie Universität, Berlin; 1997.
65. Petri B, Bootz A, Khalansky A, Hekmatara T, Müller R, Uhl R, Kreuter J, Gelperina S: **Chemotherapy of brain tumour using doxorubicin bound to surfactant-coated poly(butyl cyanoacrylate) nanoparticles: revisiting the role of surfactants.** *Journal of controlled release* 2007, **117**:51–8.
66. Kreuter J, Shamenkov D, Petrov V, Ramge P, Cychutek K, Koch-Brandt C, Alyautdin R: **Apolipoprotein-mediated transport of nanoparticle-bound drugs across the blood-brain barrier.** *Journal of drug targeting* 2002, **10**:317–25.
67. Kreuter J: **Mechanism of polymeric nanoparticle-based drug transport across the blood-brain barrier (BBB).** *Journal of microencapsulation* 2013, **30**:49–54.
68. Meister S, Zlatev I, Stab J, Docter D, Baches S, Stauber RH, Deutsch M, Schmidt R, Ropele S, Windisch M, Langer K, Wagner S, von Briesen H, Weggen S, Pietrzik CU: **Nanoparticulate flurbiprofen reduces amyloid- β 42 generation in an in vitro blood-brain barrier model.** *Alzheimer's research & therapy* 2013, **5**:51.
69. Alyautdin RN, Reichel A, Löbenberg R, Ramge P, Kreuter J, Begley DJ: **Interaction of Poly(butylcyanoacrylate) Nanoparticles with the Blood-Brain Barrier in vivo and in vitro.** *Journal of Drug Targeting* 2001, **9**:209–221.
70. Borchard G, Audus KL, Shi F, Kreuter J: **Uptake of surfactant-coated poly(methyl methacrylate)-nanoparticles by bovine brain microvessel endothelial cell monolayers.** *International Journal of Pharmaceutics* 1994, **110**:29–35.
71. Ramge P, Unger RE, Oltrogge JB, Zenker D, Begley D, Kreuter J, von Briesen H: **Polysorbate-80 coating enhances uptake of polybutylcyanoacrylate (PBCA)-nanoparticles by human and bovine primary brain capillary endothelial cells.** *European Journal of Neuroscience* 2000, **12**:1931–1940.
72. Hasadsri L, Kreuter J, Hattori H, Iwasaki T, George JM: **Functional protein delivery into neurons using polymeric nanoparticles.** *The Journal of biological chemistry* 2009, **284**:6972–81.
73. Juan BS De, Briesen H Von, Gelperina SE, Kreuter J: **Cytotoxicity of doxorubicin bound to poly(butyl cyanoacrylate) nanoparticles in rat glioma cell lines using different assays.** 2008.
74. Tahara K, Kato Y: **Intracellular drug delivery using polysorbate 80-modified poly (D, L-lactide-co-glycolide) nanospheres to glioblastoma cells.** *Journal of Microencapsulation* 2011, **28**(1):29-36.
75. Kreuter J: **Drug targeting with nanoparticles.** *European journal of drug metabolism and pharmacokinetics* 1994, **19**:253–6.
76. Chen Y-C, Hsieh W-Y, Lee W-F, Zeng D-T: **Effects of surface modification of PLGA-PEG-PLGA nanoparticles on loperamide delivery efficiency across the blood-brain barrier.** *Journal of Biomaterials Applications* 2011, **27**:909–922.
77. Michaelis K, Hoffmann MM, Dreis S, Herbert E, Alyautdin RN, Michaelis M, Kreuter J, Langer K: **Covalent linkage of apolipoprotein e to albumin nanoparticles strongly enhances drug transport into the brain.** *The Journal of pharmacology and experimental therapeutics* 2006, **317**:1246–53.
78. Kreuter J, Hekmatara T, Dreis S, Vogel T, Gelperina S, Langer K: **Covalent attachment of apolipoprotein A-I and apolipoprotein B-100 to albumin nanoparticles enables drug transport into the brain.** *Journal of controlled release* 2007, **118**:54–8.

79. Lucarelli M, Borrelli V, Fiori A, Cucina A, Granata F, Potenza RL, Scarpa S, Cavallaro A, Strom R: **The expression of native and oxidized LDL receptors in brain microvessels is specifically enhanced by astrocytes-derived soluble factor(s)**. *FEBS Letters* 2002, **522**:19–23.
80. Lajoie JM, Shusta E V: **Targeting receptor-mediated transport for delivery of biologics across the blood-brain barrier**. *Annual review of pharmacology and toxicology* 2015, **55**:613–31.
81. Wagner S, Zensi A, Wien SL, Tschickardt SE, Maier W, Vogel T, Worek F, Pietrzik CU, Kreuter J, von Briesen H: **Uptake mechanism of ApoE-modified nanoparticles on brain capillary endothelial cells as a blood-brain barrier model**. *PLoS one* 2012, **7**:e32568.
82. Herz J, Strickland DK: **LRP: a multifunctional scavenger and signaling receptor**. *The Journal of clinical investigation* 2001, **108**:779–84.
83. Li J, Sabliov C: **PLA/PLGA nanoparticles for delivery of drugs across the blood-brain barrier**. *Nanotechnology Reviews* 2013, **2**:241–257.
84. Yang SC, Lu LF, Cai Y, Zhu JB, Liang BW, Yang CZ: **Body distribution in mice of intravenously injected camptothecin solid lipid nanoparticles and targeting effect on brain**. *Journal of controlled release* 1999, **59**:299–307.
85. Kim D-H, Martin DC: **Sustained release of dexamethasone from hydrophilic matrices using PLGA nanoparticles for neural drug delivery**. *Biomaterials* 2006, **27**:3031–7.
86. Gulyaev AE, Gelperina SE, Skidan IN, Antropov AS, Kivman GY, Kreuter J: **Significant transport of doxorubicin into the brain with polysorbate 80-coated nanoparticles**. *Pharmaceutical research* 1999, **16**:1564–9.
87. Reddy LH, Sharma RK, Chuttani K, Mishra AK, Murthy RR: **Etoposide-incorporated tripalmitin nanoparticles with different surface charge: formulation, characterization, radiolabeling, and biodistribution studies**. *The AAPS journal* 2004, **6**:e23.
88. Sun W, Xie C, Wang H, Hu Y: **Specific role of polysorbate 80 coating on the targeting of nanoparticles to the brain**. *Biomaterials* 2004, **25**:3065–71.
89. Wang C-X, Huang L-S, Hou L-B, Jiang L, Yan Z-T, Wang Y-L, Chen Z-L: **Antitumor effects of polysorbate-80 coated gemcitabine polybutylcyanoacrylate nanoparticles in vitro and its pharmacodynamics in vivo on C6 glioma cells of a brain tumor model**. *Brain research* 2009, **1261**:91–9.
90. Alyautdin RN, Petrov VE, Langer K, Berthold A, Kharkevich DA, Kreuter J: **Delivery of Loperamide Across the Blood-Brain Barrier with Polysorbate 80-Coated Polybutylcyanoacrylate Nanoparticles**. *Pharmaceutical Research* 1997, **14**:325–328.
91. Tosi G, Costantino L, Rivasi F, Ruozi B, Leo E, Vergoni A V, Tacchi R, Bertolini A, Vandelli MA, Forni F: **Targeting the central nervous system: in vivo experiments with peptide-derivatized nanoparticles loaded with Loperamide and Rhodamine-123**. *Journal of controlled release* 2007, **122**:1–9.
92. Gao K, Jiang X: **Influence of particle size on transport of methotrexate across blood brain barrier by polysorbate 80-coated polybutylcyanoacrylate nanoparticles**. *International journal of pharmaceutics* 2006, **310**:213–9.
93. Wilson B, Samanta MK, Santhi K, Kumar KPS, Paramakrishnan N, Suresh B: **Poly(n-butylcyanoacrylate) nanoparticles coated with polysorbate 80 for the targeted delivery of rivastigmine into the brain to treat Alzheimer's disease**. *Brain research* 2008, **1200**:159–68.
94. Parikh T, Bommana MM, Squillante E: **Efficacy of surface charge in targeting pegylated nanoparticles of sulphuride to the brain**. *European journal of pharmaceutics and biopharmaceutics* 2010, **74**:442–50.
95. Wilson B, Samanta MK, Santhi K, Kumar KPS, Paramakrishnan N, Suresh B: **Targeted delivery of tacrine into the brain with polysorbate 80-coated poly(n-butylcyanoacrylate) nanoparticles**. *European journal of pharmaceutics and biopharmaceutics* 2008, **70**:75–84.

96. Alyautdin RN, Tezikov EB, Ramge P, Kharkevich DA, Begley DJ, Kreuter J: **Significant entry of tubocurarine into the brain of rats by adsorption to polysorbate 80-coated polybutylcyanoacrylate nanoparticles: an in situ brain perfusion study.** *Journal of microencapsulation* 1998, **15**:67–74.
97. **2014 Alzheimer's Disease Facts and Figures, Alzheimer's Association, date accessed 18-03-15** [<https://www.alz.org/facts/>]
98. **2015 World Population Data Sheet, population reference bureau, date accessed 12-01-16** [www.prb.org]
99. Prince M, Wimo A, Guerchet M, Gemma-Claire A, Wu Y-T, Prina M: *World Alzheimer Report 2015: The Global Impact of Dementia - An Analysis of Prevalence, Incidence, Cost And Trends.* 2015 *Alzheimer's disease International.* [<https://www.alz.co.uk/research/WorldAlzheimerReport2015.pdf>]
100. Sosa-Ortiz AL, Acosta-Castillo I, Prince MJ: **Epidemiology of Dementias and Alzheimer's Disease.** *Archives of Medical Research* 2012, **43**:600–608.
101. Sindi S, Mangialasche F, Kivipelto M: **Advances in the prevention of Alzheimer's Disease.** *F1000Prime Reports* 2015, **7**(May):1–12.
102. Riley JC: **Estimates of Regional and Global Life Expectancy, 1800–2001.** *Population and Development Review* 2005, **31**:537–543.
103. Mölsä PK, Marttila RJ, Rinne UK: **Survival and cause of death in Alzheimer's disease and multi-infarct dementia.** *Acta Neurologica Scandinavica* 1986, **74**:103–107.
104. Lambracht-Washington D, Rosenberg RN: **Advances in the development of vaccines for Alzheimer's disease.** *Discovery medicine* 2013, **15**:319–26.
105. Tinetti ME, McAvay GJ, Murphy TE, Gross CP, Lin H, Allore HG: **Contribution of individual diseases to death in older adults with multiple diseases.** *Journal of the American Geriatrics Society* 2012, **60**:1448–56.
106. Maier W, Jessen F, Schneider F, Deuschl G, Spottke A, Reichmann H: *Diagnose- Und Behandlungsleitlinie Demenz.* Berlin, Heidelberg: Springer Berlin Heidelberg; 2010.
107. Kaduszkiewicz H, Zimmermann T, Beck-Bornholdt H-P, van den Bussche H: **Cholinesterase inhibitors for patients with Alzheimer's disease: systematic review of randomised clinical trials.** *BMJ (Clinical research ed)* 2005, **331**:321–7.
108. Aisen PS, Cummings J, Schneider LS: **Symptomatic and nonamyloid/tau based pharmacologic treatment for Alzheimer disease.** *Cold Spring Harbor perspectives in medicine* 2012, **2**:a006395.
109. McShane R, Areosa Sastre A, Minakaran N: **Memantine for dementia.** *The Cochrane database of systematic reviews* 2006, **19**(2):CD003154.
110. Fischer-Terworth C: *Evidenzbasierte Demenztherapie: Wissenschaftlich fundierte neuropsychiatrisch-psychologische Therapien für den ambulanten und stationären Bereich.* Pabst Science Publishers, D-49525 Lengerich, Germany; 2013.
111. Morimoto SS, Kanellopoulos D, Manning KJ, Alexopoulos GS: **Diagnosis and Treatment of Depression and Cognitive Impairment in Late-Life.** *Annals of the New York Academy of Sciences* 2015, **1345**:36–46.
112. Vandenberghe R, Rinne JO, Boada M, Katayama S, Scheltens P, Vellas B, Tuchman M, Gass A, Fiebach JB, Hill D, Lobello K, Li D, McRae T, Lucas P, Evans I, Booth K, Luscan G, Wyman BT, Hua L, Yang L, Brashear HR, Black RS: **Bapineuzumab for mild to moderate Alzheimer's disease in two global, randomized, phase 3 trials.** *Alzheimer's research & therapy* 2016, **8**:18.
113. Hippus H, Neundörfer G: **The discovery of Alzheimer's disease.** *Dialogues in clinical neuroscience* 2003, **5**:101–8.
114. Alzheimer A, Stelzmann RA, Schnitzlein HN, Murtagh FR: **An English translation of Alzheimer's 1907 paper, "Über eine eigenartige Erkrankung der Hirnrinde".** *Clinical anatomy (New York, NY)* 1995, **8**:429–31.
115. Alzheimer A: **Über eine eigenartige Erkrankung der Hirnrinde.** *Allg Zeitschr Psychiatr* 1907, **64**:146–148.

116. Kraepelin E: **Psychiatrie. 8th Ed. Vol I: Allgemeine Psychiatrie; Vol II: Klinische Psychiatrie.** Barth Verlag 1909/1910. 8th edition. Leipzig, Germany
117. Giannakopoulos P, Herrmann FR, Bussi re T, Bouras C, K vari E, Perl DP, Morrison JH, Gold G, Hof PR: **Tangle and neuron numbers, but not amyloid load, predict cognitive status in Alzheimer's disease.** *Neurology* 2003, **60**:1495–500.
118. Neumann K, Fari s G, Slachevsky A, Perez P, Maccioni RB: **Human platelets tau: a potential peripheral marker for Alzheimer's disease.** *Journal of Alzheimer's disease* 2011, **25**:103–9.
119. Proft J, Weiss N: **A protective mutation against Alzheimer disease?** *Communicative & integrative biology* 2012, **5**:301–3.
120. McGeer PL, McGeer EG: **NSAIDs and Alzheimer disease: epidemiological, animal model and clinical studies.** *Neurobiology of aging* 2007, **28**:639–47.
121. Perl DP: **Neuropathology of Alzheimer's disease.** *The Mount Sinai journal of medicine, New York* 2010, **77**:32–42.
122. Citron M: **Alzheimer's disease: strategies for disease modification.** *Nature Reviews Drug Discovery* 2010, **9**:387–398.
123. Querfurth HW, LaFerla FM: **Alzheimer's disease.** *The New England journal of medicine* 2010, **362**:329–44.
124. F rstl H, Kurz A: **Clinical features of Alzheimer's disease.** *European Archives of Psychiatry and Clinical Neuroscience* 1999, **249**:288–290.
125. Page S, Fletcher T: **Auguste D: One hundred years on: 'The person' not 'the case'.** *Dementia* 2006, **5**:571–583.
126. Maurer K, Volk S, Gerbaldo H: **Auguste D and Alzheimer's disease.** *Lancet* 1997, **349**:1546–9.
127. Bird TD: **Genetic Aspects of Alzheimer Disease.** *Genetics in Medicine* 2008, **10**:231–239.
128. Hardy J, Bogdanovic N, Winblad B, Portelius E, Andreassen N, Cedazo-Minguez A, Zetterberg H: **Pathways to Alzheimer's disease.** *Journal of internal medicine* 2014, **275**:296–303.
129. Mullan M, Houlden H, Windelspecht M, Fidani L, Lombardi C, Diaz P, Rossor M, Crook R, Hardy J, Duff K: **A locus for familial early-onset Alzheimer's disease on the long arm of chromosome 14, proximal to the alpha 1-antichymotrypsin gene.** *Nature genetics* 1992, **2**:340–342.
130. Mullan M: **Familial Alzheimer's disease: second gene locus located.** *BMJ (Clinical research ed)* 1992, **305**:1108–9.
131. Haass C, Lemere CA, Capell A, Citron M, Seubert P, Schenk D, Lannfelt L, Selkoe DJ: **The Swedish mutation causes early-onset Alzheimer's disease by β -secretase cleavage within the secretory pathway.** *Nature Medicine* 1995, **1**:1291–1296.
132. Hardy J, Selkoe DJ: **The amyloid hypothesis of Alzheimer's disease: progress and problems on the road to therapeutics.** *Science (New York, NY)* 2002, **297**:353–6.
133. Bartus RT, Dean RL, Beer B, Lippa AS: **The cholinergic hypothesis of geriatric memory dysfunction.** *Science (New York, NY)* 1982, **217**:408–14.
134. Hardy J, Allsop D: **Amyloid deposition as the central event in the aetiology of Alzheimer's disease.** *Trends in Pharmacological Sciences* 1991, **12**:383–388.
135. Bartzokis G: **Age-related myelin breakdown: a developmental model of cognitive decline and Alzheimer's disease.** *Neurobiology of aging* 2004, **25**:5–18; author reply 49–62.
136. Bartzokis G: **Alzheimer's disease as homeostatic responses to age-related myelin breakdown.** *Neurobiology of aging* 2011, **32**:1341–71.
137. Geula C, Mesulam MM, Saroff DM, Wu CK: **Relationship between plaques, tangles, and loss of cortical cholinergic fibers in Alzheimer disease.** *Journal of neuropathology and experimental neurology* 1998, **57**:63–75.

138. Bartus RT: **On neurodegenerative diseases, models, and treatment strategies: lessons learned and lessons forgotten a generation following the cholinergic hypothesis.** *Experimental neurology* 2000, **163**:495–529.
139. Davies P, Maloney AJ: **Selective loss of central cholinergic neurons in Alzheimer's disease.** *Lancet* 1976, **2**:1403.
140. Hardy J, Higgins G: **Alzheimer's disease: the amyloid cascade hypothesis.** *Science* 1992, **256**:184–185.
141. Selkoe DJ: **The molecular pathology of Alzheimer's disease.** *Neuron* 1991, **6**:487–98.
142. Artavanis-Tsakonas S, Rand MD, Lake RJ: **Notch signaling: cell fate control and signal integration in development.** *Science (New York, NY)* 1999, **284**:770–6.
143. LaFerla FM, Green KN, Oddo S: **Intracellular amyloid-beta in Alzheimer's disease.** *Nature reviews Neuroscience* 2007, **8**:499–509.
144. Crump CJ, Johnson DS, Li Y-M: **Target of γ -secretase modulators, presenilin marks the spot.** *The EMBO journal* 2011, **30**:4696–8.
145. Müller U, Winter P, Graeber MB: **A presenilin 1 mutation in the first case of Alzheimer's disease.** *Lancet neurology* 2013, **12**:129–30.
146. Chouraki V, Seshadri S: **Genetics of Alzheimer's disease.** *Advances in genetics* 2014, **87**:245–94.
147. Naj AC, Jun G, Reitz C, Kunkle BW, Perry W, Park YS, Beecham GW, Rajbhandary RA, Hamilton-Nelson KL, Wang L-S, Kauwe JSK, Huentelman MJ, Myers AJ, Bird TD, Boeve BF, Baldwin CT, Jarvik GP, Crane PK, Rogava E, Barmada MM, Demirci FY, Cruchaga C, Kramer PL, Ertekin-Taner N, Hardy J, Graff-Radford NR, Green RC, Larson EB, St George-Hyslop PH, Buxbaum JD, et al.: **Effects of multiple genetic loci on age at onset in late-onset Alzheimer disease: a genome-wide association study.** *JAMA neurology* 2014, **71**:1394–404.
148. Cedazo-Mínguez A: **Apolipoprotein E and Alzheimer's disease: molecular mechanisms and therapeutic opportunities.** *Journal of cellular and molecular medicine* 2007, **11**:1227–38.
149. Riddell DR, Christie G, Hussain I, Dingwall C: **Compartmentalization of beta-secretase (Asp2) into low-buoyant density, noncaveolar lipid rafts.** *Current biology* 2001, **11**:1288–93.
150. Liu Q, Zerbinatti C V, Zhang J, Hoe H-S, Wang B, Cole SL, Herz J, Muglia L, Bu G: **Amyloid precursor protein regulates brain apolipoprotein E and cholesterol metabolism through lipoprotein receptor LRP1.** *Neuron* 2007, **56**:66–78.
151. Jiang Q, Lee CYD, Mandrekar S, Wilkinson B, Cramer P, Zelcer N, Mann K, Lamb B, Willson TM, Collins JL, Richardson JC, Smith JD, Comery TA, Riddell D, Holtzman DM, Tontonoz P, Landreth GE: **ApoE promotes the proteolytic degradation of A β .** *Neuron* 2008, **58**:681–93.
152. Deane R, Sagare A, Hamm K, Parisi M, Lane S, Finn MB, Holtzman DM, Zlokovic B V: **apoE isoform-specific disruption of amyloid beta peptide clearance from mouse brain.** *The Journal of clinical investigation* 2008, **118**:4002–13.
153. Wang H, Anderson LG, Lascola CD, James ML, Venkatraman TN, Bennett ER, Acheson SK, Vitek MP, Laskowitz DT: **ApolipoproteinE mimetic peptides improve outcome after focal ischemia.** *Experimental neurology* 2013, **241**:67–74.
154. Ghosal K, Stathopoulos A, Thomas D, Phenis D, Vitek MP, Pimplikar SW: **The apolipoprotein-E-mimetic COG112 protects amyloid precursor protein intracellular domain-overexpressing animals from Alzheimer's disease-like pathological features.** *Neuro-degenerative diseases* 2013, **12**:51–8.
155. Jones L, Holmans PA, Hamshere ML, Harold D, Moskvina V, Ivanov D, Pocklington A, Abraham R, Hollingworth P, Sims R, Gerrish A, Pahwa JS, Jones N, Stretton A, Morgan AR, Lovestone S, Powell J, Proitsis P, Lupton MK, Brayne C, Rubinsztein DC, Gill M, Lawlor B, Lynch A, Morgan K, Brown KS, Passmore PA, Craig D, McGuinness B, Todd S, et al.: **Genetic evidence implicates the immune system and cholesterol metabolism in the aetiology of Alzheimer's disease.** *PloS one* 2010, **5**:e13950.

156. McGeer PL, McGeer EG: **The possible role of complement activation in Alzheimer disease.** *Trends in molecular medicine* 2002, **8**:519–23.
157. Velazquez P, Cribbs DH, Poulos TL, Tenner AJ: **Aspartate residue 7 in amyloid beta-protein is critical for classical complement pathway activation: implications for Alzheimer's disease pathogenesis.** *Nature medicine* 1997, **3**:77–79.
158. Rogers J, Cooper NR, Webster S, Schultz J, McGeer PL, Styren SD, Civin WH, Brachova L, Bradt B, Ward P: **Complement activation by beta-amyloid in Alzheimer disease.** *Proceedings of the National Academy of Sciences of the United States of America* 1992, **89**:10016–20.
159. Rogers J, Schultz J, Brachova L, Lue LF, Webster S, Bradt B, Cooper NR, Moss DE: **Complement activation and beta-amyloid-mediated neurotoxicity in Alzheimer's disease.** *Research in immunology* 1992, **143**:624–30.
160. Daborg J, Andreasson U, Pekna M, Lautner R, Hanse E, Minthon L, Blennow K, Hansson O, Zetterberg H: **Cerebrospinal fluid levels of complement proteins C3, C4 and CR1 in Alzheimer's disease.** *Journal of neural transmission (Vienna, Austria : 1996)* 2012, **119**:789–97.
161. Mattsson N, Tabatabaei S, Johansson P, Hansson O, Andreasson U, Månsson J-E, Johansson J-O, Olsson B, Wallin A, Svensson J, Blennow K, Zetterberg H: **Cerebrospinal fluid microglial markers in Alzheimer's disease: elevated chitotriosidase activity but lack of diagnostic utility.** *Neuromolecular medicine* 2011, **13**:151–9.
162. Craig-Schapiro R, Perrin RJ, Roe CM, Xiong C, Carter D, Cairns NJ, Mintun MA, Peskind ER, Li G, Galasko DR, Clark CM, Quinn JF, D'Angelo G, Malone JP, Townsend RR, Morris JC, Fagan AM, Holtzman DM: **YKL-40: a novel prognostic fluid biomarker for preclinical Alzheimer's disease.** *Biological psychiatry* 2010, **68**:903–12.
163. Jonsson T, Atwal JK, Steinberg S, Snaedal J, Jonsson P V, Bjornsson S, Stefansson H, Sulem P, Gudbjartsson D, Maloney J, Hoyte K, Gustafson A, Liu Y, Lu Y, Bhangale T, Graham RR, Huttenlocher J, Bjornsdottir G, Andreassen OA, Jönsson EG, Palotie A, Behrens TW, Magnusson OT, Kong A, Thorsteinsdottir U, Watts RJ, Stefansson K: **A mutation in APP protects against Alzheimer's disease and age-related cognitive decline.** *Nature* 2012, **488**:96–9.
164. Schaefer EJ, Bongard V, Beiser AS, Lamon-Fava S, Robins SJ, Au R, Tucker KL, Kyle DJ, Wilson PWF, Wolf PA: **Plasma phosphatidylcholine docosaehaenoic acid content and risk of dementia and Alzheimer disease: the Framingham Heart Study.** *Archives of neurology* 2006, **63**:1545–50.
165. Heude B, Ducimetière P, Berr C: **Cognitive decline and fatty acid composition of erythrocyte membranes-The EVA Study.** *The American journal of clinical nutrition* 2003, **77**:803–8.
166. Freund-Levi Y, Eriksdotter-Jönhagen M, Cederholm T, Basun H, Faxén-Irving G, Garlind A, Vedin I, Vessby B, Wahlund L-O, Palmblad J: **Omega-3 fatty acid treatment in 174 patients with mild to moderate Alzheimer disease: OmegAD study: a randomized double-blind trial.** *Archives of neurology* 2006, **63**:1402–8.
167. Barberger-Gateau P: **Nutrition and brain aging: how can we move ahead?** *European journal of clinical nutrition* 2014, **68**:1245–1249.
168. Mayeux R: **Alzheimer's disease: epidemiology.** *Handbook of clinical neurology* 2008, **89**:195–205.
169. Launer L: **Nonsteroidal anti-inflammatory drug use and the risk for Alzheimer's disease: dissecting the epidemiological evidence.** *Drugs* 2003, **63**:731–9.
170. McGeer PL, McGeer E, Rogers J, Sibley J: **Anti-inflammatory drugs and Alzheimer disease.** *Lancet* 1990, **335**:1037.
171. Cole GM, Morihara T, Lim GP, Yang F, Begum A, Frautschy SA: **NSAID and antioxidant prevention of Alzheimer's disease: lessons from in vitro and animal models.** *Annals of the New York Academy of Sciences* 2004, **1035**:68–84.
172. Gasparini L, Ongini E, Wenk G: **Non-steroidal anti-inflammatory drugs (NSAIDs) in Alzheimer's disease: old and new mechanisms of action.** *Journal of neurochemistry* 2004, **91**:521–36.
173. Leuchtenberger S, Behr D, Weggen S: **Selective modulation of Abeta42 production in Alzheimer's disease: non-steroidal anti-inflammatory drugs and beyond.** *Current pharmaceutical design* 2006, **12**:4337–55.

174. Combs CK, Johnson DE, Karlo JC, Cannady SB, Landreth GE: **Inflammatory mechanisms in Alzheimer's disease: inhibition of beta-amyloid-stimulated proinflammatory responses and neurotoxicity by PPARgamma agonists.** *The Journal of neuroscience* 2000, **20**:558–67.
175. Heneka MT, Landreth GE, Feinstein DL: **Role for peroxisome proliferator-activated receptor-gamma in Alzheimer's disease.** *Annals of neurology* 2001, **49**:276.
176. Beher D, Clarke EE, Wrigley JDJ, Martin ACL, Nadin A, Churcher I, Shearman MS: **Selected non-steroidal anti-inflammatory drugs and their derivatives target gamma-secretase at a novel site. Evidence for an allosteric mechanism.** *The Journal of biological chemistry* 2004, **279**:43419–26.
177. Eriksen JL, Sagi SA, Smith TE, Weggen S, Das P, McLendon DC, Ozols V V, Jessing KW, Zavitz KH, Koo EH, Golde TE: **NSAIDs and enantiomers of flurbiprofen target gamma-secretase and lower Abeta 42 in vivo.** *The Journal of clinical investigation* 2003, **112**:440–9.
178. Morihara T, Chu T, Ubada O, Beech W, Cole GM: **Selective inhibition of Abeta42 production by NSAID R-enantiomers.** *Journal of neurochemistry* 2002, **83**:1009–12.
179. **Myriad Genetics Reports Results of U.S. Phase 3 Trial of Flurizan™ in Alzheimer's Disease**, date accessed **28-11-14** [<http://web.archive.org/web/20080730012308/http://www.myriad.com/news/release/1170283>]
180. **Myriad Genetics Reports Results of U.S. Phase 2 Trial of Flurizan™ in Alzheimer's Disease**, date accessed **28-11-14** [<http://investor.myriad.com/releasedetail.cfm?ReleaseID=326077>]
181. **MPC-7869 Clinical Study, EU Clinical Trials Register**, date accessed **2016-05-20** [<https://www.clinicaltrialsregister.eu/ctr-search/search?query=alzheimer+flurbiprofen>]
182. Wilcock GK, Black SE, Hendrix SB, Zavitz KH, Swabb EA, Laughlin MA: **Efficacy and safety of tarenflurbil in mild to moderate Alzheimer's disease: a randomised phase II trial.** *The Lancet Neurology* 2008, **7**:483–93.
183. Green RC, Schneider LS, Amato DA, Beelen AP, Wilcock G, Swabb EA, Zavitz KH: **Effect of tarenflurbil on cognitive decline and activities of daily living in patients with mild Alzheimer disease: a randomized controlled trial.** *JAMA : the journal of the American Medical Association* 2009, **302**:2557–64.
184. Wilcock GK, Black SE, Balch AH, Amato DA, Beelen AP, Schneider LS, Green RC, Swabb EA, Zavitz KH, Group. & the TP 3 S: *Safety and Efficacy of Tarenflurbil in Subjects With Mild Alzheimer's Disease: Results From an 18-Month International Multi-Center Phase 3 Trial.* AAIC 2009, Abstract O1-04-07. 2009.
185. Parepally JMR: **Factors limiting nonsteroidal anti-inflammatory drug uptake and distribution in central nervous system, Dissertation.** Texas Tech University Health Sciences Center; 2005.
186. Mannila A, Rautio J, Lehtonen M, Järvinen T, Savolainen J: **Inefficient central nervous system delivery limits the use of ibuprofen in neurodegenerative diseases.** *European Journal of Pharmaceutical Sciences* 2005, **24**:101–105.
187. Bannwarth B, Lopicque F, Pehourcq F, Gillet P, Schaeffer T, Laborde C, Dehais J, Gaucher A, Netter P: **Stereoselective disposition of ibuprofen enantiomers in human cerebrospinal fluid.** *British journal of clinical pharmacology* 1995, **40**:266–269.
188. Matoga M, Péhourcq F, Lagrange F, Tramu G, Bannwarth B: **Influence of molecular lipophilicity on the diffusion of arylpropionate non-steroidal anti-inflammatory drugs into the cerebrospinal fluid.** *Arzneimittel-Forschung* 1999, **49**:477–82.
189. **Measuring the Impedance of Cell Layers**, date accessed **2015-09-03** [<http://www.nanoanalytics.com/en/hardwareproducts/cellscope/howitworks/chapter02/index.php>]
190. Meister S: **Blood-CNS barriers in neurodegenerative diseases, Dissertation.** Johannes Gutenberg Universität Mainz; 2013.
191. Back SA, Khan R, Gan X, Rosenberg PA, Volpe JJ: **A new Alamar Blue viability assay to rapidly quantify oligodendrocyte death.** *Journal of neuroscience methods* 1999, **91**:47–54.
192. Mehta R, Kumar V, Bhunia H, Upadhyay SN: **Synthesis of Poly(Lactic Acid): A Review.** *Journal of Macromolecular Science, Part C: Polymer Reviews* 2005, **45**:325–349.

193. Arakawa T, Kita Y, Timasheff SN: **Protein precipitation and denaturation by dimethyl sulfoxide.** *Biophysical chemistry* 2007, **131**:62–70.
194. Koo EH, Squazzo SL: **Evidence that production and release of amyloid beta-protein involves the endocytic pathway.** *The Journal of biological chemistry* 1994, **269**:17386–9.
195. Stab J, Zlatev I, Raudszus B, Meister S, Langer K, Pietrzik CU, von Briesen H, Wagner S: **Flurbiprofen-loaded nanoparticles can cross a primary porcine in vitro blood-brain barrier model to reduce amyloid- β 42 burden.** *Journal of Nanomedicine & Biotherapeutic Discovery* 2016 **6**:140.
196. Butt AM, Jones HC, Abbott NJ: **Electrical resistance across the blood-brain barrier in anaesthetized rats: a developmental study.** *The Journal of physiology* 1990, **429**:47–62.
197. Zlatev I: **Entwicklung von Nanopartikeln als Träger für Alzheimer-Therapeutika, Dissertation.** Westfälische Wilhelms-Universität Münster; 2014.
198. Kulkarni RK, Pani KC, Neuman C, Leonard F: **Polylactic acid for surgical implants.** *Archives of surgery (Chicago, Ill : 1960)* 1966, **93**:839–43.
199. Kreuter J, Hekmatara T, Dreis S, Vogel T, Gelperina S, Langer K: **Covalent attachment of apolipoprotein A-I and apolipoprotein B-100 to albumin nanoparticles enables drug transport into the brain.** *Journal of controlled release* 2007, **118**:54–8.
200. Zensi A, Begley D, Pontikis C, Legros C, Mihoreanu L, Büchel C, Kreuter J: **Human serum albumin nanoparticles modified with apolipoprotein A-I cross the blood-brain barrier and enter the rodent brain.** *Journal of drug targeting* 2010, **18**:842–8.
201. Salmaso S, Caliceti P: **Stealth properties to improve therapeutic efficacy of drug nanocarriers.** *Journal of drug delivery* 2013, **2013**:374252.
202. Bauer B: **In vitro Zellkulturmodelle der Blut-Hirn-Schranke zur Untersuchung der Permeation und P-Glycoprotein-Interaktion von Arzneistoffen, Dissertation.** Ruprecht-Karls-Universität Heidelberg; 2002.
203. Garinot M, Fiévez V, Pourcelle V, Stoffelbach F, des Rieux A, Plapied L, Theate I, Freichels H, Jérôme C, Marchand-Brynaert J, Schneider Y-J, Prétat V: **PEGylated PLGA-based nanoparticles targeting M cells for oral vaccination.** *Journal of controlled release* 2007, **120**:195–204.
204. Gu F, Zhang L, Teplý BA, Mann N, Wang A, Radovic-Moreno AF, Langer R, Farokhzad OC: **Precise engineering of targeted nanoparticles by using self-assembled biointegrated block copolymers.** *Proceedings of the National Academy of Sciences of the United States of America* 2008, **105**:2586–91.
205. Bolton AE, Hunter WM: **The labelling of proteins to high specific radioactivities by conjugation to a 125I-containing acylating agent.** *The Biochemical journal* 1973, **133**:529–39.
206. Pieri M, Christian HC, Wilkins RJ, Boyd CAR, Meredith D: **The apical (hPepT1) and basolateral peptide transport systems of Caco-2 cells are regulated by AMP-activated protein kinase.** *American journal of physiology Gastrointestinal and liver physiology* 2010, **299**:G136–43.
207. Tran SB, Maxwell BD, Cao K, Bonacorsi SJ: **The synthesis of (14)C-labeled, (13)CD2-labeled saxagliptin, and its (13)CD2-labeled 5-hydroxy metabolite.** *Journal of labelled compounds & radiopharmaceuticals* 2014, **57**:136–40.
208. **Carbon 14 Labelled Peptides | Cambridge Research Biochemicals, date accessed 2016-05-19** [<http://www.crbdiscovery.com/technical/radiolabelling/carbon14-labelled-peptides.php>]
209. Martínez Vera NP, Schmidt R, Langer K, Zlatev I, Wronski R, Auer E, Havas D, Windisch M, von Briesen H, Wagner S, Stab J, Deutsch M, Pietrzik C, Fazekas F, Ropele S: **Tracking of magnetite labeled nanoparticles in the rat brain using MRI.** *PLoS one* 2014, **9**:e92068.
210. Gómez-Lopera SA, Arias JL, Gallardo V, Delgado A V: **Colloidal stability of magnetite/poly(lactic acid) core/shell nanoparticles.** *Langmuir* 2006, **22**:2816–21.
211. Frounchi M, Shamschiri S: **Magnetic nanoparticles-loaded PLA/PEG microspheres as drug carriers.** *Journal of biomedical materials research Res A* 2015, **103**(5):1893-8

212. **Basel Declaration A call for more trust, transparency and communication on animal research, date accessed 12/03/15** [<http://www.basel-declaration.org/>]
213. Israel M a., Yuan SH, Bardy C, Reyna SMS, Mu Y, Herrera C, Hefferan MP, Van Gorp S, Nazor KL, Boscolo FS, Carson CT, Laurent LC, Marsala M, Gage FH, Remes AM, Koo EH, Goldstein LSB: **Probing sporadic and familial Alzheimer's disease using induced pluripotent stem cells.** *Nature* 2012, **482**:216–220.
214. Choi SH, Kim YH, Hebisch M, Sliwinski C, Lee S, D'Avanzo C, Chen H, Hooli B, Asselin C, Muffat J, Klee JB, Zhang C, Wainger BJ, Peitz M, Kovacs DM, Woolf CJ, Wagner SL, Tanzi RE, Kim DY: **A three-dimensional human neural cell culture model of Alzheimer's disease.** *Nature* 2014, **515**:274–278.
215. Wyss-Coray T: **Inflammation in Alzheimer disease: driving force, bystander or beneficial response?** *Nature medicine* 2006, **12**:1005–15.
216. Hsiao K, Chapman P, Nilsen S, Eckman C, Harigaya Y, Younkin S, Yang F, Cole G: **Correlative memory deficits, Abeta elevation, and amyloid plaques in transgenic mice.** *Science (New York, NY)* 1996, **274**:99–102.
217. Santacruz K, Lewis J, Spires T, Paulson J, Kotilinek L, Ingelsson M, Guimaraes A, DeTure M, Ramsden M, McGowan E, Forster C, Yue M, Orne J, Janus C, Mariash A, Kuskowski M, Hyman B, Hutton M, Ashe KH: **Tau suppression in a neurodegenerative mouse model improves memory function.** *Science (New York, NY)* 2005, **309**:476–81.
218. Deacon R, Altimiras F, Bazan-Leon E, Pyarasani R, Nachtigall F, Santos L, Tsolaki A, Pednekar L, Kishore U, Biekofsky R, Vasquez R, Cogram P: **Natural AD-Like Neuropathology in Octodon degus: Impaired Burrowing and Neuroinflammation.** *Current Alzheimer research* 2015, **12**:314–322.
219. Patabendige A, Abbott NJ: **Primary porcine brain microvessel endothelial cell isolation and culture.** *Current protocols in neuroscience* 2014, **69**:3.27.1–3.27.17.
220. Walters EM, Agca Y, Ganjam V, Evans T: **Animal models got you puzzled?: think pig.** *Annals of the New York Academy of Sciences* 2011, **1245**:63–4.
221. Siddharthan V, Kim Y V, Liu S, Kim KS: **Human astrocytes/astrocyte-conditioned medium and shear stress enhance the barrier properties of human brain microvascular endothelial cells.** *Brain research* 2007, **1147**:39–50.
222. Kuo Y-C, Lu C-H: **Effect of human astrocytes on the characteristics of human brain-microvascular endothelial cells in the blood-brain barrier.** *Colloids and surfaces B, Biointerfaces* 2011, **86**:225–31.
223. Tan KH, Dobbie MS, Felix RA, Barrand MA, Hurst RD: **A comparison of the induction of immortalized endothelial cell impermeability by astrocytes.** *Neuroreport* 2001, **12**:1329–34.
224. Deane R, Bell RD, Sagare A, Zlokovic B V: **Clearance of amyloid-beta peptide across the blood-brain barrier: implication for therapies in Alzheimer's disease.** *CNS & neurological disorders drug targets* 2009, **8**:16–30.
225. Burgmans S, van de Haar HJ, Verhey FRJ, Backes WH: **Amyloid- β interacts with blood-brain barrier function in dementia: a systematic review.** *Journal of Alzheimer's disease* 2013, **35**:859–73.
226. van de Haar HJ, Burgmans S, Hofman PAM, Verhey FRJ, Jansen JFA, Backes WH: **Blood-brain barrier impairment in dementia: Current and future in vivo assessments.** *Neuroscience and biobehavioral reviews* 2015, **49C**:71–81.
227. Jack CR, Lowe VJ, Weigand SD, Wiste HJ, Senjem ML, Knopman DS, Shiung MM, Gunter JL, Boeve BF, Kemp BJ, Weiner M, Petersen RC: **Serial PIB and MRI in normal, mild cognitive impairment and Alzheimer's disease: implications for sequence of pathological events in Alzheimer's disease.** *Brain* 2009, **132**(Pt 5):1355–65.
228. Souza LC de, Sarazin M, Teixeira-Júnior AL, Caramelli P, Santos AE dos, Dubois B: **Biological markers of Alzheimer's disease.** *Arquivos de neuro-psiquiatria* 2014, **72**:227–31.
229. Dubois B, Epelbaum S, Santos A, Di Stefano F, Julian A, Michon A, Sarazin M, Hampel H: **Alzheimer disease: from biomarkers to diagnosis.** *Revue neurologique* 2013, **169**:744–51.

230. Dubois B, Feldman HH, Jacova C, Dekosky ST, Barberger-Gateau P, Cummings J, Delacourte A, Galasko D, Gauthier S, Jicha G, Meguro K, O'Brien J, Pasquier F, Robert P, Rossor M, Salloway S, Stern Y, Visser PJ, Scheltens P: **Research criteria for the diagnosis of Alzheimer's disease: revising the NINCDS-ADRDA criteria.** *Lancet neurology* 2007, **6**:734–46.
231. Möllmann H, Elsässer A, Hamm CW: **Oral antithrombotic therapy in primary and secondary prevention.** *Herz* 2005, **30**:181–8.
232. Becker RC, Meade TW, Berger PB, Ezekowitz M, O'Connor CM, Vorchheimer DA, Guyatt GH, Mark DB, Harrington RA: **The primary and secondary prevention of coronary artery disease: American College of Chest Physicians Evidence-Based Clinical Practice Guidelines (8th Edition).** *Chest* 2008, **133**(6 Suppl):776S–814S.
233. Vyas D, Castro P, Saadeh Y, Vyas A: **The role of nanotechnology in gastrointestinal cancer.** *Journal of biomedical nanotechnology* 2014, **10**:3204–18.
234. Prados J, Melguizo C, Perazzoli G, Cabeza L, Carrasco E, Oliver J, Jiménez-Luna C, Leiva MC, Ortiz R, Álvarez PJ, Aranega A: **Application of nanotechnology in the treatment and diagnosis of gastrointestinal cancers: review of recent patents.** *Recent patents on anti-cancer drug discovery* 2014, **9**:21–34.
235. Brakmane G, Winslet M, Seifalian AM: **Systematic review: the applications of nanotechnology in gastroenterology.** *Alimentary pharmacology & therapeutics* 2012, **36**:213–21.
236. de Souza LC, Sarazin M, Teixeira-Júnior AL, Caramelli P, Santos AE dos, Dubois B: **Biological markers of Alzheimer's disease.** *Arquivos de neuro-psiquiatria* 2014, **72**:227–31.
237. Engelborghs S: **Clinical indications for analysis of Alzheimer's disease CSF biomarkers.** *Revue Neurologique* 2013, **169**:709–714.
238. Molinuevo JL, Blennow K, Dubois B, Engelborghs S, Lewczuk P, Perret-Liaudet A, Teunissen CE, Parnetti L: **The clinical use of cerebrospinal fluid biomarker testing for Alzheimer's disease diagnosis: a consensus paper from the Alzheimer's Biomarkers Standardization Initiative.** *Alzheimer's & dementia* 2014, **10**:808–17.
239. Selkoe DJ, Schenk D: **Alzheimer's disease: molecular understanding predicts amyloid-based therapeutics.** *Annual review of pharmacology and toxicology* 2003, **43**:545–84.
240. Walsh DM, Selkoe DJ: **A beta oligomers - a decade of discovery.** *Journal of neurochemistry* 2007, **101**:1172–84.
241. Wong GT, Manfra D, Poulet FM, Zhang Q, Josien H, Bara T, Engstrom L, Pinzon-Ortiz M, Fine JS, Lee H-JJ, Zhang L, Higgins GA, Parker EM: **Chronic treatment with the gamma-secretase inhibitor LY-411,575 inhibits beta-amyloid peptide production and alters lymphopoiesis and intestinal cell differentiation.** *The Journal of biological chemistry* 2004, **279**:12876–82.
242. Milano J, McKay J, Dagenais C, Foster-Brown L, Pognan F, Gadiant R, Jacobs RT, Zacco A, Greenberg B, Ciaccio PJ: **Modulation of notch processing by gamma-secretase inhibitors causes intestinal goblet cell metaplasia and induction of genes known to specify gut secretory lineage differentiation.** *Toxicological sciences* 2004, **82**:341–58.
243. Fleisher AS, Raman R, Siemers ER, Becerra L, Clark CM, Dean RA, Farlow MR, Galvin JE, Peskind ER, Quinn JF, Sherzai A, Sowell BB, Aisen PS, Thal LJ: **Phase 2 safety trial targeting amyloid beta production with a gamma-secretase inhibitor in Alzheimer disease.** *Archives of neurology* 2008, **65**:1031–8.
244. Bateman RJ, Siemers ER, Mawuenyega KG, Wen G, Browning KR, Sigurdson WC, Yarasheski KE, Friedrich SW, Demattos RB, May PC, Paul SM, Holtzman DM: **A gamma-secretase inhibitor decreases amyloid-beta production in the central nervous system.** *Annals of neurology* 2009, **66**:48–54.

245. Martone RL, Zhou H, Atchison K, Comery T, Xu JZ, Huang X, Gong X, Jin M, Kreft A, Harrison B, Mayer SC, Aschmies S, Gonzales C, Zaleska MM, Riddell DR, Wagner E, Lu P, Sun S-C, Sonnenberg-Reines J, Oganessian A, Adkins K, Leach MW, Clarke DW, Huryn D, Abou-Gharbia M, Magolda R, Bard J, Frick G, Raje S, Forlow SB, et al.: **Begacestat (GSI-953): a novel, selective thiophene sulfonamide inhibitor of amyloid precursor protein gamma-secretase for the treatment of Alzheimer's disease.** *The Journal of pharmacology and experimental therapeutics* 2009, **331**:598–608.
246. Imbimbo BP: **Therapeutic potential of gamma-secretase inhibitors and modulators.** *Current topics in medicinal chemistry* 2008, **8**:54–61.
247. Chávez-Gutiérrez L, Bammens L, Benilova I, Vandersteen A, Benurwar M, Borgers M, Lismont S, Zhou L, Van Cleynebreugel S, Esselmann H, Wiltfang J, Serneels L, Karran E, Gijzen H, Schymkowitz J, Rousseau F, Broersen K, De Strooper B: **The mechanism of γ -Secretase dysfunction in familial Alzheimer disease.** *The EMBO journal* 2012, **31**:2261–74.
248. Karran E: **Current status of vaccination therapies in Alzheimer's disease.** *Journal of neurochemistry* 2012, **123**:647–51.
249. Coric V, van Dyck CH, Salloway S, Andreasen N, Brody M, Richter RW, Soininen H, Thein S, Shiovitz T, Pilcher G, Colby S, Rollin L, Dockens R, Pachai C, Portelius E, Andreasson U, Blennow K, Soares H, Albright C, Feldman HH, Berman RM: **Safety and Tolerability of the γ -Secretase Inhibitor Avagacestat in a Phase 2 Study of Mild to Moderate Alzheimer Disease.** *Archives of Neurology* 2012, **69**:1430.
250. Jarrett JT, Berger EP, Lansbury PT: **The carboxy terminus of the beta amyloid protein is critical for the seeding of amyloid formation: implications for the pathogenesis of Alzheimer's disease.** *Biochemistry* 1993, **32**:4693–7.
251. Weggen S, Eriksen JL, Das P, Sagi S a, Wang R, Pietrzik CU, Findlay K a, Smith TE, Murphy MP, Bulter T, Kang DE, Marquez-Sterling N, Golde TE, Koo EH: **A subset of NSAIDs lower amyloidogenic Abeta42 independently of cyclooxygenase activity.** *Nature* 2001, **414**:212–6.
252. Kukar TL, Ladd TB, Bann MA, Fraering PC, Narlawar R, Maharvi GM, Healy B, Chapman R, Welzel AT, Price RW, Moore B, Rangachari V, Cusack B, Eriksen J, Jansen-West K, Verbeeck C, Yager D, Eckman C, Ye W, Sagi S, Cottrell BA, Torpey J, Rosenberry TL, Fauq A, Wolfe MS, Schmidt B, Walsh DM, Koo EH, Golde TE: **Substrate-targeting gamma-secretase modulators.** *Nature* 2008, **453**:925–9.
253. Parepally JMR, Mandula H, Smith QR: **Brain uptake of nonsteroidal anti-inflammatory drugs: ibuprofen, flurbiprofen, and indomethacin.** *Pharmaceutical research* 2006, **23**:873–81.
254. Citron M: **Beta-secretase inhibition for the treatment of Alzheimer's disease—promise and challenge.** *Trends in pharmacological sciences* 2004, **25**:92–7.
255. Leung D, Abbenante G, Fairlie DP: **Protease inhibitors: current status and future prospects.** *Journal of medicinal chemistry* 2000, **43**:305–41.
256. Nitsch RM, Slack BE, Wurtman RJ, Growdon JH: **Release of Alzheimer amyloid precursor derivatives stimulated by activation of muscarinic acetylcholine receptors.** *Science (New York, NY)* 1992, **258**:304–7.
257. Gervais F, Paquette J, Morissette C, Krzywkowski P, Yu M, Azzi M, Lacombe D, Kong X, Aman A, Laurin J, Szarek WA, Tremblay P: **Targeting soluble Abeta peptide with Tramiprosate for the treatment of brain amyloidosis.** *Neurobiology of aging* 2007, **28**:537–47.
258. Eckman EA, Eckman CB: **Abeta-degrading enzymes: modulators of Alzheimer's disease pathogenesis and targets for therapeutic intervention.** *Biochemical Society transactions* 2005, **33**(Pt 5):1101–5.
259. Gardell SJ, Krueger JA, Antrilli TA, Elokda H, Mayer S, Orcutt SJ, Crandall DL, Vlasuk GP: **Neutralization of plasminogen activator inhibitor I (PAI-1) by the synthetic antagonist PAI-749 via a dual mechanism of action.** *Molecular pharmacology* 2007, **72**:897–906.

260. Goedert M, Klug A, Crowther RA: **Tau protein, the paired helical filament and Alzheimer's disease.** *Journal of Alzheimer's disease* 2006, **9**(3 Suppl):195–207.
261. Thal DR, Holzer M, Rüb U, Waldmann G, Günzel S, Zedlick D, Schober R: **Alzheimer-related tau-pathology in the perforant path target zone and in the hippocampal stratum oriens and radiatum correlates with onset and degree of dementia.** *Experimental neurology* 2000, **163**:98–110.
262. Hutton M, Lendon CL, Rizzu P, Baker M, Froelich S, Houlden H, Pickering-Brown S, Chakraverty S, Isaacs A, Grover A, Hackett J, Adamson J, Lincoln S, Dickson D, Davies P, Petersen RC, Stevens M, de Graaff E, Wauters E, van Baren J, Hillebrand M, Joosse M, Kwon JM, Nowotny P, Che LK, Norton J, Morris JC, Reed LA, Trojanowski J, Basun H, et al.: **Association of missense and 5'-splice-site mutations in tau with the inherited dementia FTDP-17.** *Nature* 1998, **393**:702–5.
263. Lee VM-Y, Trojanowski JQ: **Progress from Alzheimer's tangles to pathological tau points towards more effective therapies now.** *Journal of Alzheimer's disease* 2006, **9**(3 Suppl):257–62.
264. Schneider A, Mandelkow E: **Tau-based treatment strategies in neurodegenerative diseases.** *Neurotherapeutics : the journal of the American Society for Experimental NeuroTherapeutics* 2008, **5**:443–57.
265. **TRx-237-005 Clinical Study, EU Clinical Trials Register, date accessed 2016-05-20** [<https://www.clinicaltrialsregister.eu/ctr-search/search?query=TRx-237-005>]
266. **TRx-237-015 Clinical Study, EU Clinical Trials Register, date accessed 2016-05-20** [<https://www.clinicaltrialsregister.eu/ctr-search/search?query=TRx-237-015>]
267. **TRx-237-020 Clinical Study, EU Clinical Trials Register, date accessed 2016-05-20** [<https://www.clinicaltrialsregister.eu/ctr-search/search?query=TRx-237-020>]
268. Finch CE, Morgan TE: **Systemic inflammation, infection, ApoE alleles, and Alzheimer disease: a position paper.** *Current Alzheimer research* 2007, **4**:185–9.
269. Mrak RE, Griffin WST: **Glia and their cytokines in progression of neurodegeneration.** *Neurobiology of aging* 2005, **26**:349–54.
270. Griffin WST, Mrak RE: **Interleukin-1 in the genesis and progression of and risk for development of neuronal degeneration in Alzheimer's disease.** *Journal of leukocyte biology* 2002, **72**:233–8.
271. Cacquevel M, Lebourrier N, Chéenne S, Vivien D: **Cytokines in neuroinflammation and Alzheimer's disease.** *Current drug targets* 2004, **5**:529–34.
272. Mrak RE, Sheng JG, Griffin WST: **Glial cytokines in Alzheimer's disease: Review and pathogenic implications.** *Human Pathology* 1995, **26**:816–823.
273. Akiyama H, Barger S, Barnum S, Bradt B, Bauer J, Cole GM, Cooper NR, Eikelenboom P, Emmerling M, Fiebich BL, Finch CE, Frautschy S, Griffin WS, Hampel H, Hull M, Landreth G, Lue L, Mrak R, Mackenzie IR, McGeer PL, O'Banion MK, Pachter J, Pasinetti G, Plata-Salaman C, Rogers J, Rydel R, Shen Y, Streit W, Strohmeyer R, Tooyoma I, et al.: *Inflammation and Alzheimer's Disease. Volume 21*; 2000.
274. Frank-Cannon TC, Alto LT, McAlpine FE, Tansey MG: **Does neuroinflammation fan the flame in neurodegenerative diseases?** *Molecular neurodegeneration* 2009, **4**:47.
275. Vlad SC, Miller DR, Kowall NW, Felson DT: **Protective effects of NSAIDs on the development of Alzheimer disease.** *Neurology* 2008, **70**:1672–7.
276. Mackenzie IRA, Munoz DG: **Nonsteroidal anti-inflammatory drug use and Alzheimer-type pathology in aging.** *Neurology* 1998, **50**:986–990.
277. Sastre M, Dewachter I, Rossner S, Bogdanovic N, Rosen E, Borghgraef P, Evert BO, Dumitrescu-ozimek L, Thal DR, Landreth G, Walter J, Klockgether T, Leuven F Van, Heneka MT: **Nonsteroidal anti-inflammatory drugs repress beta-secretase gene promoter activity by the activation of PPARgamma.** *Proceedings of the National Academy of Sciences of the United States of America* 2006, **103**(2):443–8.

278. Zhou Y, Su Y, Li B, Liu F, Ryder JW, Wu X, Gonzalez-DeWhitt PA, Gelfanova V, Hale JE, May PC, Paul SM, Ni B: **Nonsteroidal anti-inflammatory drugs can lower amyloidogenic Abeta42 by inhibiting Rho.** *Science (New York, NY)* 2003, **302**:1215–7.
279. Takahashi Y, Hayashi I, Tominari Y, Rikimaru K, Morohashi Y, Kan T, Natsugari H, Fukuyama T, Tomita T, Iwatsubo T: **Sulindac sulfide is a noncompetitive gamma-secretase inhibitor that preferentially reduces Abeta 42 generation.** *The Journal of biological chemistry* 2003, **278**:18664–70.
280. Lleó A, Berezovska O, Herl L, Raju S, Deng A, Bacskai BJ, Frosch MP, Irizarry M, Hyman BT: **Nonsteroidal anti-inflammatory drugs lower Abeta42 and change presenilin 1 conformation.** *Nature medicine* 2004, **10**:1065–6.
281. Gasparini L, Rusconi L, Xu H, del Soldato P, Ongini E: **Modulation of beta-amyloid metabolism by non-steroidal anti-inflammatory drugs in neuronal cell cultures.** *Journal of neurochemistry* 2004, **88**:337–48.
282. Kukar T, Murphy MP, Eriksen JL, Sagi SA, Weggen S, Smith TE, Ladd T, Khan MA, Kache R, Beard J, Dodson M, Merit S, Ozols V V, Anastasiadis PZ, Das P, Fauq A, Koo EH, Golde TE: **Diverse compounds mimic Alzheimer disease-causing mutations by augmenting Abeta42 production.** *Nature medicine* 2005, **11**:545–50.
283. Sung S, Yang H, Uryu K, Lee EB, Zhao L, Shineman D, Trojanowski JQ, Lee VM-Y, Praticò D: **Modulation of nuclear factor-kappa B activity by indomethacin influences A beta levels but not A beta precursor protein metabolism in a model of Alzheimer's disease.** *The American journal of pathology* 2004, **165**:2197–206.
284. Warner TD, Mitchell JA: **Cyclooxygenases: new forms, new inhibitors, and lessons from the clinic.** *FASEB journal* 2004, **18**:790–804.
285. Lehmann JM, Lenhard JM, Oliver BB, Ringold GM, Kliewer SA: **Peroxisome proliferator-activated receptors alpha and gamma are activated by indomethacin and other non-steroidal anti-inflammatory drugs.** *The Journal of biological chemistry* 1997, **272**:3406–10.
286. Bernardo A, Ajmone-Cat MA, Gasparini L, Ongini E, Minghetti L: **Nuclear receptor peroxisome proliferator-activated receptor-gamma is activated in rat microglial cells by the anti-inflammatory drug HCT1026, a derivative of flurbiprofen.** *Journal of neurochemistry* 2005, **92**:895–903.
287. Preisner A, Albrecht S, Cui Q-L, Hucke S, Ghelman J, Hartmann C, Taketo MM, Antel J, Klotz L, Kuhlmann T: **Non-steroidal anti-inflammatory drug indometacin enhances endogenous remyelination.** *Acta neuropathologica* 2015, **130**(2):247–61.
288. Norflus F, Nanje A, Gutekunst C-A, Shi G, Cohen J, Bejarano M, Fox J, Ferrante RJ, Hersch SM: **Anti-inflammatory treatment with acetylsalicylate or rofecoxib is not neuroprotective in Huntington's disease transgenic mice.** *Neurobiology of disease* 2004, **17**:319–25.
289. Esposito E, Di Matteo V, Benigno A, Pierucci M, Crescimanno G, Di Giovanni G: **Non-steroidal anti-inflammatory drugs in Parkinson's disease.** *Experimental neurology* 2007, **205**:295–312.
290. Deleidi M, Gasser T: **The role of inflammation in sporadic and familial Parkinson's disease.** *Cellular and molecular life science* 2013, **70**(22):4259–73.
291. Casper D, Yaparpalvi U, Rempel N, Werner P: **Ibuprofen protects dopaminergic neurons against glutamate toxicity in vitro.** *Neuroscience letters* 2000, **289**:201–4.
292. Brown AD, McMorris CA, Longman RS, Leigh R, Hill MD, Friedenreich CM, Poulin MJ: **Effects of cardiorespiratory fitness and cerebral blood flow on cognitive outcomes in older women.** *Neurobiology of aging* 2010, **31**:2047–57.
293. Larson EB, Wang L: **Exercise, aging, and Alzheimer disease.** *Alzheimer disease and associated disorders* 2004, **18**:54–6.
294. Aisen PS, Schneider LS, Sano M, Diaz-Arrastia R, van Dyck CH, Weiner MF, Bottiglieri T, Jin S, Stokes KT, Thomas RG, Thal LJ: **High-dose B vitamin supplementation and cognitive decline in Alzheimer disease: a randomized controlled trial.** *JAMA* 2008, **300**:1774–83.

295. Liu Q-P, Wu Y-F, Cheng H-Y, Xia T, Ding H, Wang H, Wang Z-M, Xu Y: **Habitual coffee consumption and risk of cognitive decline/dementia: a systematic review and meta-analysis of prospective cohort studies.** *Nutrition* 2016, **32**(6):628-36.
296. Kim Y-S, Kwak SM, Myung S-K: **Caffeine intake from coffee or tea and cognitive disorders: a meta-analysis of observational studies.** *Neuroepidemiology* 2015, **44**:51-63.
297. Gamoh S, Hashimoto M, Hossain S, Masumura S: **Chronic Administration Of Docosahexaenoic Acid Improves The Performance Of Radial Arm Maze Task In Aged Rats.** *Clinical and Experimental Pharmacology and Physiology* 2001, **28**:266-270.
298. Hashimoto M, Hossain S, Shimada T, Shido O: **Docosahexaenoic acid-induced protective effect against impaired learning in amyloid beta-infused rats is associated with increased synaptosomal membrane fluidity.** *Clinical and experimental pharmacology & physiology* 2006, **33**:934-9.
299. Lim S, Suzuki H: **Changes in maze behavior of mice occur after sufficient accumulation of docosahexaenoic acid in brain.** *The Journal of nutrition* 2001, **131**:319-24.
300. Sugimoto Y, Taga C, Nishiga M, Fujiwara M, Konishi F, Tanaka K, Kamei C: **Effect of docosahexaenoic acid-fortified *Chlorella vulgaris* strain CK22 on the radial maze performance in aged mice.** *Biological & pharmaceutical bulletin* 2002, **25**:1090-2.
301. Suzuki H, Park SJ, Tamura M, Ando S: **Effect of the long-term feeding of dietary lipids on the learning ability, fatty acid composition of brain stem phospholipids and synaptic membrane fluidity in adult mice: a comparison of sardine oil diet with palm oil diet.** *Mechanisms of ageing and development* 1998, **101**:119-28.
302. Kalmijn S, Launer LJ, Ott A, Witteman JC, Hofman A, Breteler MM: **Dietary fat intake and the risk of incident dementia in the Rotterdam Study.** *Annals of neurology* 1997, **42**:776-82.
303. Connor WE: **Importance of n-3 fatty acids in health and disease.** *The American journal of clinical nutrition* 2000, **71**(1 Suppl):171S-5S.
304. Barberger-Gateau P, Letenneur L, Deschamps V, Pérès K, Dartigues J-F, Renaud S: **Fish, meat, and risk of dementia: cohort study.** *BMJ (Clinical research ed)* 2002, **325**:932-3.
305. Morris MC, Evans DA, Bienias JL, Tangney CC, Bennett DA, Wilson RS, Aggarwal N, Schneider J: **Consumption of fish and n-3 fatty acids and risk of incident Alzheimer disease.** *Archives of neurology* 2003, **60**:940-6.
306. Cunnane SC, Plourde M, Pifferi F, Bégin M, Féart C, Barberger-Gateau P: **Fish, docosahexaenoic acid and Alzheimer's disease.** *Progress in lipid research* 2009, **48**:239-56.
307. Loef M, Walach H: **The omega-6/omega-3 ratio and dementia or cognitive decline: a systematic review on human studies and biological evidence.** *Journal of nutrition in gerontology and geriatrics* 2013, **32**:1-23.
308. Dacks PA, Shineman DW, Fillit HM: **Current evidence for the clinical use of long-chain polyunsaturated n-3 fatty acids to prevent age-related cognitive decline and Alzheimer's disease.** *The journal of nutrition, health & aging* 2013, **17**:240-51.
309. Huang TL: **Omega-3 fatty acids, cognitive decline, and Alzheimer's disease: a critical review and evaluation of the literature.** *Journal of Alzheimer's disease* 2010, **21**:673-90.
310. Lee J, Jung S, Kim I, Jeong Y, Kim H, Kim S: **Polymeric nanoparticle composed of fatty acids and poly(ethylene glycol) as a drug carrier.** *Int J Pharm.* 2003, **251**:23-32.

8 APPENDIX

8.1 List of publications

Journals

Flurbiprofen-loaded nanoparticles can cross a primary porcine *in vitro* blood-brain barrier model to reduce amyloid- β 42 burden.

Stab J, Zlatev I, Raudszus B, Meister S, Langer K, Pietrzik CU, von Briesen H, Wagner S. *J Nanomedicine Biotherapeutic Discov* 2016, 6:140

Transport of treosulfan and temozolomide across an *in vitro* blood-brain barrier model.

Linz U, Hupert M, Santiago-Schübel B, Wien S, **Stab J**, Wagner S, 2015, *Anticancer Drugs*. 2015; 26(7):728-36

Tracking of magnetite labeled nanoparticles in the rat brain using MRI.

Martínez V, Schmidt R, Langer K, Zlatev I, Wronski R, Auer E, Havas D, Windisch M, von Briesen H, Wagner S, **Stab J**, Deutsch M, Pietrzik CU, Fazekas F, Ropele S, *PLoS ONE*, 2014, 9(3): e92068.

Nanoparticulate flurbiprofen reduces amyloid- β 42 generation in an *in vitro* blood-brain barrier model.

Meister S, Zlatev I, **Stab J**, Docter D, Baches S, Stauber RH, Deutsch M, Schmidt R, Ropele S, Windisch M, Langer K, Wagner S, von Briesen H, Weggen S, Pietrzik CU, *Alzheimers Res Ther*. 2013; 5(6):51.

Citrus fruit and fabacea secondary metabolites potently and selectively block TRPM3.

Straub I, Mohr F, **Stab J**, Konrad M, Philipp S, Oberwinkler J, Schaefer M.; *Br J Pharmacol*. 2013, 168(8):1835-50

TRPM3 is a nociceptor channel involved in the detection of noxious heat.

Vriens J, Owsianik G, Hofmann T, Philipp SE, **Stab J**, Chen X, Benoit M, Xue F, Janssens A, Kerselaers S, Oberwinkler J, Vennekens R, Gudermann T, Nilius B, Voets T.; *Neuron*. 2011, 70(3):482-94.

Orals

Speaker at NanoBioMed Conference in Graz, Austria, April 2015

Posters

Trojan Horses for Alzheimer's disease treatment - Flurbiprofen-loaded poly(lactic acid) nanoparticles reduce A β 42 levels in a primary porcine *in vitro* blood-brain barrier model.

Stab J, Zlatev I, Meister S, Langer K, Wronski R, Windisch M, Ropele S, Schmidt R, Deutsch M, Pietrzik C, von Briesen H, Wagner S, Bad Herrenalber Transporter- und Barriere- Tage 2014, Bad Herrenalb, Germany, 2014

Painkillers for Alzheimer's disease – A nanoparticle-based approach to transport flurbiprofen to the brain.

Stab J, Zlatev I, Meister S, Langer K, Wronski R, Windisch M, Ropele S, Schmidt R, Deutsch M, Pietrzik C, von Briesen H, Wagner S, 9th World Meeting on Pharmaceutics, Biopharmaceutics and Pharmaceutical Technology, Lisbon, Portugal, 2014

Making transport possible: Flurbiprofen-loaded nanoparticles for the treatment of Alzheimer's disease.

Stab J, Zlatev I, Meister S, Langer K, Wronski R, Windisch M, Ropele S, Schmidt R, Deutsch M, Pietrzik C, von Briesen H, Wagner S, Bad Herrenalber Transporter- und Barriere- Tage 2013, Bad Herrenalb, Germany, 2013

Nanoparticle-mediated transport of drugs over the blood-brain barrier: Hope for Alzheimer's disease.

Stab J, Zlatev I, Langer K, Wronski R, Windisch M, Ropele S, Schmidt R, Deutsch M, Pietrzik C, von Briesen H, Wagner S, 8th World Meeting on Pharmaceutics, Biopharmaceutics and Pharmaceutical Technology, Istanbul, Turkey, 2012

Nanoparticle-mediated transport of drugs over the blood-brain barrier: Hope for Alzheimer's disease.

Stab J, Zlatev I, Langer K, Wronski R, Windisch M, Ropele S, Schmidt R, Deutsch M, Pietrzik C, von Briesen H, Wagner S, Bad Herrenalber Transporter- und Barriere- Tage 2012, Bad Herrenalb, Germany, 2012

8.2 Curriculum Vitae

Julia Stab

* 10.02.1985 in Paderborn, Germany

Studies, academic degrees & current position:

Since June 2011 Lab member of research group of Dr. Sylvia Wagner at the Fraunhofer Institute for Biomedical Engineering (IBMT), St. Ingbert and Sulzbach, Germany

2010 - 2011 Lab member of research group of Dr. Johannes Oberwinkler at the Institute for Experimental and Clinical Pharmacology & Toxicology of Saarland University, Germany

2010 Diploma in human & molecular biology from Saarland University, Homburg/Saar, Germany, Title of thesis: *“Characterization of TRPM3 Channels in Cells of the Peripheral Nervous System”*

2009 Scientific assistant at the Institute for Experimental and Clinical Pharmacology & Toxicology of Saarland University, Germany

2007 Pre-Diploma in Biology from Technical University Kaiserslautern, Germany

2004 Abitur at Reismann-Gymnasium Paderborn, Germany

Additional education

“Writing in the Sciences” Coursera certificate from Stanford University, Stanford School of Medicine, USA, 2014

8.3 Acknowledgements

Herzlichen Dank!

Die vorliegende Arbeit wurde am Fraunhofer IBMT im Saarland angefertigt. Mein besonderer Dank gilt Herrn Prof. Dr. Fuhr, der meine Arbeit angeleitet und betreut hat. Herrn Prof. Dr. von Briesen und Herrn Prof. Dr. Zimmermann danke ich für ihr Interesse und Ihre konstruktive Kritik an meiner Arbeit und für die Möglichkeit die Arbeit am Fraunhofer IBMT durchzuführen. Frau Dr. Sylvia Wagner danke ich ganz besonders für die Überlassung des Themas, die fortwährende Unterstützung, die wissenschaftlichen Beiträge und Ihre Diskussionsbereitschaft. Herrn Prof. Dr. Marc Schneider danke ich für die Begutachtung dieser Dissertation und für seine hilfreichen wissenschaftlichen Beiträge und Diskussionen.

Am Institut für Pharmazeutische Technologie und Biopharmazie der Westfälischen Wilhelms-Universität in Münster möchte ich mich bei Herrn Prof. Dr. Langer und seiner Arbeitsgruppe für die gelungene Kooperation und die daraus entstandenen gemeinsamen Publikationen bedanken. Mein besonderer Dank gilt Herrn Dr. Iavor Zlatev und Herrn Bastian Raudszus, für die Herstellung und stetige Optimierung der Nanopartikel, die in dieser Arbeit verwendet wurden.

Am Institut für Physiologische Chemie und Pathobiochemie der Universitätsmedizin der Johannes Gutenberg-Universität in Mainz möchte ich Prof. Dr. Pietrzik und besonders auch Dr. Sabrina Meister für die gelungene Kooperation, die daraus entstandenen gemeinsamen Publikationen, das zur Verfügung stellen diverser Antikörper und Zellen danken. Weiterhin danke ich ihr für die Erlaubnis die Ergebnisse bezüglich der nanopartikelären Proteinkorona in dieser Arbeit abzubilden, sowie für die steten wissenschaftlichen Beiträge und zahlreichen Diskussionen und Telefonate bezüglich der Blut-Hirn-Schranken-Modelle danken.

Einen ganz herzlichen Dank möchte ich auch meinen lieben Mit-Promovenden, Büronachbarn und Kollegen aussprechen: Dr. Nadine Wilhelm, Linda Elberskirch (auch für die Unterstützung bei HPLC Analysen), Aline Moosmann, Elmar Mohrhardt und Dr. Erwin Gorjup, die meine Zeit am Fraunhofer IBMT maßgeblich geprägt haben. Vielen Dank auch an unsere hervorragenden technischen Assistenten Sascha Wien und Judith Bungert, deren Erfahrung und Motivation unsere Doktorarbeiten begleitet haben. Für die Unterstützung und den ungebrochenen Eifer bei zahlreichen Experimenten bedanke ich mich ganz herzlich bei Kristina Golfmann, Theresa Siebert und Stefan Ohlinger, die ihre Bachelor- bzw. Masterarbeit am Fraunhofer IBMT absolviert haben und mich tatkräftig unterstützt haben.

Für die Korrekturen der englischen Sprache bedanke ich mich ganz herzlich bei Herrn Matthew Zion.

Thank you, dear friend!